AD_____

Award Number: DAMD17-03-C-0089

TITLE: Biomarker Development for TLR4 Agonists

PRINCIPAL INVESTIGATOR: David H. Persing, M.D., Ph.D.

CONTRACTING ORGANIZATION: Corixa Corporation
Seattle, Washington 98104

REPORT DATE: October 2004

TYPE OF REPORT: Annual

PREPARED FOR: U.S. Army Medical Research and Materiel Command
Fort Detrick, Maryland 21702-5012

DISTRIBUTION STATEMENT: Approved for Public Release;
Distribution Unlimited

The views, opinions and/or findings contained in this report are those of the author(s) and should not be construed as an official Department of the Army position, policy or decision unless so designated by other documentation.

20050218 090

REPORT DOCUMENTATION PAGE

Form Approved
OMB No. 074-0188

Public reporting burden for this collection of information is estimated to average 1 hour per response, including the time for reviewing instructions, searching existing data sources, gathering and maintaining the data needed, and completing and reviewing this collection of information. Send comments regarding this burden estimate or any other aspect of this collection of information, including suggestions for reducing this burden to Washington Headquarters Services, Directorate for Information Operations and Reports, 1215 Jefferson Davis Highway, Suite 1204, Arlington, VA 22202-4302, and to the Office of Management and Budget, Paperwork Reduction Project (0704-0188), Washington, DC 20503

1. AGENCY USE ONLY (Leave blank)	2. REPORT DATE	3. REPORT TYPE AND DATES COVERED
	October 2004	Annual (8 Oct 2003 - 7 Sep 2004)

4. TITLE AND SUBTITLE
Biomarker Development for TLR4 Agonists

5. FUNDING NUMBERS
DAMD17-03-C-0089

6. AUTHOR(S)
David H. Persing, M.D., Ph.D.

7. PERFORMING ORGANIZATION NAME(S) AND ADDRESS(ES)
Corixa Corporation
Seattle, Washington 98104

E-Mail: David.persing@corixa.com

8. PERFORMING ORGANIZATION REPORT NUMBER

9. SPONSORING / MONITORING AGENCY NAME(S) AND ADDRESS(ES)
U.S. Army Medical Research and Materiel Command
Fort Detrick, Maryland 21702-5012

10. SPONSORING / MONITORING AGENCY REPORT NUMBER

11. SUPPLEMENTARY NOTES

12a. DISTRIBUTION / AVAILABILITY STATEMENT
Approved for Public Release; Distribution Unlimited

12b. DISTRIBUTION CODE

13. ABSTRACT (Maximum 200 Words)

In DARPA-supported studies, we have shown that a family of novel synthetic glycolipids known as the aminoalkyl glucosaminide phosphates (AGPs) act as potent agonists of Toll-like receptor 4 (TLR4), and that administration of AGPs to the airways results in protection against lethal challenge with virulent bacterial and viral agents. Preliminary toxicological studies indicate that intranasal delivery of the compounds is safe, and human clinical trials with aerosolized TLR4 agonists are now anticipated. To monitor the effectiveness of immunoprophylaxis in human trials, it may become necessary to develop surrogate biomarkers of protection since experimental challenge endpoints are not readily available. Under the current contract, we have completed a series of *in vitro* and *in vivo* studies to identify candidate biomarkers via microarray-based transcriptional profiling, conventional multiplex cytokine and flow cytometric analyses. Through these studies we have identified biomarkers suitable for clinical monitoring of AGP mediated protection. Synthesis and scale-up requirements have been established and carried out for a single lead AGP candidate, CRX-527, for production of GMP grade material suitable for clinical trials. Formal GLP toxicology studies with CRX-527 will be initiated in early 2005 with a Phase I Clinical trial planned for the first quarter of 2006. Pre-IND documents for this phase I clinical trial are currently being assembled and will be submitted to the FDA for approval in mid-October.

14. SUBJECT TERMS
TLR4 agonists, innate immunity, synthetic lipid A mimetics, cytokines, biomarkers, surface markers, DNA microarray, synthesis, scale-up, analytical assays

15. NUMBER OF PAGES
76

16. PRICE CODE

17. SECURITY CLASSIFICATION OF REPORT	18. SECURITY CLASSIFICATION OF THIS PAGE	19. SECURITY CLASSIFICATION OF ABSTRACT	20. LIMITATION OF ABSTRACT
Unclassified	Unclassified	Unclassified	Unlimited

TABLE OF CONTENTS

I. INTRODUCTION

Scientists at Corixa have developed a library of synthetic lipid A mimetics known chemically as aminoalkyl 2-amino-2-deoxy-4-phosphono-beta-D-glucopyranosides (aminoalkyl glucosaminide 4-phosphates, AGPs). These synthetic molecules are structurally related to the major hexa-acyl component present in MPL (trademarked) adjuvant, whereby the reducing sugar has been replaced with an aminoalkyl aglycon. The conformationally flexible N-acylated aglycon arm permits energetically favored close packing of the fatty acyl chains. Tight packing of six fatty acids in a hexagonal array is believed to play an essential role in the bioactivity of lipid A-like molecules. Corixa's library of AGPs is divided into several families based on the specific aglycon moiety: L-seryl, L-serinamide, serinol, aminoethyl, and "cyclic" families.

As part of a DARPA contract initiated in 2000, we screened all available AGP compounds for in vivo and in vitro immunostimulatory activity in models of innate immunity. The top candidates from these studies represented each of the AGP families, respectively: RC527, RC522, RC545, RC524 and RC590. While each of these AGPs differs with respect to the aglycon unit, they all have identical fatty acid chain length pattern, i.e. three pairs of a 14-carbon fatty acid with a ten-carbon fatty acid branch. These AGPs were further evaluated in vivo and in vitro for a variety of parameters including dose response, time-of-protection, tolerance (repeated dosing), route of delivery, and induction of adaptive immunity following pathogen challenge. Two AGPs, CRX-527 and CRX-524, emerged as the top candidates from the DARPA project and have low inflammatory potential in vitro while maintaining potency in mouse in vivo assays. Due to it's higher in vivo and in vitro immunostimulatory activity, therapeutic index, and greater solubility CRX-527 was chosen as the lead candidate for further development under the current U.S. Army Medical Research and Materiel Command contract. The specific aims of this contract are as follows:

Task 1) Biomarker Discovery. Microarray analysis using CRX-524 and CRX-527 will be performed to identify mRNA expression of novel and previously identified markers during the period immediately following AGP exposure (< 6 hours) and up to 168 hours for human monocyte derived macrophages, and/or human PBMC.

Task 2) *In vivo* Detection of Soluble Biomarkers. Biomarker candidates identified in Task 1 will be tested by using commercially available ELISA kits or commercial available antibodies in an in-house-developed immunoassay. Candidate biomarkers will be evaluated in mouse and primate sera to determine the sensitivity, specificity, accuracy, and precision of each marker. Mouse and primate sera will be obtained at a series of timepoints after intranasal exposure to CRX-524 or CRX-527.

Task 3) Cellular Biomarkers. Mouse splenocytes and PBMC of responsive donors will be cultured, cell subsets will be identified and stained for intracellular cytokines followed by flow cytometry in order to determine cell types that are activated in response to CRX-524 or CRX-527. PBMC harvested from mice and primates at several timepoints after intranasal AGP exposure will then be tested for surface marker expression that tracks with the protective effect of the AGPs CRX-524 and CRX-527.

Task 4) AGP Process Development and GMP Manufacturing. Corixa synthetic chemists will investigate a scale up strategy for increased production of CRX-527 with the goal of GMP synthesis at a scale larger than 5 grams. A 20 gram quantity of material

sufficient for formulation testing, stability analysis, toxicological testing, and up to phase 3 clinical trials will be synthesized via subcontract.

Task 5) Phase I Clinical Trial Evaluation. A phase I dose escalation study will be performed in 4 cohorts of 8 volunteers. Drug will be administered into the upper airways via the Pfeiffer uni-dose device. Signs and symptoms post-exposure will be monitored and biomarkers identified in aims 1-3 will be studied as surrogate markers of protective efficacy.

II. BODY

Task 1: Biomarker Discovery (Microarray)

Over the previous year the microarray team initiated and completed the biomarkers discovery phase of the contract. Pilot and full-scale microarray biomarker discovery experiments were designed and completed. The pilot study was performed in November 2003 to arrive at doses of AGP to use in the final microarray study and to select an appropriate sample size. From this pilot experiment, 3 PBMC donors (PBMCs were collected under DARPA contract) were chosen for the full-scale study and a dose range for the AGP was selected. Starting in December 2003 and continuing through April 2004, these samples were used to isolate adherent macrophages as outlined in the experimental design below.

Large Scale biomarkers experiment: 3 donors (45, 77 and 466)

5 time pts: 2,6,24,72, 96 and 168hrs
3 treatments: CRX524 (5ug/ml), CRX527 (1ug/ml and 0.1ug/ml), media only (+/- IFN-γ pre-treatment)

1. Plate 1.92 $X10^8$ PBMC per condition (at 30 pts/ $6x10^9$ cells required)
2. Retain adherent cells after 2 hrs
3. Culture for 5 days
4. Stimulate with A GPs (with and without IFN-γ) for time periods shown above
5. Harvest supernatants and freeze at -80C
6. Harvest cells in Trizol for mRNA extraction
7. Test supernatants by TNF-α ELISA to confirm activity
8. Isolate total RNA convert to amplified RNA
9. Make labeled cDNA probes
10. Hybridize to Inflammation Chip (printed in-house, containing app. 1100 inflammation relevant genes)
11. Perform Genespring Analysis (looking for statistically relevant markers that may be useful to assay the effects of AGP's in vivo)

Two lots of in-house microarray chips were printed with approximately 1100 inflammation relevant cDNAs and controls on each slide. 58 of these slides were hybridized to cDNA generated from the amplified RNA. Analysis of the data was completed in May, 2004. The 24 - 48hr time period provides the best window for collection of clinical samples. Genes that are over-expressed in this time frame may be suitable biomarkers to track AGP administration and duration of the ensuing innate immune response. Table 1 shows the genes which were 2-fold or greater over-expressed at 48hrs following CRX-524 administration.

Table 1: Microarray summary

Common name	d466	d45	d77	Average expression 48hr (IFN-γ)	Location
TNF alpha	4.2	3.3	2.1	3.2	Soluble
RANTES	8.9	8.2	7.8	8.3	Soluble
CCL4	8.8	25.1	16.6	16.8	Soluble
MARCKS	5.0	3.9	5.0	4.6	Soluble
CXCL3	2.9	12.9	29.5	15.1	Soluble
MMP7	7.7	5.0	14.7	9.1	Soluble
IL8	9.4	30.8	48.0	29.4	Soluble
IL1 beta	5.8	17.6	52.1	25.2	Soluble
Cox2	2.4	2.7	7.0	4.0	Soluble
CCL2	2.8	9.3	19.4	10.5	Soluble
CCL15	3.2	2.7	1.7	2.5	Soluble
beta2 microglobin	2.5	2.7	2.5	2.6	Soluble
Tap1	2.8	2.9	2.3	2.7	ER, Cytoplasm
Viperin	9.7	13.2	9.4	10.7	ER, Cell surface?
NAF-1	4.0	4.8	3.8	4.2	Cytoplasm, Nuclear
STAT1	2.8	2.9	4.5	3.4	Cytoplasm, Nuclear
STAT3	4.0	2.6	7.2	4.6	Cytoplasm, Nuclear
STAT4	2.6	2.6	9.1	4.8	Cytoplasm, Nuclear
OIP106	2.6	8.7	6.7	6.0	Cytoplasm, Nuclear
DIF-2	5.5	2.4	3.7	3.9	Cytoplasm, Nuclear
IFP35	4.4	4.0	3.2	3.9	Cytoplasm, Nuclear
OAS1	3.4	3.7	4.0	3.7	Cytoplasm
KYNU	2.7	2.6	12.0	5.7	Cytoplasm
INDO	3.4	26.4	6.4	12.1	Cytoplasm
IkBa	2.3	4.6	2.3	3.1	Cytoplasm
TNFIAP6	6.6	37.8	40.2	28.2	Cell surface
TLR2	2.1	3.1	8.8	4.7	Cell surface
SLC3A2	2.2	13.5	1.5	5.7	Cell surface
LY75	7.2	2.0	3.7	4.3	Cell surface
IL7 receptor	3.4	6.5	9.9	6.6	Cell surface
HxCT	7.1	3.3	8.0	6.1	Cell surface
CD80	4.3	13.1	8.6	8.7	Cell surface
CD38	3.4	16.1	ND	9.8	Cell surface
CCR7	2.9	10.0	4.2	5.7	Cell surface

In addition to the genes previously discovered by soluble or cell surface biomarker discovery experiments, two genes of particular interest as biomarkers were elevated at 24-48hrs. MMP-7 (matrilysin), a secreted metalloproteinases, and therefore measurable by ELISA, and CCR7 (chemokine receptor) a potential cell surface marker, were induced by CRX-524. These genes and others on the table have now been confirmed by Real time-PCR and are being further characterized by ELISA or FACS.

Two other genes that were elevated at 24-48 hrs were also of interest, Indolamine-pyrrole 2,3 dioxygenase (IDO or INDO) and Kynureninase (KYNU). Both are enzymes essential in the

degradation of Tryptophan. IDO degrades Tryptophan to N-formyl Kynurenine, which is then further degraded to Kynurenine. Kynureninase metabolizes Kynurenine to Anthranilate.

Degradation of Tryptophan by IDO has been shown to slow bacterial growth, stabilize IL6 and IL8 mRNA and suppress T-cell proliferation. (1,2,3). Dubener et al. (4) demonstrated a simple assay to detect Kynurenine in cell supernatants. This colorimetric assay, using Erlich's reagent, was used as a bioassay for IFN-γ (which also induces IDO). This assay was used to test frozen supernatants from our time course experiments. A detectable increase in Kynurenine over background, w/ and w/o IFN-γ, peaking at 24-48 hrs, was demonstrated (Figure 1). The Kynenurenine increase indicates the degradation of Tryptophan via the induction of IDO by the AGP's. Another version of this assay using HPLC to detect Tryptophan and Kynurenine in serum has been published (5).

The HPLC assay for determining tryptophan and kynurenine levels in serum was tested using mouse serum collected from mice treated with LPS (100 ng), CRX-527 (10 ug) or vehicle, via intranasal or IV administration Serum was harvested at 48 hrs following treatment and frozen at –80deg C until assayed.

The HPLC assay was performed as follows. 100ul of serum was mixed w/ 100ul phosphate buffer containing 10umol/L of 3-nitro-L-tyrosine as an internal control. The sample was then precipitated w/ TCA and 100ul loaded into a Waters analytical HPLC machine with an auto-sampler. Kynurenine and nitrotyrosine were detected via UV absorbance at 360nm wavelength, and tryptophan was detected via fluorescence at 285nm extinction and 365nm emission (Widner et.al). The serums and controls were run over an Agilent Zorbax C-18 column w/ a guard column in place. The area under the curve of each of the relevant peaks was used to calculate the kynurenine to tryptophan ratios using the nitro-tyrosine as an internal standard.

The results were as anticipated (Figure 2 and Table 2). The two mice treated with 10 ug CRX-527, I.V., had the highest levels of kynurenine, >2 fold over vehicle alone. The mice treated with 10 ug CRX527 via intranasal/intrapulmonary delivery had the next highest levels of kynurenine followed by the LPS (I.V.) treated mice. Mice treated with 10 ug CRX-527 via strict intranasal delivery showed no change in serum kynurenine levels above vehicle alone.

The tryptophan levels in the mice were much higher (3x) than that reported for normal human patients (5). This lowered the kynurenine/trptophan ratios. However, the CRX-527 treated mice still showed approximately 2 fold higher ratio than in the vehicle controls (Table 2). This assay is simple, inexpensive and relatively high throughput. With further refinements it may prove useful as a biomarker assay to measure the effects of AGP's on human patients by indirectly measuring the induction of indoleamine 2,3 dioxygenase (IDO).

(1) MacKenzie et al., Eur. J Immunol. 29, (1999) 3254-3261
(2) Wissen et al., J of Immunology, Vol 169, 2002, 7039-7044
(3) Munn et al., J Exp.Med., Vol. 189, (No. 9), (1999) 1363-1372
(4) Dubener et al., JIM, 168 (1994), 39-47
(5) Widner et al., Tryptophan, Serotonin and Melatonin: Basic Aspects and Applications, edited by Huether et al., Kluwer Acedemic/ Plenum publishers, New York, 1999

Figure 1: Kynurenine assay w/ Erlich's reagent (donor 77)

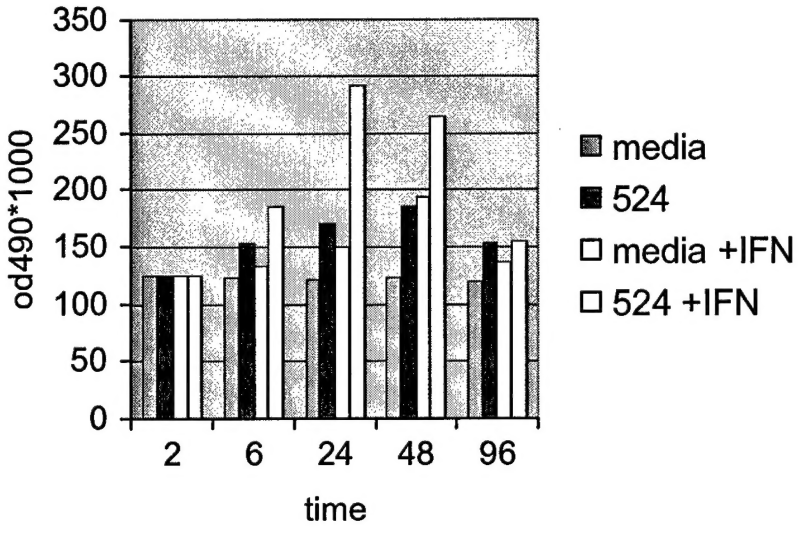

Figure 2: Kynurenine HPLC assay

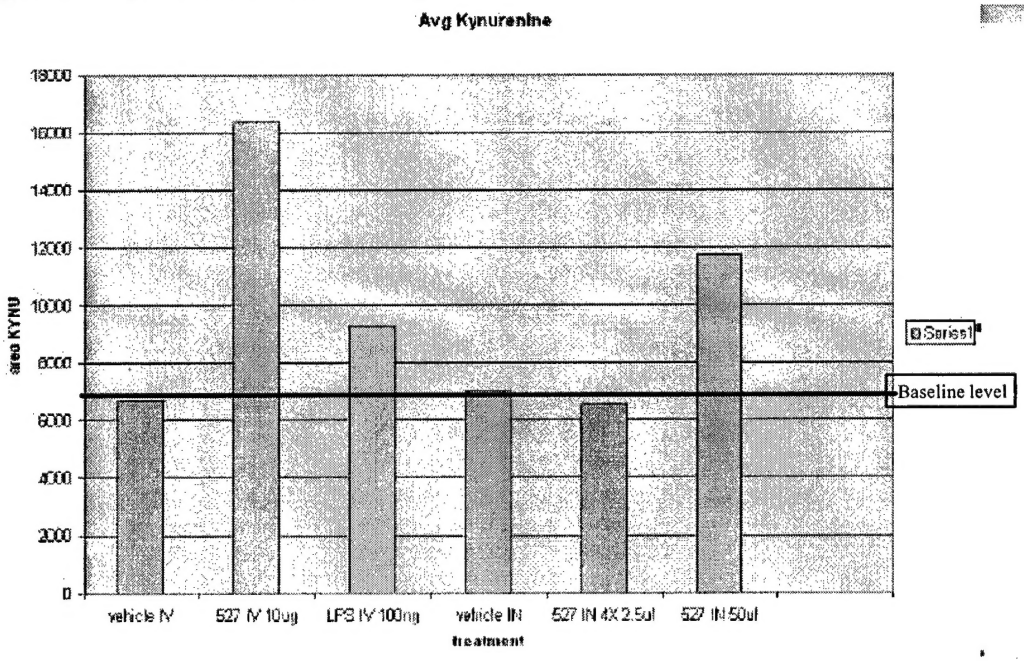

Table 2: Data from Kynurenine/Tryptophan HPLC assay

	umol/ trp	umol/kynu	ratio kynu/trp	avg nmol/mmol
vehicle IV	82.8	0.5	0.006	
vehicle IV	90.4	0.7	0.008	7.0
527 IV 10ug	108.5	1.6	0.015	
527 IV 10ug	131.2	1.5	0.012	13.5
LPS IV 100ng	139.8	0.9	0.006	
LPS IV 100ng	106.0	0.9	0.009	7.5
527 IN 4X 2.5ul	112.3	0.7	0.007	
527 IN 4X 2.5ul	90.2	0.5	0.006	6.5
527 IN 50ul	111.1	1.1	0.010	
527 IN 50ul	144.0	1.2	0.008	9.0
vehicle IN	104.6	0.7	0.007	
vehicle IN	84.0	0.6	0.007	7.0

Task 1: Biomarker Discovery (real-time RT-PCR).

During the previous year the RT-PCR team specifically targeted biomarkers that could be analyzed from small, easily collected clinical samples that would be identical or similar to samples to be collected during toxicology and/or phase I clinical studies. A pilot study was performed during January-February 2004 to validate RNA isolation and biomarker PCR protocols. Test samples were harvested in RLT buffer and RNA later, frozen at –80C, and RNA was extracted by Qiagen RNeasy kit. It was determined that RLT buffer-treated samples had greater RNA yield, even when used in PBMC-cell spiking experiments. RNA quality was initially assessed by agarose gel, but quantities were so low that RNA visualization was not possible in most cases. Several samples were evaluated for quality using the Agilent Bioanalyzer and were found to be in sufficient quality and quantity to reverse transcribe into cDNA, which was used as a template for real-time PCR. We determined that spectrophotometric analysis was sufficient to monitor the quantity and quality (A260:A280 ratio) of RNA prior to cDNA synthesis. The quantity, quality, and volume of cDNA available from the test samples indicated we should be able to assay at least 5-7 genes; the actual yield from the cynomolgus trial allowed us to test at least 20 biomarkers.

Primers and probes were selected for various cytokines, chemokines, and cell surface markers of interest (identified through microarray and serologic response to AGP compounds) for use in cynomolgus monkey experiments with potential to be used in future human clinical trials. Sequence analysis was performed during November 2003-February 2004 to determine likelihood of detection of both cynomolgus and human genes of interest. Ultimately, Applied Biosystems TaqMan Gene Expression Assays (TGEA) were selected to assay for most biomarkers. Housekeeping genes Actin, HPRT, 18S rRNA, and PBGD were evaluated for their utility in normalizing cytokine gene expression in monkey nasal scrapings by real-time RT-PCR (Actin, HPRT, and PBGD assays were designed in-house). It was found that all housekeeping genes yielded good signal and normalization of genes of interest were not significantly affected in nasal scraping samples.

Several cynomolgus and human PBMC *in vitro* stimulation experiments were performed between February and July 2004. Real-time RT-PCR assays have been tested for 20 biomarkers on

two cynomolgus PBMC experiments (untreated and CRX-524 treated) and 4 pilot cynomolgus nasal scraping samples (2 untreated, 2 treated). Expression of 18 biomarkers was detected in monkey PBMCs and nasal scraping specimens and is summarized in the Table 3 below. Expression of 8 biomarkers were stimulated in PBMCs by CRX-524 treatment *in vitro*. One biomarker (CCR7) was clearly upregulated (3-6 times higher expression) in CRX-524-treated monkey nasal scrapings in comparison to untreated animals. The upregulation of additional biomarkers in nasal scrapings may be detected by establishing individual baseline expression prior to AGP treatment.

Table 3: Real-time RT-PCR analysis of PBMCs

Gene of Interest	Cynomolgus PBMCs	Nasal scrapings (4 pilot samples)
IL-4	no expression	no expression
IL-6	no expression	no expression
IL-10	some expression + stim*	medium expression
TNF alpha	Expression stim*	medium expression
MCP-1 (CCL2)	low expression	medium expression
IL-1 beta	Expression stim*	high expression
IP-10 (CxCl10)	low expression	very low expression level
MIP-1a (CCL3)	low expression	medium expression
MIP-1b (CCL4)	Expression stim*	high expression
RANTES (CCL5)	Expression stim*	med/high expression
CD69	very low signal	low expression
CCR7	Expression stim*	expression stim*
MMP7	low signal	high expression
CD38	low signal	low expression
INDO	Expression stim*	high expression
CD80	low signal	med/low expression
IL-7 Receptor	very low signal	med/low expression level
CxCl3 (MIP-2B)	very low signal	med expression level
CxCl9 (MIG)	very low signal	medium expression
IL-8 (CCL8)	Expression stim*	high expression

* Clear expression upregulation observed in AGP treated samples

Additionally, a time course experiment was performed where cynomolgus PBMCs were stimulated *in vitro* with CRX-524 (0.1ug/ml or 10ug/ml) and harvested at 2, 8, and 24 hours post-stimulation for evaluation by RT-PCR. We saw the best responses with the high dose of CRX-524. We detected clear upregulation of TNF-α by two hours (6 times higher expression that vehicle controls) and 10-fold increase in INDO expression 8-24 hours post treatment with CRX-524. We also detected a 1.2-1.5 increase in RANTES expression between 2-24hrs, 2-8-fold increase in CCR7 at 2hrs, and up to 17 fold increase in CxCl9. MMP7 had minimal expression in stimulated PBMCs, but no expression in vehicle controls. Based on the cynomolgus monkey pilot nasal scraping and PBMC data presented here, a priority list of real-time RT-PCR assays, including TNF-α, CCR7, MMP7, CxCl9, and INDO, was established.

RNA extraction from monkey nasal scrapings was completed and cDNA was synthesized (60 samples total). Real-time RT-PCR assays for the five priority biomarkers were tested on cynomolgus nasal scraping samples (5 monkeys treated with CRX-524, 5 vehicle treated; scrapings performed on day –13, -7, +1, +3, +5, and +7) (Cynomolgus Macaque biomarker study was funded by the DARPA contract). The expression of all 5 biomarkers were detected in all nasal scraping

specimens. Individual responses were evaluated for each biomarker. Unfortunately, many monkeys in both treatment groups showed some high biomarker signals on day –13 and/or day –7 indicating a possible problem with infection, inflammation, or injury in some animals. Likewise, expression of biomarkers was observed at elevated levels in some vehicle treated monkeys due to inflammation caused by repeated nasal scrapings on days +3, +5, and +7. We did see upregulation of CCR7 in 3/5 CRX-524 treated monkeys at day +3 to +5. All CRX-524 treated monkeys had upregulated levels of TNF-α between day +1 to day +7. Two CRX-524 treated monkeys had upregulated levels of CxCl9 and day +3 or day +5, while 3 monkeys showed upregulation of INDO at day +3 and/or day +5.

Additional candidate markers will be evaluated on the nasal scrapings in the future. During the next year, real-time RT-PCR will be used to evaluate biomarkers in a variety of samples to prepare assays for use in toxicology and clinical trials. We hope to identify surrogate biomarkers indicative of CRX-527 mechanism of action and will support additional CRX-527 and CRX-524 studies.

Influenza Challenge in Ferrets Treated with CRX-524. RNA was isolated from 99 + 8 control nasal wash specimens from the ferret influenza transmission study completed at RetroScreen in early 2004 (Ferret influenza transmission study at Retroscreen was funded by DARPA contract). Quantitative real-time RT-PCR was performed on all the nasal wash specimens from day 6 and day 27 washes and controls including Influenza A/Panama and Influenza B/Johannesburg allantoic fluid samples. At day 6, most ferrets in all groups had influenza titers above 10,000 copies/ ul nasal wash. The vehicle treated group had influenza titers that were lower than CRX-527 and CRX-524 treated groups. Influenza titers varied between individual animals (Figure 3). By day 27, most ferrets had no detectable influenza titer by real-time RT-PCR except for 3 ferrets treated with 20ug CRX-524 and two ferrets treated with 200ug CRX-524.

We will be comparing clinical observations to viral titers once the Retroscreen report is received at Corixa. We plan to develop this assay for use in clinical viral load monitoring for a future human phase I/II clinical trials with CRX-527 treatment and subsequent viral challenge.

Figure 3: Real-time RT-PCR titers of influenza virus from ferret study.

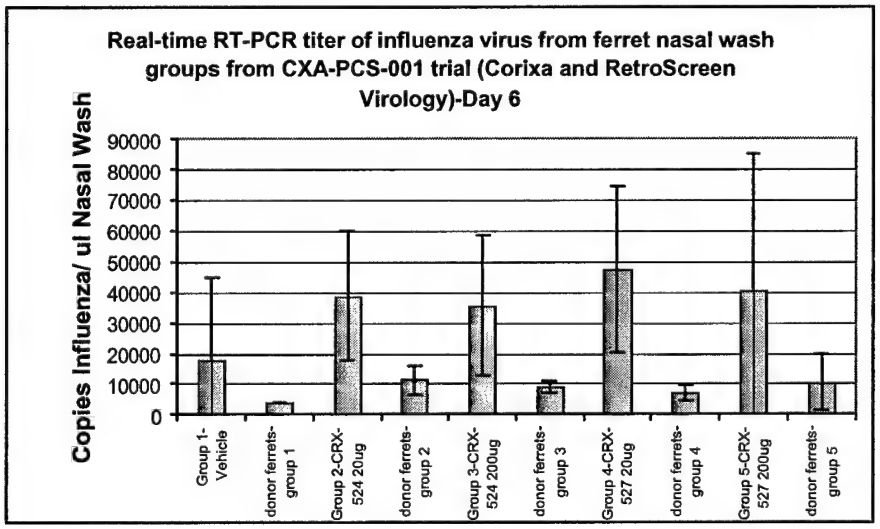

Task 2: Soluble Biomarkers.

The identification of soluble biomarkers up-regulated in serum or nasal wash fluids following intranasal AGP delivery may be useful to track the strength and duration of the non-specific resistance (NSR) afforded by AGPs. These markers may also prove useful to track the dosing and breadth of responses observed at various AGP doses in the upcoming phase I clinical trial. To this end, we have evaluated a variety of serum cytokines and chemokines in vivo following I.V. or I.N. delivery of CRX-524 or CRX-527. Previous studies have demonstrated that while many inflammatory cytokines and chemokines can be detected in the serum following I.V. or I.N. delivery of AGPs, these cytokines reach peak levels by 2-8 hrs following AGP administration and return to baseline levels by 24 hrs. This reduces the potential utility of these cytokines as biomarkers to track the strength and duration of AGP mediated protection. Based on microarray studies (reported above) and further literature review, a second list of potential soluble biomarkers was identified that might remain at elevated levels in the serum or nasal wash fluids beyond 24 hrs following AGP administration (IP-10, MIG, CRP, SAA, IL-1ra, MIP-1β). These soluble markers were evaluated in the serum of mice treated I.V. or I.N. with CRX-524 (Figure 4, SAA not shown). From these studies three soluble markers were identified (IP-10, MIG and SAA) that increased significantly in the serum following I.N. administration of CRX-524 and remained at elevated levels beyond 24 hrs. To evaluated the duration of the cytokine response in greater detail a second I.N. dosing time course experiment was performed for which serum was collected at 0, 24, 48, 96, 120 and 144 hrs following CRX-527 administration and evaluated for these three cytokines by ELISA (Figure 5). Based on these studies IP-10, MIG and SAA have become our lead serum and/or nasal wash biomarker candidates for further evaluation. As a follow-up to these in vivo studies, CRX-527 was delivered to BALB/c mice via strict (low volume) intranasal delivery, groups of 5 mice were treated with 20 ug CRX-527 and serum was harvested at 0hr, 6hr, 24hr, 48hr, 72hr, 96hr and 120hr following AGP delivery. While no significant increases in IP-10 or MIG were detected following strict I.N. administration increases in Serum Amyloid A were measured at 6-48 hrs following intranasal delivery of CRX-527 (Figure 6).

Figure 4: Serum cytokine levels at various times following I.V. or I.N. CRX-524 treatment of BALB/c mice.

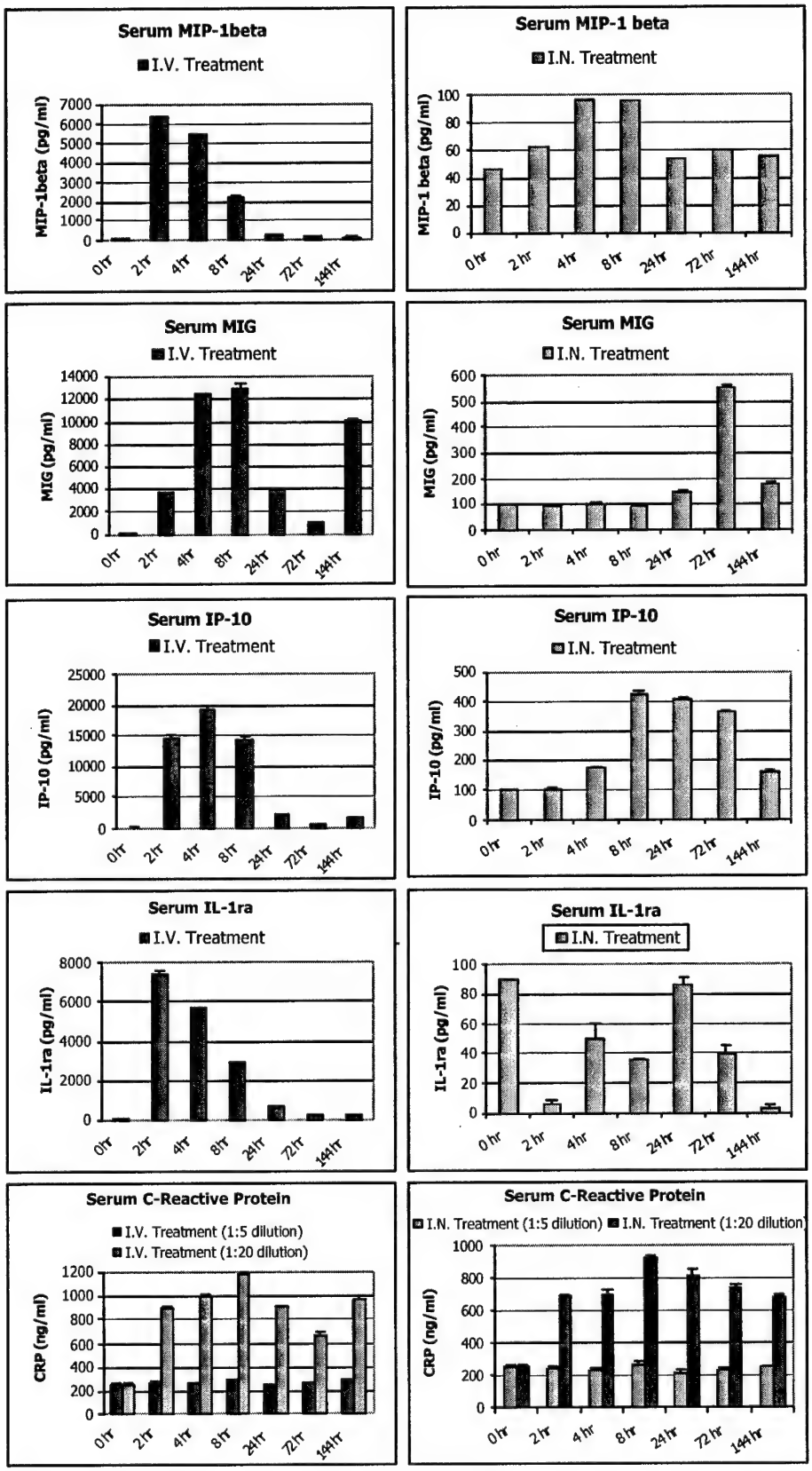

Figure 5: Serum cytokine levels at various times following I.N. CRX-527 treatment of BALB/c mice.

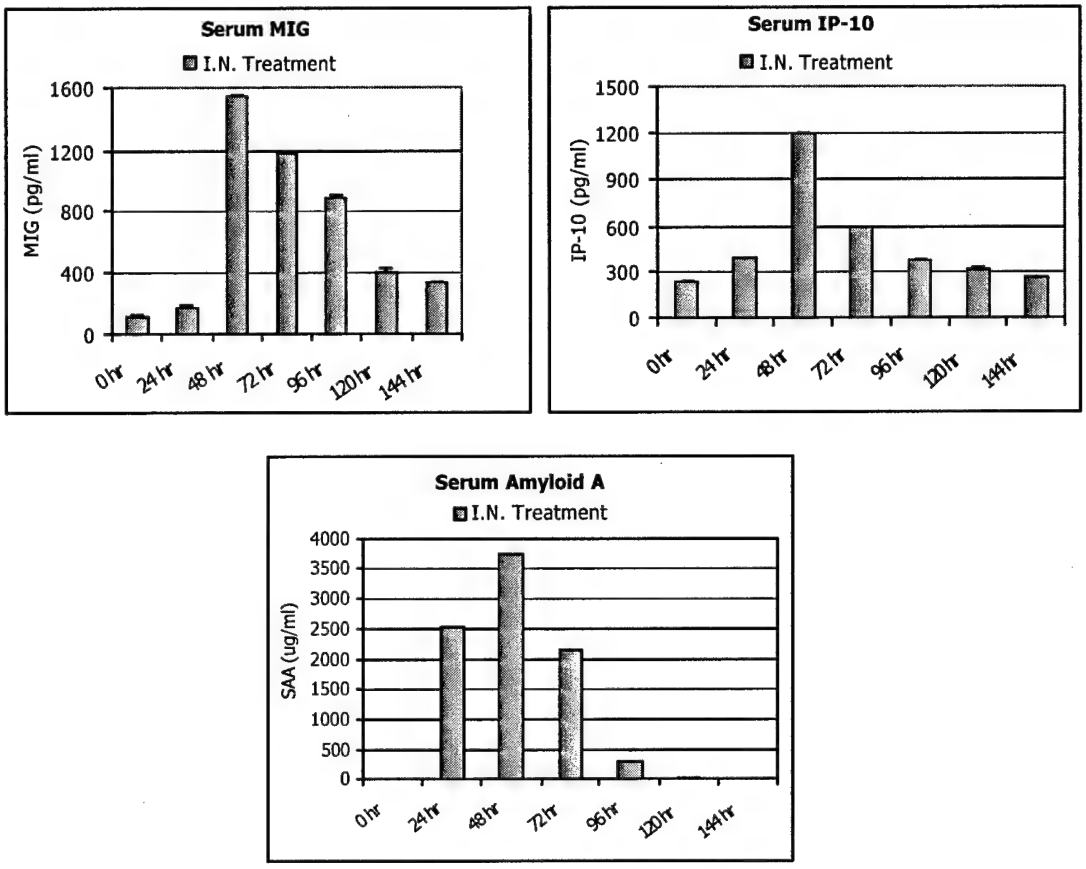

Figure 6: Serum Amyloid A levels at various times following strict (low volume) I.N. CRX-527 treatment of BALB/c mice.

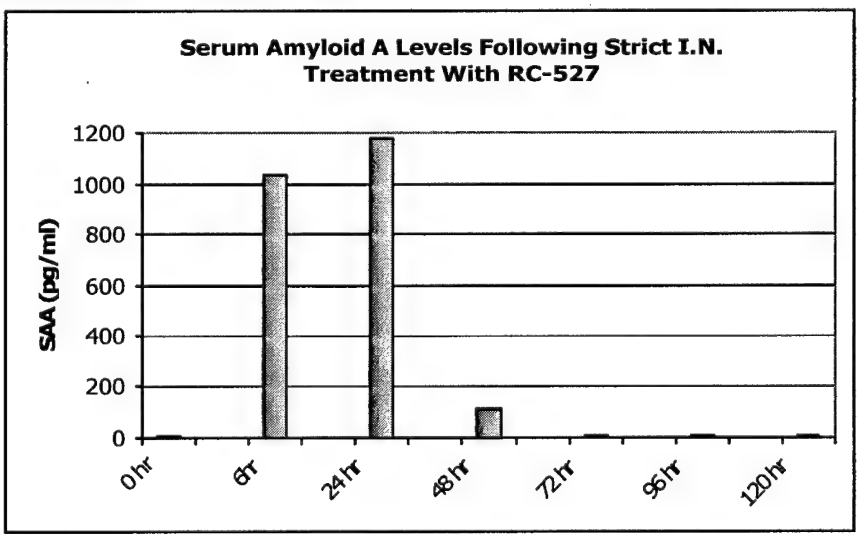

Task 2: Potency Assay Development.

Development efforts to measure the biologic potency of CRX-524 and CRX-527 have focused on measuring cytokine release from target monocyte cell lines in vitro by ELISA as a surrogate marker for receptor:ligand interactions and concomitant intracellular signaling.

The human monocytic line, MonoMac 6, was chosen as a reporter cell line from which to elicit a TLR4 mediated response. This line has inherent advantages of reproducible response to the agent without pre-stimulation or manipulation to force responsiveness.

A number of potential reporter molecules were examined for their ability to be assayed in a relatively short assay period. These included Indoleamine 2,3-Dioxygenase (IDO), inducible Nitric Oxide Synthatase (iNOS), Caspase activity via Bioluminescence Resonance Energy Transfer (BRET) and Macrophage Inhibitory Protein-1β (MIP-1β, CCL4). Based on commercial availability of reagent kits and biological response to CRX-527, MIP-1β was chosen as the reporter cytokine moving forward.

A matrix of potential test variables that could affect MIP-1β secretion post CRX-527::receptor engagement was set up and assay conditions manipulated to examine the effect of agent concentration, vehicle composition, cell culture conditions and duration of treatment.

Figure 7: Dose responsiveness for MIP-1β as measured by ELISA can be captured across a range.

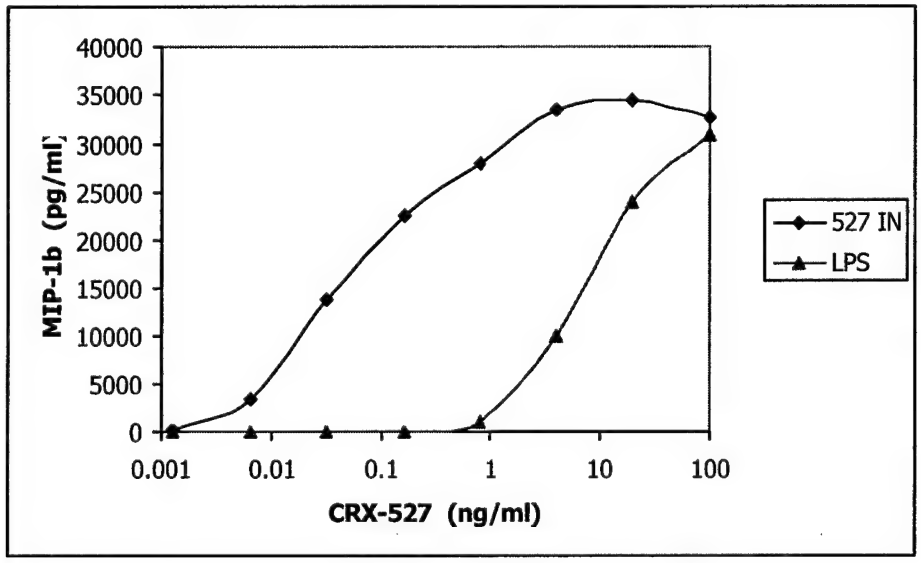

Future experiments include determining the reproducibility, durability and variability of the assay, examining lot to lot consistency of the agent, and preparing an SOP for Quality Control use.

Task 3: Cellular Biomarkers.

The identification of cell surface biomarkers up-regulated following AGP exposure may be useful to track the strength and duration of the non-specific resistance (NSR) afforded by AGPs. The specific lineage and activation markers used in these studies were chosen based on previous human PBMC in vitro studies, microarray data, literature searches, and the availability of fluorochrome conjugated antibodies. Throughout the first year of this contract, these cell-surface markers were evaluated in a series of in vitro and in vivo experiments following AGP activation. The AGPs CRX-527 and CRX-524 were chosen for these studies due to their earlier success in DARPA supported experiments. CRX-526 was also included in some experiments as an AGP/vehicle negative control. From an initial series of experiments (see December 2003 quarterly report), four candidate biomarkers were identified that warranted further investigations in vivo (CD69, CD54, CD38, MHC-I). These four biomarkers were evaluated in a series of in vivo time course and dose response experiments following intravenous (I.V.) or intranasal (I.N.) administration of CRX-524 to determine if the increased cell surface expression of these markers noted in previous experiments tracks with the duration or strength of the protective response.

I.V. administration of CRX-524 to BALB/c mice resulted in significant increases in the cell surface expression of CD69, CD54, CD38 and MHC-I (data from these studies were included in the January 2004 monthly report). While all of these markers increased in one or more cell lineages following CRX-524 treatment, the normal levels of CD54 and CD38 on the cell surface without AGP activation made tracking of changes in the cell surface density of these markers over time difficult. Due to these difficulties, CD54 and CD38 were excluded from further in vivo biomarker studies. The expression of CD69 increased significantly in all lineages tested (T-cells, B-cells, monocytes, dendritic cells, NK cells, granulocytes) in both the spleen and periphery within 24 hrs following CRX-524 treatment. As previously noted, the percentage of activated T-cells and B-cells in the spleen was significantly higher than detected in the periphery (PBMCs) whereas the percentage of activated monocytes and dendritic cells were highest in the periphery. Cell surface expression of CD69 in the spleen peaked at 24 hrs and returned to background levels by 72-96 hr following CRX-524 administration. In contrast, CD69 expression in the periphery peaked at 24 hrs but remained slightly elevated throughout the course of the experiment (120 hrs). MHC-I is expressed at 100% on all of the lineages evaluated, so measurement of the mean fluorescent intensity was used to determine changes in the cell surface density of this marker. All of the lineages tested showed significant increases in MHC-I density on the cell surface following I.V. CRX-524 treatment. Interestingly, unlike CD69, MHC-I remained at high levels throughout the course of the experiment in both the spleen and periphery (120 hr).

Large increases in the relative percentage of circulating monocytes, granulocytes and dendritic cells were also detected in mice treated I.V. with CRX-524 (data not shown). Increased numbers of mono/gran/DCs were found in both the spleen and PBMC samples with the largest increases at 24-48 hrs following AGP delivery. While concomitant reductions in T-cells, B-cells, and NK-cells were also observed, these lower numbers may simply reflect an increased number of circulating mono/gran/DC since identical numbers of live cells were acquired with the flow cytometer.

The lead candidate biomarkers identified from the I.V. CRX-524 time course experiments (CD69 and H-2K^d (MHC-I)) were further evaluated in a time course experiment following the intranasal/intrapulmonary administration of CRX-524. For these experiments, BALB/c mice were administered 20 ug of CRX524-AF in a total volume of 20 ul (10 ul per nare) while under

anesthesia. Spleens and PBMC were harvested from five mice at 24, 48, 72, 96, 144 and 196 hrs following AGP administration and immediately stained for lineage markers and cell surface CD69 or H-2K^d expression

Table 4: CRX-524 Time Course: Cell surface expression of CD69 and MHC-I in the indicated cell lineages following intranasal/intrapulmonary CRX-524 treatment.

PBMC	0 hr	24 hr	48 hr	72 hr	96 hr	144 hr	192 hr
T-cells (CD3c+)*		*1.0*	*0.9*	*0.9*	*0.9*	*0.9*	*0.9*
CD69+**	1.0	1.1	1.2	0.6	1.3	1.8	1.5
H-2K^d+ MFI***	104	95	97	107	115	105	100
Mono/Macs (CD11b+)		*1.9*	*2.1*	*3.4*	*4.0*	*2.9*	*1.7*
CD69+	5.0	5.4	8.4	16.3	13.5	4.5	6.0
H-2K^d + MFI	207	213	279	358	378	379	261
B-cells (CD19+)		*0.9*	*0.7*	*0.8*	*0.9*	*0.9*	*0.8*
CD69+	0.3	0.4	0.5	1.1	1.2	1.7	0.7
H-2K^d + MFI	145	131	132	181	204	180	149
NK-Cells (CD49b+)		*1.3*	*1.2*	*0.8*	*1.1*	*0.9*	*0.8*
CD69+	8.6	7.5	12.4	13.4	22.1	18.4	12.4
H-2K^d + MFI	126	114	121	151	169	149	127
CD3+ CD69+	15.2	17.4	16.4	19.9	26.7	30.0	18.1
CD3+ H-2K^d + MFI	153	137	144	201	210	202	162
Granulocyte (Ly-6G+)		*1.2*	*3.1*	*3.0*	*1.5*	*1.1*	*1.0*
CD69+	6.6	4.9	4.7	6.0	9.0	6.0	5.3
H-2K^d + MFI	83	69	67	120	161	124	92
Dendritic Cells (CD11c+)		*0.9*	*1.2*	*1.7*	*2.2*	*1.8*	*1.0*
CD69+	6.5	11.3	12.9	16.4	10.9	11.3	19.0
H-2K^d + MFI	176	194	237	321	294	246	195

* Fold increase in lineage cell number relative to the no activation (0 hr) control following I.N. RC524 administration. This number is based on the collection of 100,000 live cells by flow cytometry and therefore represents a relative number of cells in the spleen or periphery.

** Percent CD69+ cells in the indicated cell lineage.

*** Values for MHC-I (H-2K^d) cell surface expression are shown as mean fluorescent intensity (MFI) because H-2K^d is expressed on 100% of cells in the indicated lineage.

I.N. administration of CRX-524 to BALB/c mice resulted in a significant increase in the cell surface expression of CD69 and MHC-I on multiple cell lineages (Tables 4 and 5). CD69 increased on the cell surface of monocytes, dendritic cells, NK cells, and granulocytes in both the spleen and periphery of mice treated with CRX-524. Peak levels of CD69 expression were detected at 3-4 days and returned to background levels by 6-8 days following CRX-524 administration. This finding is significant because the increased expression of CD69 on these lineages correlates with the window-of-protection from pathogen challenge afforded to mice following I.N. AGP administration (Table 4 and Figure 8). Similar to previous I.V. experiments, the largest increases in CD69 expression were detected in the periphery when compared to increased cell surface expression on cells from the spleen. Unlike the previous I.V. delivery experiments, no significant T-cell or B-cell CD69 activation was detected in the spleen or periphery following I.N. CRX-524 administration. This may prove beneficial in a clinical setting by reducing the potential for autoimmune induction

resulting from polyclonal T- and B-cell activation. MHC-I (H-2K^d) is expressed at 100% on all of the lineages evaluated, so measurement of the mean fluorescent intensity was used to determine changes in the cell surface density of this marker. All of the lineages tested showed increases in MHC-I density on the cell surface 2-3 days following I.N. CRX-524 treatment with peak responses at 4-6 days and returned to baseline levels by 8 days following treatment. Similar to the results obtained in earlier serum cytokine experiments, I.N. administration of CRX-524 delays the onset and duration of systemic inflammatory responses relative to I.V. administration. In the case of serum cytokines, the peak response is delayed by 6-12 hrs (2 hrs for I.V. and 8 hrs for I.N.) whereas the peak cell surface expression of CD69 and MHC-I is delayed by 24-48 hrs (24 hr for I.V. and 48-72 hr for I.N.). As discussed earlier, the timing of these inflammatory responses following I.N. delivery correlates with the window-of-protection to pathogen challenge afforded by CRX-524 following I.N. delivery.

Table 5: CRX-524 Time Course: Cell surface expression of CD69 and MHC-I in the indicated cell lineages following intranasal/intrapulmonary CRX-524 treatment.

Spleen	0 hr	24 hr	48 hr	72 hr	96 hr	144 hr	192 hr
T-cells (CD3c+)*		*1.1*	*1.1*	*0.9*	*0.8*	*0.9*	*1.0*
CD69+**	10.6	11.8	10.7	13.2	13.8	12.4	10.5
H-2K^d + MFI***	93	87	89	103	107	99	96
Mono/Macs (CD11b+)		*1.0*	*1.1*	*1.8*	*1.6*	*1.2*	*1.0*
CD69+	44.3	45.1	50.8	48.0	29.1	28.2	27.6
H-2K^d + MFI	261	225	303	387	367	294	270
B-cells (CD19+)		*0.9*	*0.9*	*1.1*	*1.0*	*1.0*	*0.9*
CD69+	2.8	3.2	2.7	3.0	2.7	2.7	2.5
H-2Kd+ MFI	147	136	144	184	204	177	153
NK-Cells (CD49b+)		*0.8*	*0.8*	*0.6*	*1.1*	*1.1*	*0.9*
CD69+	26.1	27.1	34.2	39.6	43.9	37.3	32.0
H-2K^d + MFI	135	132	150	190	189	162	145
CD3+ CD69+	69.6	73.8	73.3	81.9	73.3	68.8	61.8
CD3+ H-2K^d + MFI	230	234	228	345	273	253	215
Granulocyte (Ly-6G+)		*1.0*	*1.9*	*2.1*	*1.7*	*1.4*	*1.1*
CD69+	17.1	24.1	27.8	23.6	21.1	15.0	19.6
H-2K^d + MFI	137	127	104	159	177	132	133
Dendritic Cells (CD11c+)		*1.0*	*1.2*	*1.6*	*1.6*	*1.2*	*0.9*
CD69+	34.6	40.4	46.5	43.0	33.1	29.6	33.7
H-2K^d + MFI	180	176	187	282	266	216	198

* Fold increase in lineage cell number relative to the no activation (0 hr) control following I.N. RC524 administration. This number is based on the collection of 100,000 live cells by flow cytometry and therefore represents a relative number of cells in the spleen or periphery.

** Percent CD69+ cells in the indicated cell lineage.

*** Values for MHC-I (H-2K^d) cell surface expression are shown as mean fluorescent intensity (MFI) because H-2K^d is expressed on 100% of cells in the indicated lineage.

Large increases in the relative percentage of circulating monocytes, granulocytes and dendritic cells were also detected in mice treated I.N. with CRX-524 (fold increases are shown in italics in Table 4, Table 5, and Figure 8). Increased numbers of circulating mono/gran/DCs were

detected within 24-48 hrs following CRX-524 treatment. The numbers of circulating monocytes and DCs peaked at 4 days following AGP treatment and returned to normal levels by day 8. The increases in circulating granulocytes reached maximal levels at 48 hrs and returned to baseline levels by 6-8 days following treatment. While concomitant reductions in T-cells, B-cells, and NK-cells were also observed, these lower numbers are most likely the result of increased numbers of circulating mono/gran/DC since identical numbers of total live cells were acquired for each sample with the flow cytometer. The close correlation between the window of protective efficacy and increases in circulating mono/gran/DCs may prove valuable in monitoring future upcoming clinical trials since confirmation of adequate patient dosing and correlative window-of-protection data may only require differential cell counts from nasal washes (local responses) and/or PBMCs (systemic responses) (Figure 8).

Figure 8: Fold change in lineage specific cell number following I.N. CRX-524

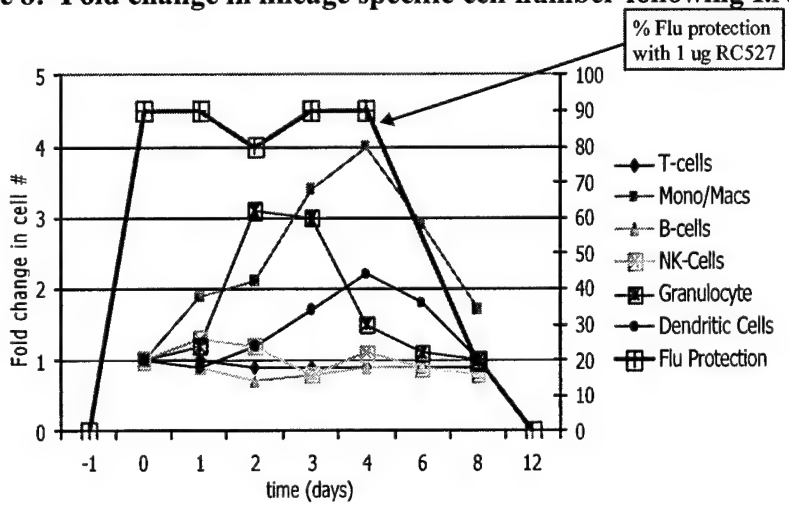

Using the data from time-course experiments shown above we selected a single time point to evaluate the intranasal administration of CRX524 at various doses. For these experiments, BALB/c mice were administered increasing doses of CRX-524 (0.008 ug to 20 ug) in a total volume of 20 ul (10 ul per nare) while under anesthesia. Spleens and PBMC were harvested from five mice at 96 hrs following CRX-524 administration and immediately stained for lineage markers and cell surface CD69 or H-2K^d expression.

I.N. administration of CRX-524 to BALB/c mice resulted in a dose-responsive increase in the cell surface expression of CD69 and MHC-I on multiple cell lineages (Tables 6, 7 and Figure 9). Increases in cell surface CD69 were detected on monocytes, dendritic cells, and granulocytes in the periphery of mice treated with 20 ug CRX-524. No significant increases in cell surface CD69 were observed at lower CRX-524 doses. MHC-I (H-2K^d) is expressed at 100% on all of the lineages evaluated, so measurement of the mean fluorescent intensity was used to determine changes in the cell surface density of this marker. All of the lineages tested showed increases in MHC-I density on the cell surface at 96 hrs following I.N. CRX-524 treatment. The largest increases in MHC-I were observed on monocytes and dendritic cells in the periphery of mice (PBMCs) with measurable increases down to a 1 ug dose of CRX-524 (Figure 9).

Increases in the relative percentage of circulating monocytes, granulocytes and dendritic cells previously reported in mice treated with CRX-524 were not as robust in this experiment when compared to earlier experiments. Increased numbers of circulating mono/gran/DCs were detected at

96 hrs following I.N. administration of 20 ug CRX-524; however, no significant increases were observed at lower doses of CRX-524 (Tables 6 and 7).

Table 6: CRX-524 Dose Response: Cell surface expression of CD69 and MHC-I in the indicated cell lineages following intranasal/intrapulmonary CRX-524 treatment.

(PBMC)							
RC524 dose (ug)	**0**	**0.008**	**0.04**	**0.2**	**1.0**	**5**	**20**
T-cells (CD3c+)*		*1.0*	*1.0*	*1.0*	*0.9*	*1.0*	*0.9*
CD69+**	1.5	1.0	1.5	1.6	1.4	1.0	1.2
H-2Kd+ MFI***	108	104	106	107	106	105	114
Mono/Macs (CD11b+)		*0.9*	*1.0*	*1.0*	*0.7*	*1.2*	*2.2*
CD69+	4.7	5.1	5.8	3.9	4.4	7.0	10.6
H-2Kd+ MFI	218	199	216	206	231	285	343
B-cells (CD19+)		*1.1*	*1.1*	*1.1*	*1.3*	*1.1*	*1.1*
CD69+	0.6	0.6	0.8	0.7	0.7	0.9	1.0
H-2Kd+ MFI	148	141	139	140	148	170	192
NK-Cells (CD49b+)		*1.1*	*1.2*	*1.2*	*1.1*	*1.1*	*1.2*
CD69+	6.7	5.1	5.8	6.5	5.7	7.6	9.7
H-2Kd+ MFI	125	121	120	122	123	133	148
CD3+ CD69+	12.4	8.7	10.5	10.1	9.9	10.3	10.1
CD3+ H-2Kd+ MFI	135	128	130	132	133	140	149
Granulocyte (Ly-6G+)		*0.9*	*0.8*	*0.9*	*0.6*	*0.8*	*1.1*
CD69+	6.4	6.4	10.4	10	7.2	9.0	9.1
H-2Kd+ MFI	97	104	100	97	105	113	159
Dendritic Cells (CD11c+)		*0.9*	*1.0*	*1.1*	*0.8*	*1.2*	*2.0*
CD69+	4.8	6	8.2	5.7	7.2	7.2	8.3
H-2Kd+ MFI	159	163	153	161	172	200	270

* Fold increase in lineage cell number at 96 hr relative to the no activation (0 hr) control. This number is based on the collection of 100,000 live cells by flow cytometry and therefore represents a relative number of cells in the spleen or periphery.

** Percent CD69+ cells in the indicated cell lineage at 96 hrs.

*** Values for MHC-I (H-$2K^d$) cell surface expression are shown as mean fluorescent intensity (MFI) because H-$2K^d$ is expressed on 100% of cells in the indicated lineage.

Table 7: CRX-524 Dose Response: Cell surface expression of CD69 and MHC-I in the indicated cell lineages following intranasal/intrapulmonary CRX-524 treatment.

spleen							
RC524 dose (ug)	**0**	**0.008**	**0.04**	**0.2**	**1.0**	**5**	**20**
T-cells (CD3c+)*		*1.1*	*0.9*	*1.0*	*1.0*	*1.0*	*0.9*
CD69+**	8.5	8.3	9.4	8.9	8.9	9.5	10.5
H-2Kd+ MFI***	98	94	94	95	93	96	104
Mono/Macs (CD11b+)		*0.9*	*0.9*	*1.0*	*0.8*	*1.1*	*1.5*
CD69+	27.7	26.4	26.7	21.6	27.5	19.7	14.2
H-2Kd+ MFI	267	262	237	231	252	277	327
B-cells (CD19+)		*1.0*	*1.0*	*1.0*	*1.1*	*0.9*	*1.0*
CD69+	2.1	2.2	2.3	1.8	1.9	2.3	2.5
H-2Kd+ MFI	153	147	142	143	146	167	197
NK-Cells (CD49b+)		*0.9*	*1.0*	*1.0*	*1.1*	*0.9*	*1.0*
CD69+	22.5	20.9	22.9	22.3	22	17.1	38.7
H-2Kd+ MFI	134	135	132	132	134	147	176
CD3+ CD69+	64	61	63	58	58	64	69
CD3+ H-2Kd+ MFI	251	230	234	229	227	224	258
Granulocyte (Ly-6G+)		*1.0*	*1.0*	*1.1*	*1.2*	*1.2*	*1.6*
CD69+	16.4	24.0	22.1	19.1	23.7	18.3	20.4
H-2Kd+ MFI	129	168	140	144	135	141	163
Dendritic Cells (CD11c+)		*0.9*	*0.9*	*0.9*	*1.0*	*1.0*	*1.3*
CD69+	36.3	35.3	36.0	35.1	37.5	30.3	32.3
H-2Kd+ MFI	192	194	181	180	181	198	233

* Fold increase in lineage cell number at 96 hr relative to the no activation (0 hr) control. This number is based on the collection of 100,000 live cells by flow cytometry and therefore represents a relative number of cells in the spleen or periphery.

** Percent CD69+ cells in the indicated cell lineage at 96 hrs.

*** Values for MHC-I (H-2K^d) cell surface expression are shown as mean fluorescent intensity (MFI) because H-2K^d is expressed on 100% of cells in the indicated lineage.

Figure 9: MHC-I MFI in mouse PBMCs 96 hrs following intranasal/intrapulmonary administration of CRX-524.

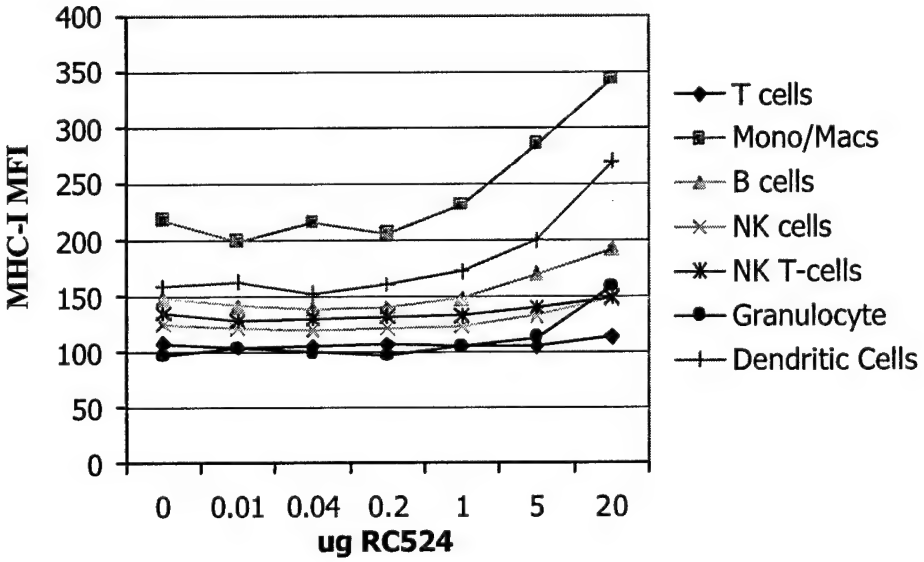

Task 4: Toxicology

With respect to the non-clinical toxicology activities, the following progress was made in the first year of this contract:

1. Decision was made to conduct two multiple-dose toxicity studies of CRX-527: one in rodents (rats) and one in dogs. The rodent study is planned for January 05 and the dog study for March 05.
2. Extensive prospecting of CROs having experience with intra-nasal delivery was conducted and two CROs were retained.
3. Exploratory toxicology studies have been initiated in house to determine the most suitable method for administering divided doses of CRX-527 repeatedly in rodents.
4. A draft toxicology protocol was developed for the multiple-dose toxicity studies of CRX-527. The rodent (rat) toxicology study outline is shown below.

4.1 Multiple-Dose GLP Toxicology Studies of CRX-527 after Intranasal Administration in Rats

A multiple-dose toxicity study of CRX-527 after intranasal administration to rats is proposed. The study is designed to evaluate the safety and potential toxicity of CRX-527 after multiple doses. The CRX-527 test article for the toxicity study will be produced using the same manufacturing process as the product for the proposed Phase 1 clinical trial.

The toxicity study will be conducted in accordance with FDA Good Laboratory Practice regulations (21 CFR 58).

Study Title. A 13-Week Multiple-Dose Toxicity Study of CRX-527 via Intranasal Administration to Rats with a 4-Week Recovery.

Performing laboratory. CIT, BP 563, 27005 Evreux, France

Purpose. The objective of the study is to evaluate the safety and potential toxicity of CRX-527 after repeated intranasal administration to rats.

Test Article. CRX-527-IN: 1000 µg/mL CRX-527 and 2% glycerol in Water for Injection, USP. Serial dilutions (10x and 100x) thereof in 2% glycerol in Water for Injection, USP.

Control Article. Vehicle-IN: 2% glycerol in Water for Injection, USP.

Test Animals. Sprague Dawley rats (200-300g)

Study Design. The study will be conducted in 136 rats for a duration of up to 116 days. There will be 4 treatment groups; vehicle control, low, mid and high dose CRX-527. Each group will be comprised of 34 animals: 17 males and 17 females per group. Test and control article will be repeatedly administered twice a week for 13 weeks for a total of 26 doses.

A subset of animals (12/sex/group) will be euthanized on study day 89, 1 day after the last treatment and the remaining animals (5/sex/group) after a 28 day recovery period (study day 116).

Table 8: Proposed Toxicology Study Design

Group	Treatment	Animal #	Dose		Dose Volume (µL)	*Day of Dosing*	Sacrifice (n/sex)	
			µg/rat	µg/ cm^2			Terminal Day 89	Recovery Day 116
1	Vehicle-IN	17M/17F	-	-	175***	0,4,7,11,14,18 ,21,25,28,32,3 5,39,42,46,49, 53,56,60,63,6 7,70,74,77,81, 84, 88	12M/12F	5M/5F
2	Low	17M/17F	1.75	0.125	175*	Ibid.	12M/12F	5M/5F
3	Mid	17M/17F	17.5	1.25	175**	Ibid.	12M/12F	5M/5F
4	High	17M/17F	175	12.5	175***	Ibid.	12M/12F	5M/5F

*test article diluted 100x
**test article diluted 10x
***undiluted

Animal will be conscious during treatment in order to minimize aspiration of the test article into the lungs. Dosing will be based on nasal surface area (µg/cm^2). The nasal surface area of rat is 14cm^2 and the human is 160cm^2 (S. Gizurarson. 1990. Acta Pharm. Nord. 2(2):105-22). Dose levels in the toxicology study will be a 10x multiple of the human dose levels in the Phase 1 clinical trial (2, 20 and 200µg per subject or 0.0125, 0.125, 1.25 µg/cm^2 of the nasal cavity surface area).

Test and Control Article Administration. Test and Control article will be administered twice a week at 4 and 3 day intervals. Doses will be administered on Study Days 4, 7, 11, 14, 18, 21, 25, 28, 32, 35, 39, 42, 46, 49, 53, 56, 60, 63,67, 70, 74, 77, 81, 84, 88 to all animals. Test and

control articles will be administered as divided or fractionated doses. There will be 5 dosing intervals per day. Both nares will be treated at each dosing interval. A volume of 35 µL will be applied to the nasal cavity (right plus left nares) at each dosing interval. The total volume administered to the nasal cavity per day will be 175 µL.

Study End-Points. Animals will be observed for a period of up to 28 days following the last treatment. Necropsy will be performed at 2 intervals on study days 89 and 116, one day and 28 days post-last dose, respectively.

The following parameters will be assessed in the study:

Morbidity and mortality (daily)
Clinical observations (d0 and then twice a week until then end of the study)
Body weight (d0 and then weekly until the end of the study)
Food consumption (daily)
Temperature (4h after each dose administration)
Hematology (d89, d116)
Clinical chemistry (d89, d116)
Gross pathology, including organs weights of selected tissue (d89, d116)
Histopathology (d89, d116)

We are particularly interested in assessing potential toxicity in the nasal cavity and in the central nervous system (CNS).

Task 4: AGP Scale-up/Chemistry. Development of cost-effective and scalable synthesis for the preparation of clinical supplies of CRX-527.

The main process development goals for the first year of this project centered on (1) developing an efficient and scalable process for the production of CRX-524 and/or -527 that would be suitable for preparation of material for toxicological evaluation, pre-formulation and other studies, (2) identifying a suitable CMO for the manufacture of clinical material, (3) technology transfer of the small-scale process to the CMO for further development/scale-up and initiation of qualifying runs as a precursor to cGMP, and (4) preparing the CMC section for 527 manufacture for pre-IND submission. These objectives have been either completed or are on track to meet projected timelines. However, the greater aqueous solubility and potency of 527 as compared with 524 recently led to the selection of 527 as the lead candidate for further development/scale-up and clinical evaluation. A smooth transition from chemical process development of 524 to the development of 527 was made possible by employing a flexible synthesis strategy which was convergent with respect to the AGP backbone and the chiral fatty acid units. A brief discussion of the progress toward achieving the above objectives is summarized below.

The syntheses of a concept lot and two toxicology batches of high purity (>95% by HPLC) of CRX-524 were completed in 12 steps from commercially available D-glucosamine hydrochloride (**1**) using carbobenzyloxycarbonyl (Cbz) protection of the amino groups. Other N-protecting schemes (Aoc, Phth, Troc) were also investigated but the use of the Cbz group lead to the most efficient preparation of the starting material **3**, which could isolated without aqueous work-up and purified readily by crystallization on over a 50-gm scale. The synthesis of the requisite fatty acid starting material, (R)-3-decanoyloxytetradecanoic acid (**4**), was also successfully scaled (to 100-gm level) using a 5-step process involving enantioselective hydrogenation in the key step. Efficient N,N,O-triacylation of pivotal intermediate **3** (>85% yield per acylation) with fatty acid **4** and further

elaboration lead to CRX-524 free acid in high chemical yield and purity after chromatographic purification on silica gel. This new synthetic approach to CRX-524 overcomes many of the deficiencies of the discovery route, such as multiple synthetic and chromatographic steps. The goal of reducing the number of chromatographic steps was achieved primarily by using trituration, reslurrying, and crystallization techniques to purify intermediates, which in turn was made possible by using the aromatic Cbz group for nitrogen protection and installing the lipophilic fatty acid moieties near the end of the synthesis.

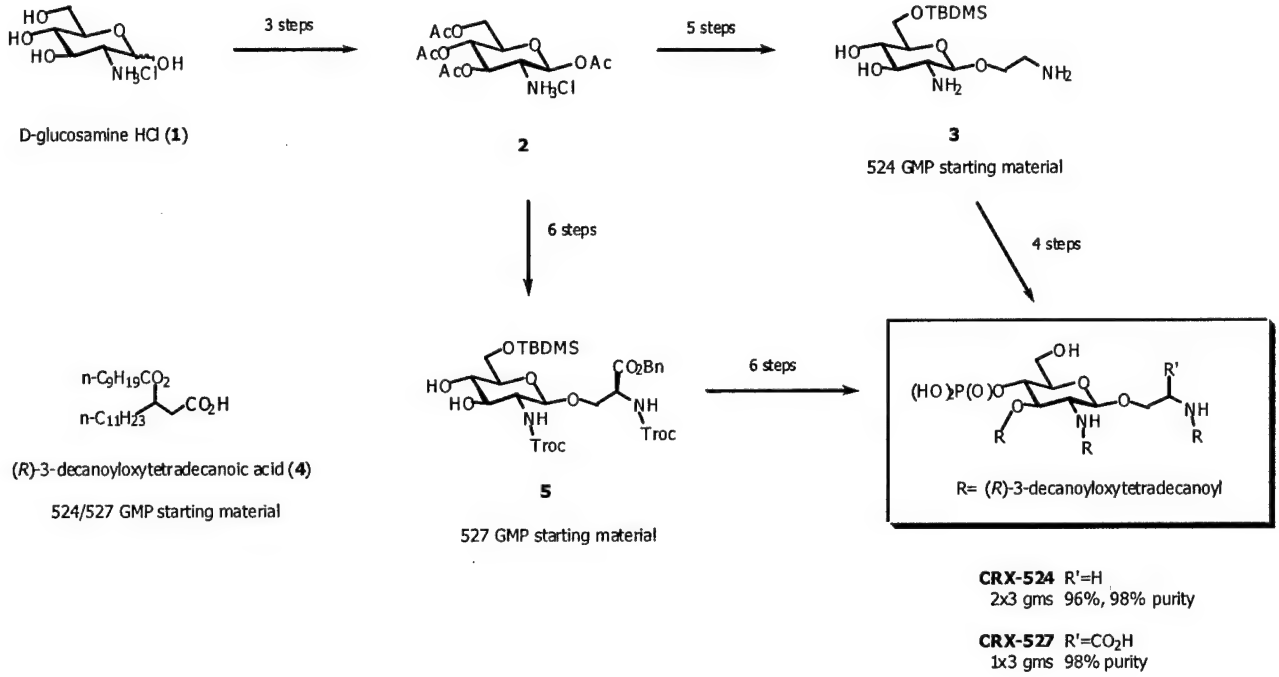

Subsequent application of this general strategy to CRX-527 was achieved with Troc protection of the amino groups and incorporating the fatty acid groups in two acylation steps instead of one using compound **5** as the 527 starting material. Elaboration of compound **5** to CRX-527 free acid in four steps has been carried out on up to a 3-gm scale. The in-house synthesis of a second 3-gm lot of CRX-527 for toxicology and other studies is nearing completion.

Earlier this year site visits were conducted at three CMOs and Tetrionics, Inc. of Madison, WI was chosen for the production of clinical supplies after completion of a QA audit. Initial scale-up/optimization work at Tetrionics focused on the synthesis of known compounds **2** and **4**, which are common to both the CRX-524 and 527 syntheses. Following the selection of 527 as the lead NSR candidate, Tetrionics carried out the concept synthesis of CRX-527 following the protocols provided by Corixa with minor modifications. The purification of 527 free acid by crystallization is currently being evaluated by the CMO in order to circumvent the chromatographic purification used by Corixa, which can lead to small amounts of de-acylation products.

The CMC section detailing the manufacture of CRX-527 via the Troc route outlined above and proposed purity specifications has been prepared for inclusion in the 527 pre-IND document.

Chemical process development plans for Year 2 will focus on (1) completing a second 3-gm lot of CRX-527 in house for use in toxicological studies, (2) completing qualifying GMP (20 g) batches of CRX-527 at CMO, (3) performing additional in-house scale-up/optimization studies on

early intermediates in the 527 synthetic process in order to facilitate preparation of Phase 1 clinical material at the CMO and later stage clinical materials, (4) preparing process-related impurities and degradates in bulk 527 for confirmation/quantitation of impurity levels and to establish routine quality profiles, and (5) synthesizing suitable derivatives of 527 for ADME(Tox) studies (e.g. precursors for possible tritium, 14C, or 32P radiolabelling).

Task 4: AGP Process Development/Formulations.

Formulation Development Activities for CRX-524

In the last quarter of 2003, additional aqueous formulations containing CRX-524 were placed on stability. Ongoing stability studies, both in vials and in nasal spray devices, were maintained. Several concentrations were formulated, reflecting potential doses for human studies. All assay testing was performed by the Analytical Development Group.

I. Stability of CRX 524-AF in vials and Syringes

At a concentration of about 1000 µg/mL, CRX 524-AF appeared stable in both vials and nasal spray syringes for up to 18 months at refrigerated temperatures. Assay results for three of the oldest lots are illustrated below **(Figure 10).**

Figure 10: CRX-524 Stability in vials and syringes

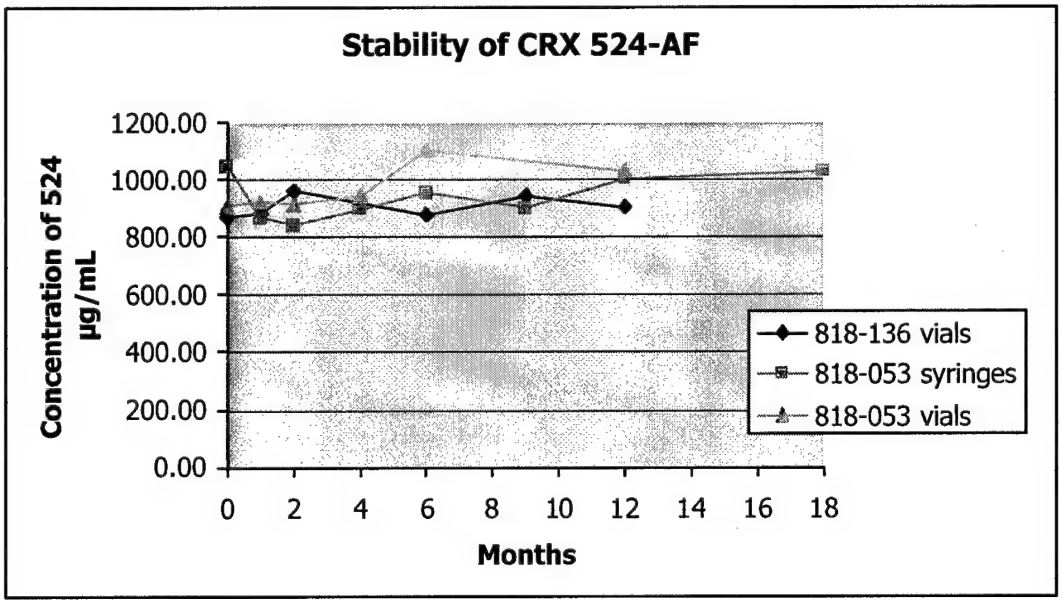

II. Nasal Spray Formulation Development for CRX-524

Development of new formulations of CRX-524 with an emphasis towards nasal spray applications was initiated. Excipients utilized in these formulation studies included amines, buffers, polymers, surfactants, and alcohols. These solutions were evaluated for ease of manufacturability, pH, isotonicity, and other criteria essential for nasal spray formulations. Any potential candidates were placed on accelerated and real time stability, and were periodically tested for determination of continued potency and suitability for this application. Accelerated data generated for solutions of varying pH is summarized in the chart below (Figure 11).

Figure 11: CRX-524 formulation studies

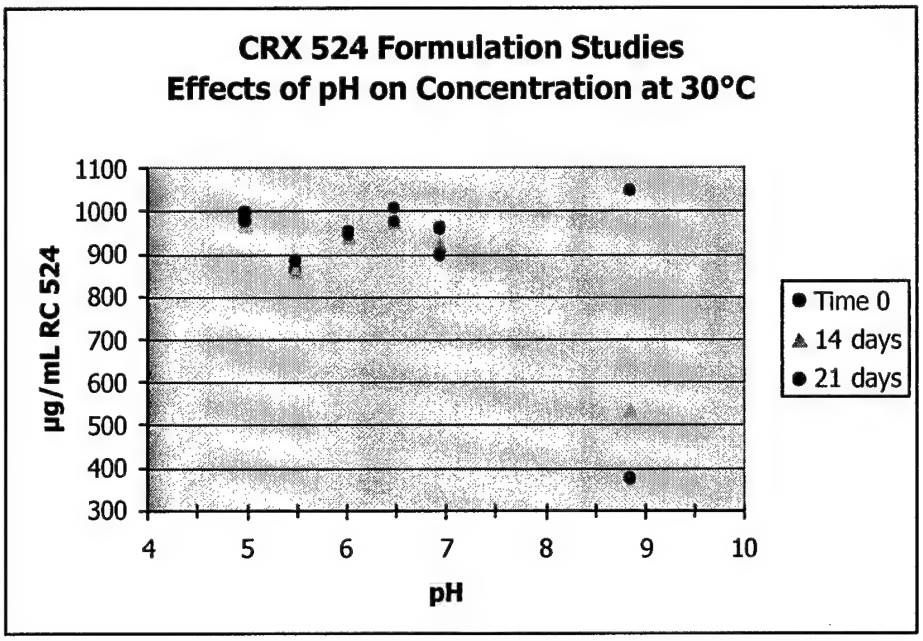

III. API Stability of CRX-524

The free acid and TEA salt of 524 was placed on stability to further define degradation pathways and illustrate optimal storage conditions. Results to date are tabulated below.

Table 9: Stability of CRX-524 TEA salt (ug/ml CRX-524)

	4 months		6 months		9 months	
Temp.	Free acid	Salt	Free acid	Salt	Free acid	Salt
-80°C	594.45	528.62	NT	NT	NT	NT
-20°C	602.78	515.38	534.43	453.09	561.62	470.17
2-8°C	605.65	522.95	527.80	464.50	556.50	480.01

IV. Formulation Preparation and Testing

Formulations of 524-AF and 527-AF were prepared and loaded into Accuspray syringe devices for the ferret influenza study and the Cebu primate study. Unused syringes were returned from the study centers and submitted for concentration verification testing. There was no loss of the active compound in the returned syringes.

V. High Concentration Toxicology Study Formulations

In anticipation of toxicity studies, efforts focused on development of higher concentration CRX 524-AF formulations. Solutions up to 4 mg/mL 524 were prepared and placed on stability. However, high concentrations of the AF formulation proved to be unstable, and the studies were discontinued.

Formulation Development Activities – CRX- 527-IN

I. Formulation and Stability Studies for CRX527-IN

Following the adoption of CRX 527 as the lead candidate, manufacturing instructions and other documentation were drafted in preparation for production of pre-clinical material. The CMC sections relating to formulations and stability in the Pre-IND document were completed. Several grams of the bulk AGP free acid were salted and characterization studies were outlined and initiated. This raw material was incorporated into several formulations and submitted to the Analytical Development Group for testing. Several lots were placed on stability, with additional stability lots planned. Ongoing stability studies were maintained and all data is being examined in an effort to establish preliminary release specifications for the final product (Figure 12). In addition, a higher concentration lot (5000 µg/mL) was successfully formulated for pilot toxicity and bioassay studies.

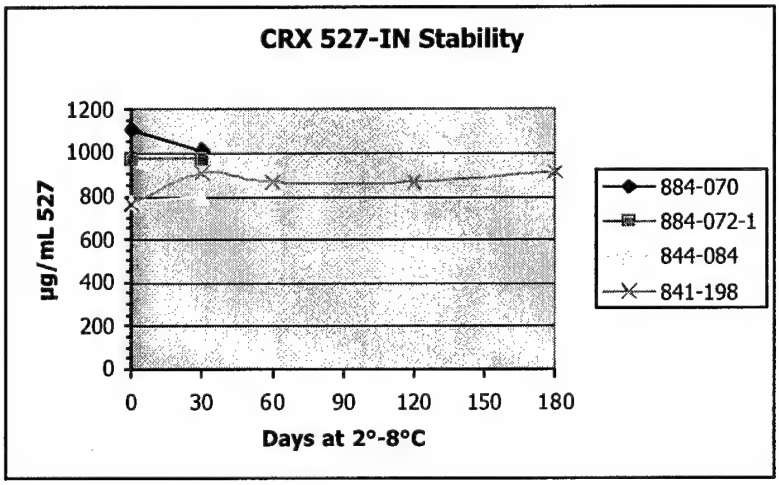

Figure 12: Stability of CRX527-IN

Buffered CRX 527-IN formulations were monitored for changes in pH over time (Figure 13). This information will help in optimizing an ideal nasal spray formulation. At accelerated storage conditions, the assay profile is shown below. Additional storage conditions are being monitored.

Figure 13: CRX527-IN pH Stability

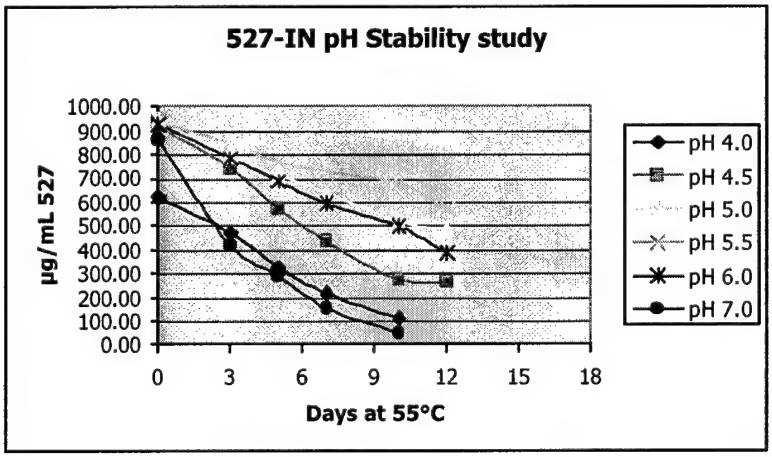

II. Evaluation of nasal spray delivery device

Several nasal spray delivery devices were examined and evaluated. Criteria included ease of manual filling and assembly, droplet size characteristics with product, cost per unit, and packaging configuration. The consensus of the project team was to move forward with the Pfeiffer Unit Dose device.

III. Formulation Development Activities with CRX-527 – Looking Ahead

Efforts will continue to focus on development of a nasal spray formulation that is optimal for the delivery device, stable, and efficacious. Optimization of the manufacturing process will be completed. Characterization of the bulk drug substance will continue in an effort to establish release specifications and solubility information. Additional lots of formulations, prepared from different raw material batches, will be placed on stability, and ongoing stability studies will be maintained. Data generated from all lots will be used to establish preliminary specification ranges for formulation release. Filter validation studies are planned, along with validation of the sterilization cycle for autoclaving device components. Spray characterization studies with the chosen formulation will be initiated, as will stability and recovery studies in the devices.

Task 4: Evaluation of new CRX-527-IN formulation and in vivo protection studies in support of Pre-IND Briefing Document.

We evaluated the protective effect of the IN formulation (2% glycerol in water) of CRX-527 in a mouse model of descending influenza infection. In these experiments, groups of mice pretreated with IN vehicle (control) or CRX-527-IN were challenged with virus while conscious by intranasal administration of a low dose of influenza in a small volume (5 uL per naris). We believe this system is a true model of descending infection for the following reasons. First, fluids administered in low volumes to conscious mice via the intranasal route should not enter the lungs, since the intact gag reflex prevents entry into the trachea of any material that gets past the nasopharynx. Consistent with this supposition is our finding that influenza is undetectable in the lungs of mice one hour after conscious intranasal challenge as determined by PCR (data not shown). We also found that influenza titers in the lungs of mice do not begin to rise above detection limits until 4-5 days after conscious intranasal challenge (data not shown), and that the increase in pulmonary viral titer correlates strongly with the kinetics of weight loss, which typically begins on day 5-6 post-challenge and is maximal by day 8-9 (see Figure 14 for kinetics of weight loss after sub-lethal influenza infection). Furthermore, because of the intact gag reflex, any influenza in the challenge bolus that gets past the nasopharynx during conscious intranasal challenge would be swallowed. Since influenza infects only respiratory epithelium in mammals (Zambon MC, *Epidemiology and Pathogenesis of Influenza*, J Antimicrob Chemo, 1999, 44, Topic B, 3-9), any virus that is swallowed would be inconsequential with regard to infection and disease. We confirmed this supposition by challenging conscious naïve mice with influenza via the gastric route using a gavage needle. These mice did not develop clinical disease (data not shown).

In an effort to mimic the intended route of administration in humans (i.e. strict intranasal), anesthetized mice were treated with CRX-527-IN in a volume (2.5 uL per naris) that has been demonstrated to remain in the nasal cavity (Visweswaraiah A, Novotny LA, Hjemdahl-Monsen EJ, Bakaletz LO, Thanavala Y., Vaccine. 2002 Aug 19;20(25-26):3209-20). Mice were anesthetized prior to CRX-527-IN administration to ensure the compound remained in contact with the nasal mucosa for an extended period of time. Progression of clinical disease was followed by measuring weight loss over time and subjectively scoring the severity of clinical disease. Disease severity was

scored on a scale from 0 to 3 (3 being the most severe) that was a compilation of observable symptoms including ruffled fur, labored breathing and hunched posture.

Strict intranasal administration of CRX-527-IN to mice one day prior to intranasal influenza challenge was found to attenuate disease in a dose-sensitive manner. Relative to untreated control mice, mice treated with CRX-527-IN experienced less severe disease, as demonstrated by extended time to appearance of symptoms, reduced peak weight loss and reduced cumulative disease scores (Figures 14 and 15). Optimal protection occurred at a dose between 1 and 10 ug.

Figure 14: Kinetics of weight loss after sub-lethal influenza infection.

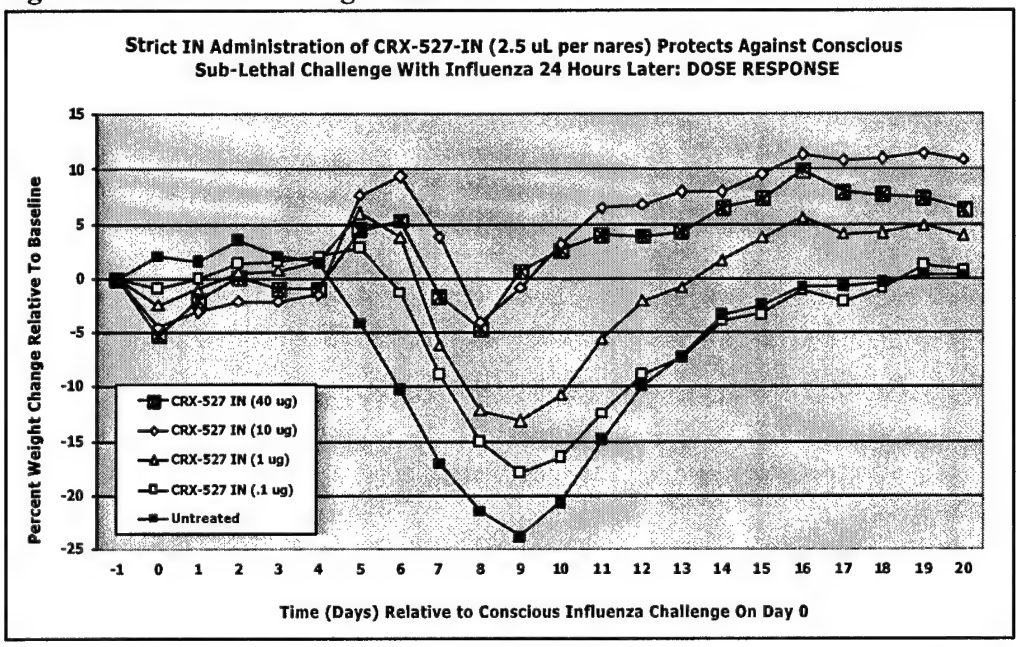

Figure 15: Strict I.N. administration of CRX-527 protects against sub-lethal influenza challenge.

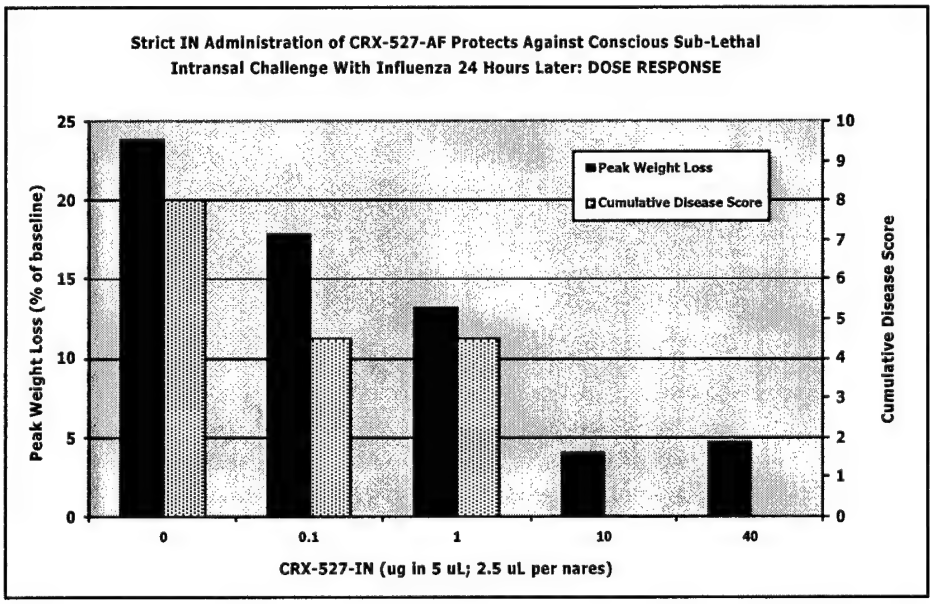

To investigate the kinetics of CRX-527-IN-mediated protection in the mouse model of descending influenza infection, the AGP (10 ug; 2.5 ug per naris) was administered to anesthetized mice at various times prior to or after conscious intranasal challenge. Again, weight change and severity of clinical disease were documented for several weeks post-challenge.

The protection induced by strict intranasal administration of CRX-527-IN was maximal one day after dosing (Figures 16 and 17). Mice in the day-1 group became sick later than the other groups, exhibited the largest reduction in peak weight loss, and demonstrated the largest reduction in cumulative disease score. Mice administered CRX-527-IN two or three days prior to influenza challenge were also protected, though to a lesser degree. Mice treated four day prior to challenge were not protected. The compound was also protective when administered the same day as or one day after the viral challenge, but afforded no protective benefit when administered 2 days after challenge. CRX-527-IN, therefore, provides prophylactic or therapeutic protection from influenza infection in mice when administered anywhere from three days prior to challenge to one day after challenge.

Figure 16: Window of protection.

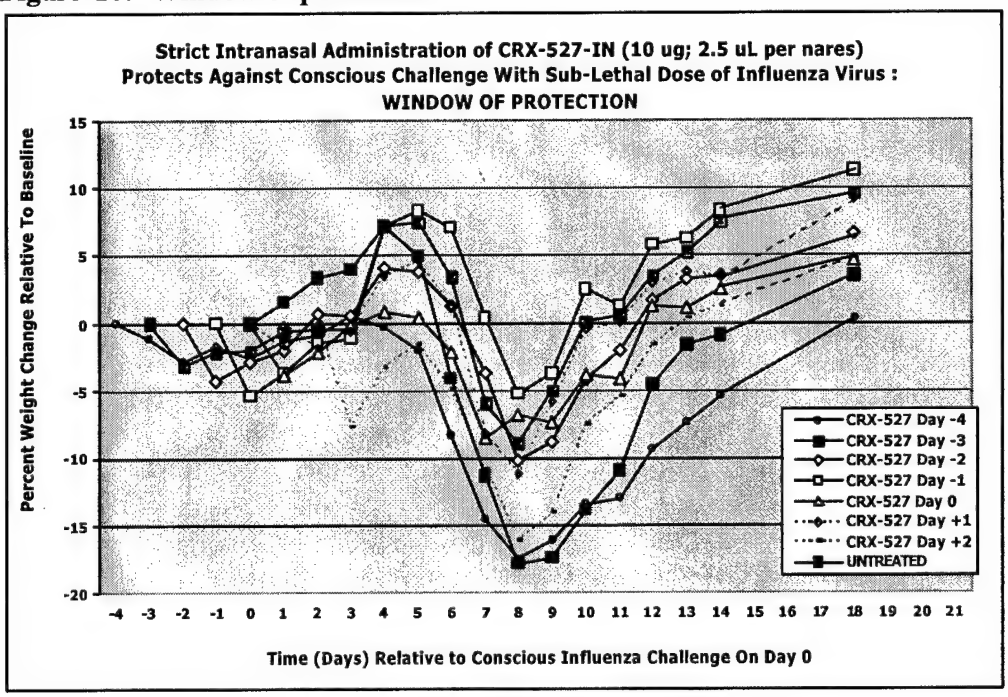

Figure 17: I.N. administration of CRX-527 protects against I.N. challenge with influenza.

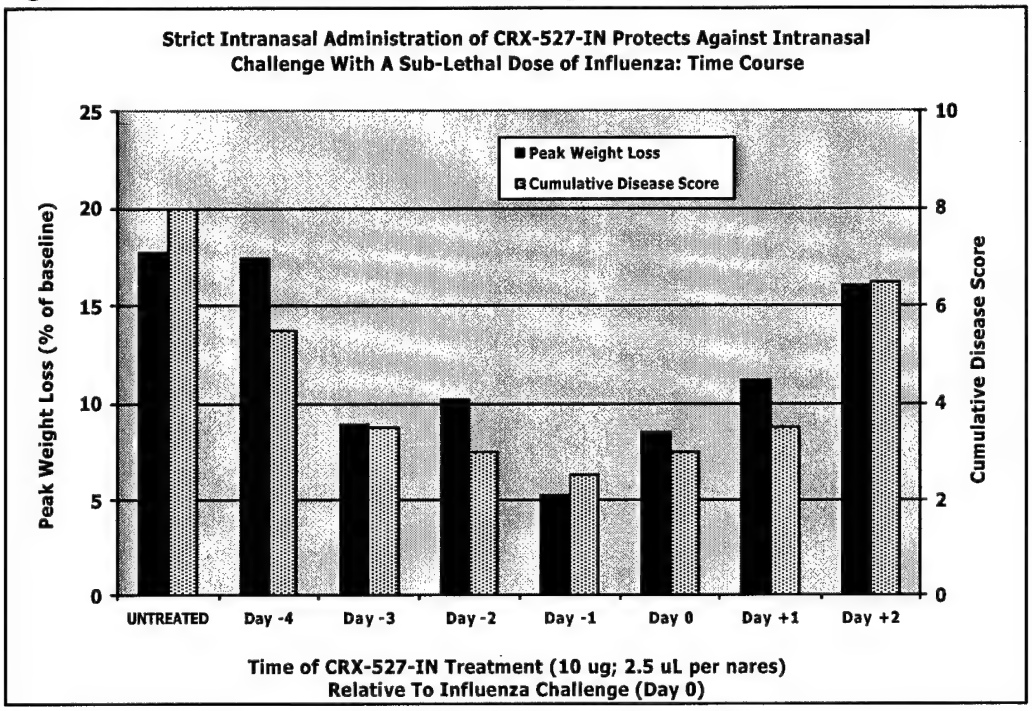

We also used the descending model of influenza infection in mice to determine whether CRX-527-IN mediated protection against challenge can be maintained for prolonged periods of time by repeated intranasal administration of the compound. Groups of mice were administered a total of five doses of CRX-527-IN (10 ug; 2.5 uL per naris at 3 or 4 day intervals), with the final dose administered one day prior to challenge. The level of protection in this group was compared to the level of protection in control mice treated one time with the same dose on the day prior to challenge (i.e. the regimen that induces the strongest protection in this system).

The results of this experiment are presented in Figure 18. The protection observed in mice treated five time with a protective dose of CRX-527 (10 ug) was as good, if not better, than the protection observed in positive control mice treated one time with the compound one day prior to infection. Mice in both the repeat dose and single dose groups lost considerably less weight than mice in the untreated control group. This experiment demonstrates that protection against influenza challenge can be maintained by repeated administration of CRX-527-IN at 3 or 4 day intervals.

Figure 18: Repeated administration of CRX-527 does not induce tolerance.

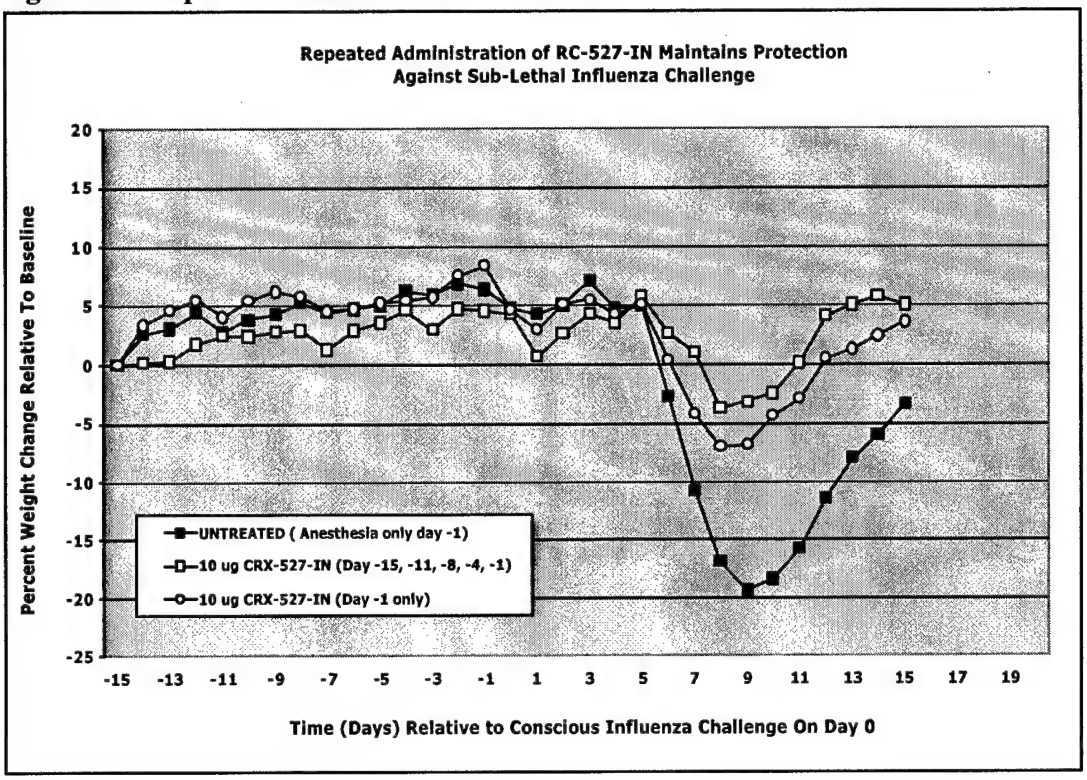

To determine whether induction of enhanced innate immunity to influenza challenge by CRX-527 interferes with the development of adaptive immunity to the virus, we evaluated the ability of mice that were protected against influenza challenge with the AGP to withstand rechallenge with lethal doses of the virus. In this experiment, the response to influenza rechallenge in mice weakly or strongly protected against primary challenge (0.1 or 40 ug of CRC-527; see Figures 14 and 15) was compared to the response in naïve mice to primary challenge.

For this experiment, mice from each group (strongly protected/recovered, weakly protected/recovered, and naïve) were split into five sub-groups (3 mice per sub-group). The sub-groups were challenged with 1:1, 1:10, 1:100, 1:1000 or 1:10,000 dilutions of influenza stock via the intranasal / intrapulmonary route (20 uL per nares with anesthesia). This method of challenge ensures delivery of virus to the lungs and has been demonstrated to result in a lethal outcome in naïve mice.

As expected, naïve mice were extremely susceptible to the influenza challenge. The sub-groups challenged with the 1:1, 1:10, 1:100 and 1:1000 dilutions of the viral stock succumbed to the disease. Though the sub-group challenged with the 1:10,000 dilution of influenza stock survived to day 14, they became quite ill, losing 15% of their baseline body weight during the peak of disease. In contrast to naïve mice, the mice from either the weakly or strongly protected groups were able to withstand rechallenge with even the 1:1 dilution of the influenza stock (Figure 19). These mice lost only several percentage points of their baseline body weight during the first few days following rechallenge, and appeared disease-free throughout the duration of the experiment (cumulative disease scores = 0 for both groups).

The results of this experiment demonstrate that CRX-527-induced enhancement of innate immunity in mice prior to influenza challenge does not interfere with the development of adaptive immunity to the virus. CRX-527-IN-protected mice became mildly ill during the course of primary infection, but did not show signs of disease when rechallenged with more than 1000 times the dose of influenza that kills naïve mice.

Figure 19: Mice protected against sub-lethal influenza challenge by prophylactic intranasal administration of CRX-527 are immune to rechallenge with lethal doses of influenza

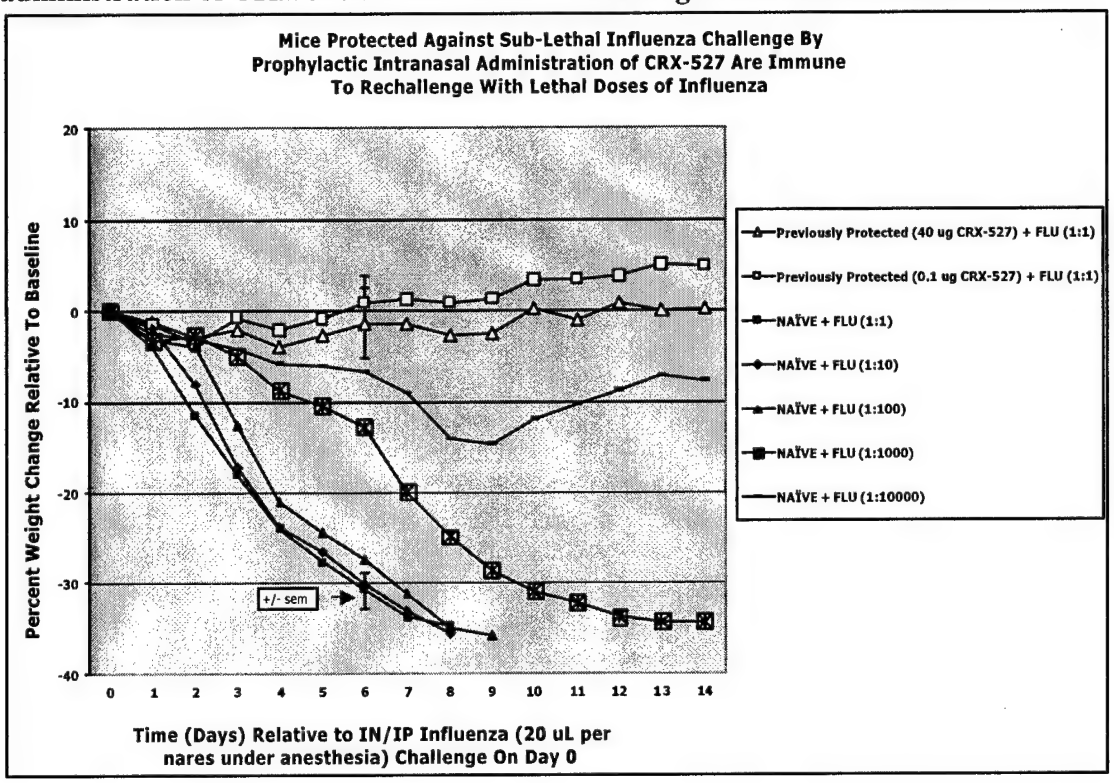

Because of safety concerns relating to the potential for inadvertent treatment with CRX-527-IN after establishment of influenza infection, we also investigated the impact of CRX-527-IN on disease outcome when administered prior to, during or after virus-induced peak weight loss. Groups of mice were treated via the strict intranasal route with 10 ug of CRX-527-IN five, nine or fourteen after challenge. An untreated/unchallenged group, as well as groups treated with CRX-527-IN one day prior to challenge or with vehicle five days post-challenge were used as controls.

Intranasal administration of CRX-527-IN prior to, during, or after influenza-induced peak weight loss did not impact disease outcome significantly (Figure 20). The weight loss curve for the mice treated with CRX-527-IN on day five was no different than the curve for mice treated with vehicle on the same day. Mice treated with the AGP on day nine post-challenge continued their recovery with no deviation in weight gain. Recovering mice treated with CRX-527-IN on day fourteen post-challenge lost a small percentage of their baseline body weight during the first day post-treatment. However, the mice recovered quickly, gaining back the lost weight during the subsequent 24 hour period. The slower recovery of mice treated with CRX-527-IN on days nine and fourteen relative to the mice treated with vehicle or the compound on day five is curious and may reflect a palliative effect of anesthesia (used during intranasal dosing on day five, nine and fourteen)

on disease outcome. Such a possibility is under investigation. Overall, these results indicate that CRX-527-IN does not significantly exacerbate illness in influenza-infected mice, even if administered at a time when disease symptoms are maximal.

Figure 20: Intranasal administration of CRX-527 after infection does not affect disease outcome.

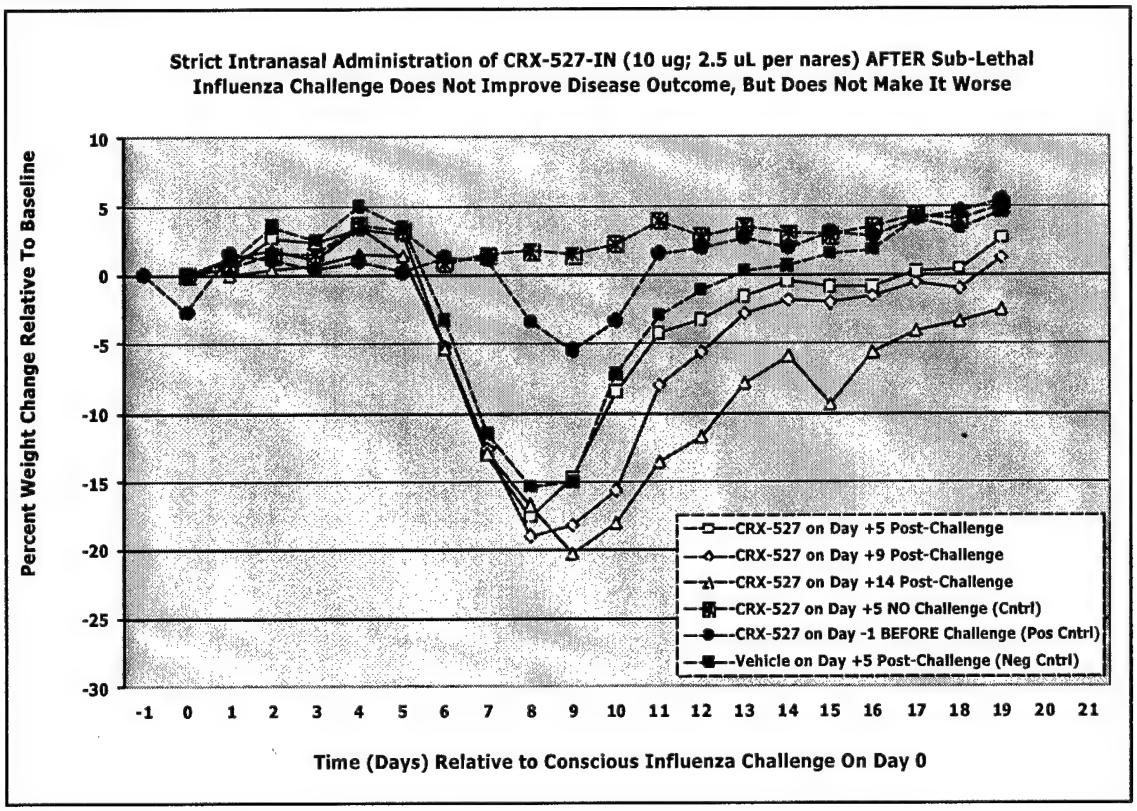

Summary of in vivo protection data. We have demonstrated that strict intranasal administration of CRX-527-IN protects mice against descending influenza infection when administered anywhere from three days prior to challenge to one day after challenge. We have also shown that protection against influenza challenge can be maintained by repeated administration of CRX-527-IN at 3 or 4 day intervals, and that the protection does not interfere with the development of adaptive immunity to the virus. Finally, our results indicate that administration of CRX-527-IN post-challenge does not significantly exacerbate illness, even if administered at a time when disease symptoms from the viral infection are maximal.

Task 4: Analytical Chemistry

Method development work was conducted on a LC method to detect free fatty acids in Bulk TEA salted RC-524 and RC-527. The method was deemed adequate to determine total free fatty acid content of either RC-524 or RC-527.

Additional work was performed on the method to improve the resolution between the decanoic acid (C10) and 3-hydroxy myristic acid (C14OH) peaks so that the contribution of individual fatty acids could be determined. Although adequate resolution between C10 and C14OH was achieved, the modifications to the elution conditions resulted in interference from other system

peaks. Additional work on this method will be needed to achieve the goal of adequate separation of all potential fatty acid peaks without interference from system related peaks.

Work was also conducted to develop a method to detect residual solvents as potential impurities in RC-527. The list of potential process related residual solvents included acetonitrile, dichloromethane, methanol, acetic acid, tetrahydrofuran, heptane, tert-butanol and ethyl acetate. A limit assay employing gas chromatography to resolve the solvents and flame ionization detection was successfully developed. A lot of RC-527 was tested using the method and was determined not to contain any of the solvents at levels approaching the ICH limits. Note that acetic acid chromatographs poorly using this method resulting in a distorted peak shape. Although it could be determined that the sample tested did not contain acetic acid at levels approaching the limit, further work may be needed to develop a method that gives adequate peak shape for acetic acid.

Task 5: Regulatory/Clinical.

With respect to the clinical/regulatory, the following progress was made during the first year of the contract:

1. A clinical development sub-team was formed to facilitate the design of the Phase 1 trial and to complete the clinical documents required for the Pre-IND Briefing Document.

2. A draft clinical plan has been developed consisting of a randomized, controlled (saline as the placebo), double-blind, dose-escalation trial in healthy adults. After reviewing all relevant pre-clinical data the CRX-527 clinical sub-team decided the phase 1 clinical trial should include bi-weekly dosing (Monday, Friday) for 6-weeks (total of 12 doses per subject) at each of four dose levels.

3. The Pre-IND Briefing Document is currently being compiled and will be submitted in mid-October 2004 to the Division of Anti-Viral Drug Products (DAVDP), Office of Drug Evaluation IV (ODE IV), at the Food and Drug Administration

III. KEY RESEARCH ACCOMPLISHMENTS

Task 1: Biomarker Discovery (Microarray).

1. Pilot experiments were completed to identify PBMC samples, time points and dose ranges for the full-scale microarray experiment.
2. A microarray experiment with over 1100 inflammatory genes was completed with AGP activated macrophages.
3. The data for all three donors was compiled using Genespring and candidate biomarkers were identified for further analysis by real time RT-PCR, ELISA, or FACS.

Task 1: Biomarker Discovery (Real Time RT-PCR).

1. RNA extraction procedure for PBMC cultures/nasal scrapings optimized: RLT-buffer and Qiagen RNeasy Kit.
2. PCR assays selected based on high level of homology between cynomolgus monkey and human biomarker sequences (Applied Biosystems, TaqMan Gene Expression Assays).
3. 20 biomarker candidates identified and validated in PBMC and nasal scraping experiments.

4. Priority biomarker candidates identified: TNF-α, CCR7, MMP7, CxCl9, and INDO based on upregulation with CRX-524 and/or CRX-527 at 8-24 hours in PBMC experiments and cynomolgus nasal scrapings.
5. Influenza extraction from nasal washes procedure optimized (Qiagen QiaAmp Viral RNA Kit).

Task 2: Soluble Biomarkers.

1. A comprehensive list of soluble biomarkers was systematically screened in human PBMC in vitro and in vivo in mice following AGP stimulation.
2. From an initial list of over 35 soluble markers screened, 22 were detected in mouse serum following I.V. delivery of an AGP, 9 were detected in mouse serum following intrapulmonary delivery. Three of these soluble markers correlated with the strength and duration of protection from infectious challenge afforded by the AGP. These three markers, IP-10, MIG and SAA, are currently being evaluated in greater detail.

Task 2: Potency Assay Development

1. The human monocytic line, MonoMac 6, was chosen as a reporter cell line from which to elicit a TLR4 mediated response. This line has inherent advantages of reproducible response to the agent without pre-stimulation or manipulation to force responsiveness.
2. A number of potential reporter molecules were examined for their ability to be assayed in a relatively short assay period. Based on commercial availability of reagent kits and biological response to CRX-527, MIP-1β was chosen as the reporter cytokine moving forward.

Task 3: Cellular Biomarkers

1. A comprehensive list of cell-surface biomarkers was systematically screened in human PBMC in vitro, mouse PBMC in vitro, and in vivo in mice following AGP stimulation.
2. The cell surface markers CD69 and MHC-I were selected as the lead candidate biomarkers for further investigation.
3. Detailed in vivo time course and dose response studies were conducted to determine the feasibility of using these candidate biomarkers for clinical monitoring the breadth and duration of AGP mediated protection.
4. For strict intranasal delivery, these markers would be of limited utility to track protection in the upper airways; however, the markers would be useful for future development and clinical monitoring of an intrapulmonary drug delivery system.

Task 4: AGP Scale-up/Chemistry.

1. New scalable syntheses of CRX-524 and CRX-527 were developed and performed at Corixa on sufficient scale and purity for toxicology and other studies.
2. Tetrionics, Inc. was selected for production of clinical supplies after conducting site visits of several CMOs and performing a QA audit.
3. Technology transfer of Corixa's 524/527 synthesis protocols to Tetrionics, Inc. was completed and an initial concept run of CRX-527 was carried out at the CMO.
4. CMC section on the manufacture of CRX-527 was prepared outlining the new scalable synthesis route.

Task 4: AGP Process Development/Formulations.

1. Real-time and accelerated stability studies were started for various formulations of CRX-524 and CRX-527.
2. A new IN formulation was developed for Corixa's lead monotherapy AGP CRX-527.
3. Various commercially available intranasal delivery devices were evaluated and the Pfeiffer uni-dose device was selected for the upcoming phase I clinical trial. Criteria included ease of manual filling and assembly, droplet size characteristics with product, cost per unit, and packaging configuration.

Task 5: Regulatory/Clinical

1. A clinical development sub-team was formed to facilitate the design of the Phase 1 trial and to complete the clinical documents required for the Pre-IND Briefing Document.
2. A draft phase I clinical plan has been developed.
3. The Pre-IND Briefing Document is currently being compiled and will be submitted in mid-October 2004 to the Division of Anti-Viral Drug Products (DAVDP), Office of Drug Evaluation IV (ODE IV), at the Food and Drug Administration

IV. REPORTABLE OUTCOMES

1. Pre-IND Briefing Document for phase I clinical trial will be submitted to the FDA in October, 2004.

2. Publications *(experiments discussed in both of these papers were completed prior to the start of the Army contract; but they are being included because the work was supported by the DARPA contract which was a precursor to the work currently being done under the Army contract – copies are included in the appendix).*

   C.W. Cluff, J.R. Baldridge, A.G. Stover, J.T. Evans, D.A. Johnson, M.J. Lacy, V.G. Clawson, V.M. Yorgenson, C.L. Johnson, M.T. Livesay, R.M. Hershberg, and D.H. Persing. 2004. Evaluation of novel synthetic TLR4 agonists for induction of innate resistance to infectious challenge. Infection and Immunity (Submitted to Infection & Immunity)

   A.G. Stöver, J.D.S. Correia, C.W. Cluff, J.T. Evans, M.W. Elliott, E.W. Jeffery, D.A. Johnson, M.J. Lacy, J.R. Baldridge, P. Probst, R.J. Ulevitch, D.H. Persing, and R.M. Hershberg. 2004. Structure-activity relationship of synthetic toll-like receptor 4 agonists. J. Biol. Chem. 279(6): 4440-4449.) (DARPA; submitted prior to start of Army contract; copy attached)

3. Public presentations resulting from DARPA and Army contracts (copies included in appendix).

   Differential induction of cytokines and type I interferons in human monocytes and dendritic cells by synthetic TLR-4 and TLR-3 agonists. P. Probst, S. Engardt, J. Stolk, J. Evans, D.A. Johnson and D. Persing. Toll Meeting, Italy 2004.

   Rapid Acting Vaccines: Synthetic Toll-Like Receptor 4 (TLR-4) Agonists Induce Sequential Innate and Adaptive Mucosal Immune Responses. J.T. Evans, C.W. Cluff, D.A. Johnson,

J.R. Baldridge, and D.H. Persing. Macrae Respiratory Viral Infections Meeting, Fort Myers, FL 2004.

Rapid Acting Vaccines: Aminoalkyl Glucosaminide 4-Phosphates (AGPs) Are Potent Inducers of Sequential Innate and Adaptive Mucosal Immune Responses. C.W. Cluff, J.T. Evans, D.A. Johnson, J.R. Baldridge, and D.H. Persing. Gordon Conference on Chemical & Biological Terrorism Defense. Buellton, CA, 2004.

Rapid Acting Vaccines: Synthetic Toll-Like Receptor 4 (TLR-4) Agonists Induce Sequential Innate and Adaptive Mucosal Immune Responses. J.T. Evans, C.W. Cluff, D.A. Johnson, J.R. Baldridge, and D.H. Persing. ASM Biodefense Meeting, Baltimore, MD, 2004.

V. CONCLUSIONS

Over the past year, significant progress was made toward the completion of all Tasks outlined in the contract. The identification of potential biomarkers via microarray using primary human macrophages was completed (Task 1). The completion of Task 1 was invaluable towards preparing a list of candidate biomarkers to screen by real time RT-PCR, ELISA or FACS. Over 20 different potential biomarkers were screened on human PBMCs and test nasal scrapings by RT-PCR and 5 of these biomarkers (TNF-α, CCR7, MMP7, CxCl9, and INDO) were selected for further evaluation and assay development. Ongoing experiments over the next year will determine the utility of these markers to track the administration and immunostimulatory effects of CRX-527 in the upcoming phase I clinical trial. Likewise, over 35 soluble biomarkers and 20 cell-surface biomarkers were screened by ELISA or FACS, respectively, using in vitro human PBMC cultures and mouse in vivo studies (Tasks 2 and 3). From these studies, a short-list of soluble and cell-surface biomarkers was selected for further in vivo evaluations and assay development. In addition to selecting surrogate biomarkers for the upcoming phase I clinical trial, these studies have provided a valuable insight into the mechanism-of-action whereby CRX-527 induces a state of non-specific resistance to pathogen challenge following intranasal delivery. Task 4 of this contract focused on 1) development of a scalable synthesis strategy for increased production of CRX-527 with the goal of GMP synthesis at a 20 gram scale 2) identification of a stable formulation for intranasal delivery 3) select an appropriate intranasal delivery device 4) design GLP toxicology studies to be initiated in year 2 of the contract. All of these tasks are on-schedule or ahead of schedule based on the proposed contract timeline. Synthesis of CRX-527 has been scaled-up from a bench-scale synthesis to over 5 grams with anticipation of a 20 gram GMP lot in early 2005 (6 months ahead of schedule). This scale should be sufficient to meet the demands of this product through phase 3 clinical trials and product launch. This is a significant accomplishment given the early stage of this clinical product. The formulations group identified a stable intranasal formulation and delivery device for the upcoming CRX-527 phase I clinical trial. All of these activities are on-track for initiation of a phase I human clinical trial in late 2005 or early 2006.

A draft clinical plan (Task 5 in contract) has been developed consisting of a randomized, controlled (saline as the placebo), double-blind, dose-escalation trial in healthy adults. After reviewing all relevant pre-clinical data, the CRX-527 clinical sub-team has proposed a phase 1 clinical trial with bi-weekly dosing (Monday, Friday) for 6-weeks (total of 12 doses per subject) at each of four dose levels. We originally proposed to do a single-dose, dose escalation study with the intranasal immunomodulator. However, several issues moved us toward development of a

multi-dose product. First, a period of several weeks to several months of protection of the airways may be desirable when an exposure event is unpredictable. The value of a multi-dose study is that the safety data generated would support multiple phase II studies of experimental viral challenge in humans and studies of natural exposure to respiratory diseases among susceptible military personnel (such as during basic training). Second, Corixa is already pursuing a TLR4 agonist for an allergic rhinitis indication (CRX-675); completion of a single dose escalation study is anticipated in May of 2005. Thus, the relative value of yet another single dose trial performed with a different molecule is only incremental, and only adds to the timeline for development of a useful multidose product. A Pre-IND Briefing Document is currently being compiled and will be submitted in mid-October 2004 to the Division of Anti-Viral Drug Products (DAVDP), Office of Drug Evaluation IV (ODE IV), at the Food and Drug Administration

Obviously, the budgetary implications of moving ahead into a multi-dose trial are substantial. As detailed under separate cover, most of the increase in costs is dictated by an increase in regulatory requirements for extra toxicological studies, increased pharmacokinetics studies, drug formulations effort, repeated-dose biomarker investigations, biomarker clinical monitoring and (most importantly) the extra time and effort associated with a multi-dose (vs. single-dose) study. Additional incremental costs have come about because we had not yet had the benefit of experience with regulatory agencies in the development of an intranasal TLR4 agonist. Indeed, the experience gained by the commencement of the CRX-675 trials can now be used to provide an accurate estimate of timelines and costs associated with the more potent TLR4 agonist CRX-527.

VI. REFERENCES

All references are included within the appropriate sections above.

VII. APPENDICES

Copies of publications and abstracts are attached.

APPENDIX

Synthetic Toll-Like Receptor 4 Agonists Stimulate Innate Resistance to Infectious Challenge

Christopher W. Cluff[2], Jory R. Baldridge [2], Axel G. Stöver [1], Jay T. Evans [2], David A. Johnson[2] Michael J. Lacy[2], Valerie G. Clawson[2], Vonnie M. Yorgensen[2], Craig L. Johnson[2], Mark T. Livesay[2], Robert M. Hershberg [1,3] and David H. Persing [1,3] *

[1] Corixa Corporation, 1900 9th Avenue, Suite 1100, Seattle, WA 98101
[2] Corixa Corporation, 553 Old Corvallis Road, Hamilton, MT 59840
[3] The Infectious Disease Research Institute, 1124 Columbia Street, Suite 600, Seattle, WA 98104

Key Words: human TLR4, LPS, Agonist, Cytokine, Listeria, Influenza, innate immunity

Abbreviations used in this manuscript: TLR, Toll-like receptor; AGP, Aminoalkyl-Glucosaminide-Phosphates. PAMP, Pathogen-Associated Molecular Pattern; LPS, Lipopolysaccharide; LBP, LPS binding protein; SAR, structure / activity relationship; sem, standard error of the mean.

Running Title: Evaluation of Novel Synthetic TLR4 Ligands For Induction of Innate Immunity

* **Corresponding Author**: Corixa Corporation, 1900 9th Avenue, Suite 1100, Seattle, WA 98101. Fax Number: (206) 366-4759. E-mail address: david.persing@corixa.com

Acknowledgements: This material is based upon work supported in part by the Defense Advanced Research Projects Agency (DARPA) under Contract No.N66001-01-C-8007.

Abstract:

A series of structurally variant synthetic lipid A mimetics (termed the aminoalkyl glucosaminide phosphates, or AGPs) were evaluated in murine infectious disease models for their ability to provide short-term protection against challenge with *Listeria monocytogenes* and influenza virus. Protection against *L. monocytogenes* challenge peaked between 8 and 24 hours after intravenous administration of agonist AGPs, remained significantly elevated though day 2, and slowly diminished to baseline levels over the next several days. The kinetics of induction and duration of protection in the influenza system were similar, though peak protection was attained approximately one day later and persisted for a day longer. Administration of AGPs via the respiratory route led to protection against airway challenge with both *Listeria* and influenza virus, as well as systemic protection against intravenous challenge with *Listeria.* The AGPs were found to be inactive in the C3H-HeJ mouse, indicating their dependence on toll-like receptor 4 (TLR4) signaling. Structure-activity relationship (SAR) studies showed that activation of innate immune effectors by AGPs depends primarily on the lengths of the secondary acyl chains within the three acyl-oxy-acyl residues, and also on nature of the functional group attached to the aglycon component. We conclude that administration of synthetic TLR4 agonists provides rapid pharmacologic induction of innate resistance to infectious challenge by two different pathogen classes, that this effect is mediated via TLR4, and that structural differences between AGPs can have dramatic effects on agonist activity *in vivo.*

Introduction:

The toll-like receptors (TLRs) represent an evolutionarily conserved means of detecting and responding to microbial challenge (1). The TLRs recognize a variety of pathogen-specific components including lipopolysaccharide (LPS), CpG DNA, and microbial membrane and cell wall components (20). Toll-like receptor 4 (TLR4) is critical for recognition of LPS (30, 31) and considerable progress has recently been made in understanding the interaction of TLR4 with critical accessory molecules implicated in LPS recognition (8, 9, 17, 21, 22, 32, 40, 41). In this regard, it appears that LBP promotes binding of LPS to CD14, which in turn facilitates the association of the lipid A component of LPS with MD-2 to form a soluble complex that serves as an activating ligand for TLR4 on the cell surface. Binding of the MD-2/LPS complex to TLR4 results in aggregation of TLR4 into lipid rafts and activation of several distinct intracellular signaling pathways that result in increased transcription of many genes encoding cytokines, defensins, chemokines, and type I interferons (28, 38). These effector molecules determine a wide range of biological activities including further production of cytokines, enhancement of microbicidal activity of phagocytic cells, and migration/maturation of dendritic cells (5, 23, 36).

Before the discovery that LPS interacts with TLR4, evidence demonstrating the importance of innate immune activation in controlling infection with gram-negative bacteria was obtained in studies of C3H/HeJ mice. These mice harbor a signaling defect in TLR4 that renders them LPS-hyporesponsive (30, 31). *Salmonella typhimurium*-induced morbidity and mortality occurs at much lower doses in C3H/HeJ mice compared to wild-type mice (27), presumably because C3H/HeJ mice are unable to mount innate immune responses early enough to control infectious burden in the period prior to the development of adaptive responses (33). Similar results have been obtained when C3H/HeJ mice are evaluated in models of infection with *E .coli* (10), *Neisseria meningitidis* (43)and *Francisella tularensis* (18).

Administration of purified LPS has been found to confer prophylactic protection from subsequent bacterial or viral challenge in various animal models (4, 25), presumably via stimulation of innate immunity. Recently, intrauterine administration of LPS in cattle was shown to facilitate clearance of chronic intrauterine infections associated with infertility (34). However, despite these potentially beneficial effects, the pharmacologic use of purified LPS (or lipid A) is precluded by its extreme toxicity; LPS is highly pyrogenic and promotes systemic inflammatory response syndrome (12). In an effort to uncouple the immunomodulatory effects of lipid A from its toxicity, Ribi et al developed monophosphoryl lipid A (MLA); MLA comprises the lipid A portion of LPS from which the (R)-3-hydroxytetradecanoyl group and the 1- phosphate have been removed (24) by successive acid and base hydrolysis. LPS and MLA induce similar cytokine profiles, but MLA but is at least 100-fold less toxic (24, 39). MLA, the active ingredient of MPL™ adjuvant has been administered to more than 12,000 human subjects in studies of next-generation vaccine adjuvants (6). MLA alone or in combination with other molecules elicits protective responses when administered prior to challenge with pathogenic viruses (influenza), bacteria (*Listeria monocytogenes* and *Salmonella enteriditis*) or parasites (*Toxoplasma gondi*) (19, 29, 39). MLA is a natural biological product composed of multiple structurally distinct pharmacophores. The intrinsic heterogeneity of MLA hinders analysis of the structural features responsible for induction of innate immune responses.

We report here the results of *in vivo* structure-function studies of a family of synthetic lipid A mimetics, the aminoalkyl glucosaminide phosphates (AGPs) (13, 14). Intravenous or intranasal/intrapulmonary administration of AGPs was evaluated in standardized murine models of nonspecific resistance to bacterial and viral challenge. Our findings indicate that the ability of the AGPs to induce protective innate immune responses is TLR4 dependent and that the biological activity of these molecules is dependent on specific structural features.

Materials and Methods:

Mice: Female BALB/c, C3H/HeOuJ and C3H/HeJ mice were obtained from Jackson Laboratories, Bar Harbor, ME. Mice were 7-9 weeks of age when the experiments were initiated. Mice were anesthetized for treatment or challenge by intraperitoneal administration of a preparation containing ketamine (100 mg/kg) and xylazine (10 mg/kg). All animals were used in accordance with guidelines established by the Public Health Service and the Institutional Animal Care and Use Committee at Corixa Corporation, Hamilton, Montana.

AGPs: All AGPs were synthesized at Corixa Corp, Hamilton, MT as previously described (13). Stock solutions (1 mg/mL) of AGPs (presented as CRX- compounds) were made in 0.2% triethanolamine (TEOA; Sigma) (pH 7). Dilutions were made in sterile phosphate buffered saline (PBS). For intravenous administration, AGPs were injected into the lateral tail vein (BALB/c mice) or retro-orbital venous plexus (C3H mice) in a volume of 100 µL. For intranasal / intrapulmonary administration, a manual pipettor was used to place 20 µL of AGP preparations up the nose (10 µL per nostril) of anesthetized mice lying on their backs.

Listeria monocytogenes challenge model: An aliquot of *Listeria monocytogenes* (serotype 10403, originally obtained from M. L. Gray, Montana State University) containing ~5 x 10^9 bacteria (stored at –70°C) was added to 24 mL of sterile brain heart infusion broth (Gibco) and incubated in a shaking water bath at 37° C until mid-log growth phase (approximately 3 hours to achieve an optical density of 0.3 at 550 nM; equivalent to ~10^9 bacteria/mL). Ten-fold serial dilutions of the *L. monocytogenes* culture were made in sterile PBS. 100 µL of the 10^3/mL dilution were spread on each of three tryptic soy agar plates to confirm bacterial concentration and lack of contamination

from other organisms. For intravenous challenge, 100 µL of the 10^6/mL dilution were administered via the tail vein (BALB/c mice) or retro-orbital plexus (C3H mice) to provide a challenge dose of ~10^5 *L. monocytogenes* organisms.

Listeria-infected mice were euthanized by CO_2 overdose two days after challenge and spleens and/or lungs were harvested and placed in 4 mL sterile PBS (16 x 100 mm glass tubes). Spleens were homogenized for 10 seconds using an Ultra-Turrax T25 probe homogenizer (Junkel & Kunkel). Five ten-fold serial dilutions of splenic homogenates were generated, and 100 µL of each dilution was spread on a 10 cm diameter tryptic soy agar plate (Remel Cat #01917). The plates were incubated at room temperature, and *Listeria* CFUs were counted 72 hours later. Protection was defined as the difference between the mean log10 number of bacteria per spleen in the treatment groups and the mean log10 number of bacteria per spleen in the control mice treated with vehicle alone.

Influenza challenge model: Stock influenza A/HK/68 (H3N2), originally obtained from Dr. Philip Wyde (Baylor College of Medicine, Houston, TX), was prepared by passage through mice and stored as 1 ml aliquots at -70°C. For intranasal delivery of AGPs or influenza, BALB/c mice were anesthetized and 20 µL containing 5 LD_{50} of influenza were administered (10 µL/nostril) using a manual pipettor. Mice were monitored for mortality, clinical signs of disease and weight change for 21 days following viral challenge.

The clinical symptoms observed for disease severity were recorded as Disease Index scores and included ruffled fur, labored breathing and hunched posture. An arbitrary scale of 0 to 3 was used to score severity of disease. The Disease Index presented in the figures is an average value for all mice within a group for the 21-day period following viral challenge. The weight of the mice is a cumulative value for all the mice in a group on each day the weights were determined. Survival rates are presented as the percentage of mice in each group that were alive at the end of the 21-day period following viral challenge. Mice alive at the end of the test period were considered to be fully recovered.

Results:

Structural features of aminoalkyl-glucosaminide-phosphates (AGPs)

Previous in vitro studies in our laboratory identified important structural requirements for signaling through TLR4 by AGPs (35). In the current study, the structural correlates of protective activity mediated by AGPs were investivated in infectious challenge models of bacterial (*Listeria monocytogenes*) and viral (influenza) agents. The synthesis of the AGPs, all of which are composed of a monosaccharide unit with an N-acylated aminoalkyl aglycon spacer arm, has been described previously (13), and the general structure is shown in Figure 1. Primary acyl chain length was standardized at 14 carbons. The biological effects of variation in secondary acyl chain length (R1, R2 and R3 in Figure 1) and the aglycon component (see Fig. 1) were the primary focus of this study.

Requirement of TLR4 for activation of innate immune effectors by AGPs

TLR4 has been identified as an integral component of the LPS receptor complex comprising TLR4, MD2, and CD14 (1). Mouse strains with mutations in the gene encoding the cytoplasmic signaling domain of TLR4, such as C3H/HeJ, are hyporesponsive to LPS stimulation. This feature was exploited in order to evaluate the requirement for functional TLR4 expression in AGP-mediated enhancement of innate immunity. Groups of C3H/HeJ or wild-type C3H/HeOuH mice

were injected via the intravenous route with CRX-524 (see Figure 1 and Table 1 for structure) in 0.2% TEOA vehicle or with vehicle alone and challenged IV 48 hours later with ~10^5 live *Listeria monocytogenes*. Two days after challenge, the mice were sacrificed for determination of splenic colony forming units (CFUs). The average number of splenic CFUs (log10 value) for CRX-524-treated groups was subtracted from the average number obtained for the vehicle-treated control group to determine the magnitude of protection (presented as Log10 protection versus vehicle control on the y-axis).

CRX-524-mediated induction of resistance to *Listeria* challenge was shown to be dependent on the presence of functional TLR4, since the AGP elicited strong protection in wild type C3H/HeOuJ mice, but not in the TLR4-mutant C3H/HeJ mice (**Figure 2; Panel A**). Similar results were observed in the influenza system, where intranasal administration of CRX-524 two days prior to intranasal challenge with a lethal dose of influenza induced protection in C3H/HeOuJ mice, but not in C3H/HeJ mice (**Figure 2; Panel B**). We have conducted similar experiments to show that the immunostimulatory activity of MPL and other AGPs also depends on expression of functional TLR4 (data not shown), implicating a general requirement of TLR4 for activation of the innate immune system by lipid A and lipid A mimetics.

Effects of secondary acyl chain length on induction of innate resistance to infectious challenge

A family of AGP molecules with an L-serine based aglycon unit (referred to as the "L-seryl" family) was used to investigate the influence of secondary acyl chain length on the ability of lipid A-related molecules to induce enhanced innate immune function *in vivo*. As is the case for all AGPs used in the experiments described in this report, each of three acyl-oxy-acyl residues on the L-seryl AGPs have 14 carbon (tetradecanoyl, or myristoyl) acyl chains in the primary positions (**Figure 1**). The compounds used in these experiments contained acyl-oxy-acyl residues with 6, 7, 8, 9, 10, 11, 12 or14 carbon acyl chains at all three (R1-R3) secondary positions (**Table 1**). In the *Listeria* system, L-seryl AGPs in 0.2% TEOA or TEOA alone (vehicle control) were tested for their ability to induce protection from intravenous challenge 24 hours after intravenous administration as described above. In the influenza system, L-seryl AGPs were administered via the intranasal route to anesthetized mice. Two days later, the mice were anesthetized again and challenged with influenza via the same route. Morbidity (body weight and disease index) and mortality (percent survival) were documented for 21 days following challenge. All mice surviving at day 21 recovered completely.

The degree of protection for the AGPs with variable length acyl chains at the R1, R2 and R3 positions is presented for the *Listeria monocytogenes* (**Figure 3, panel A**) and influenza (**Figure 3, panel B**) systems. The striking difference in protective ability of AGPs was found to depend heavily on secondary acyl chain length; compounds with 6 (CRX-526) or 7 (CRX-554) carbon acyl chains were essentially inactive, whereas compounds with 10 (CRX-527), 11 (CRX-538) or 12 (CRX-560) carbon acyl chains were highly active. The compound with 14 (CRX-512) carbon acyl chains was found to be active in both systems, though the potency of this compound was diminished relative to the compounds with 10-12 carbon acyl chains, since a larger dose (20 μg) was required to obtain maximal protection.

Relative Positional Importance of Secondary Acyl Chains

To evaluate the relative positional importance of the three secondary acyl-oxy-acyl residues with regard to activation of innate immune effectors, a series of 'substituted' L-seryl compounds were used in which one of the maximally active 10 carbon acyl chains at R1, R2 or R3 was replaced

by an "inactive" 6 carbon acyl chain (CRX-566, CRX-565 or CRX-569, respectively) (**Table 1**). In addition, three AGPs were synthesized in which two of the three acyl chains at R1, R2 or R3 were replaced by 6 carbon acyl chains (CRX-568 has the 6 carbon acyl chains at R1 and R2; CRX-570 has the 6 carbon acyl chains at R2 and R3; and CRX-567 has the 6 carbon acyl chains at R1 and R3).

These six "hybrid" AGPs were evaluated for their capacity to induce protection against intravenous challenge with *Listeria monocytogenes* or influenza. The AGPs with 6 carbon acyl chains in two of the three secondary positions (CRX-567, CRX-568 and CRX-570) induced little to no protection in either system (**Figure 4, panels A and B**). In the *Listeria* system, the compound with a single 6-carbon acyl chain at R1 (CRX-566) was relatively inactive, inducing only slightly better protection than the inactive compounds containing two or three 6-carbon secondary acyl chains. CRX-565 and CRX-569, containing a single 6 carbon secondary acyl chain substitution at R2 or R3, respectively, induced significant protection, though the activity of these compounds was reduced compared to the maximally active compound with 10 carbon acyl chains at all three secondary positions (CRX-527) (**Figure 4, panel A**). The same general pattern held for the influenza system, though only CRX-569, with a single 6-carbon acyl chain at R3, induced better protection than the compounds containing two 6-carbon acyl chains (**Figure 4, panel B**).

Importance of a negatively charged functional group at position R4 on the aglycon component of AGPs

AGPs differing only in the chemical composition of the functional group R4 (**Figure 1, Table 1**) within the aglycon portion of the molecule were used to further evaluate structure/activity relationships of these synthetic TLR4 agonists. All AGPs for this experiment comprised 14 carbon primary acyl chains and 10 carbon secondary acyl chains at R1, R2 and R3. The aminoalkyl AGP (CRX-524) carries a hydrogen atom at R4, while the L-seryl AGP (CRX-527) contains a carboxyl residue at this position. The other AGPs tested in this experiment contain a carboxamide residue (CRX-522), a hydroxymethyl residue (CRX-545) or a carboxyethyl residue (CRX-573) at R4. At a dose of 1 μg, CRX-527 was found to induce significantly better protection relative to the other four compounds (**Figure 5**). Consistent with this result was the finding that the dose of CRX-527 required to prevent death in 50% of mice challenged with a lethal dose of *Listeria* (a.k.a. the effective dose 50, or ED_{50}) was 10 to 20 times lower than the ED_{50} for any of the four other compounds (data not shown).

Importance of Acyl-oxy-axyl Juxtaposition

A family of AGPs with an ? -aminoalkanol-based aglycon unit (termed the "aminoalkyl" family) that vary in the length of the carbon-based linker arm between the sugar moiety and aglycon amino group (**Table1**) were used to evaluate the importance of the relative proximity of the three acyl-oxy-acyl residues and/or the conformation of the AGP backbone on the ability of these compounds to induce innate immune responses. Members of the aminoalkyl AGP family have 2 (CRX-529), 3 (CRX-525), 4 (CRX-557) or 6 (CRX-571) carbon atom linkers between the sugar moiety (containing two acyl-oxy-acyl residues) and the aglycon unit (containing the third acyl-oxy-acyl residue). These compounds were compared with regard to their capacity for inducing innate resistance to challenge with *Listeria*.

The compounds used in this experiment all contain 14 carbon secondary acyl chains at R1, R2 and R3. Because a 1 μg dose of AGPs with 14 carbon secondary acyl chains has consistently been found to elicit significantly lower levels of protection than 1 μg of otherwise identical

compounds containing 10 carbon secondary acyl chains (see **Figure 3a** for an example), lower levels of protection (ca. 0.5 log10 units) induced by even the most potent of these AGPs was not unexpected (**Figure 6**). Despite this limitation, the experiment demonstrated that the level of protection diminishes as the linker length between the sugar moiety and the aglycon unit is increased. Whereas the AGP with a 2-carbon linker afforded the greatest level of protection, compounds with linkers of 3 to 6 carbons provided successively lower levels of protection. The lower activity of the compounds with longer linkers could either be due to the structural alterations in the AGP backbone or to changes in the spatial orientation of the acyl-oxy-acyl residues, or both.

Discussion:

LPS and monophosphoryl lipid A were both previously shown to enhance non-specific resistance to challenge with viral and bacterial pathogens, albeit by an unknown mechanism (19, 39). We now know that both molecules work by activation of TLR4, which evolved to recognize LPS as a danger signal and to activate appropriate innate and adaptive immune responses (1). TLR4 activation leads to the initiation of the MyD88-dependent intracellular signaling pathway, which results in activation of NF-kB, a transcription factor responsible for promoting, among other things, the production of multiple inflammatory cytokines (e.g. IL-6, IL-8, IL-12). LPS exposure also results in production of defensins, which comprise several distinct families of antibacterial, antifungal, and antiviral peptides (2). In addition to activation of the MyD88-dependent signaling, TLR4 agonists activate the TRIF-dependent pathway (a.k.a. the MyD88-independent pathway), which results in expression of interferon regulatory factor 3 (IRF3) and production of type I interferons (particularly interferon ß (37)), as well as activation of MAP kinases and NF-kB (16), production of inducible nitric oxide synthetase (iNOS) and functional maturation of dendritic cells (1). Induction of interferon ß appears to be crucial for the anti-viral effects associated with activation of TLR4, since mice deficient in TRIF are highly susceptible to viral infection (11). Mice deficient in either MyD88 or TRIF produce lower levels of immune effectors, and mice deficient in both are completely non-responsive to LPS (46). Thus, TLR4 activation results in short-term antimicrobial effects, which can be observed within minutes to hours of exposure to microbial components, as well as long-term effects on the adaptive response as dictated by the tenor of the cytokine environment in which antigens are presented. The latter effect is thought to play the greatest role in determining the adjuvant effects of TLR agonists (15). It is likely that the AGP-induced protective effects observed in this study are mediated by at least a subset of the effector molecules elicited by LPS.

Two AGPs were previously reported to induce protective innate immune responses when administered prior to bacterial or viral challenge in mice, though neither the structural features responsible for this activity or its dependence on TLR4 were described (3). In this report, structural variants of these compounds were used to investigate the TLR requirement and the structure / activity relationship of lipid A-mediated induction of enhanced innate resistance to infectious challenge. The protective effect is clearly mediated by TLR4, since LPS-hyporesponsive C3H/HeJ mice with a mutation in TLR4 did not develop resistance to infection with *Listeria* or influenza after treatment with doses of AGP that were effective at producing strong protection in wild-type C3H/HeOuJ mice (**Figure 2**). With regard to TLR specificity, AGPs do not appear to activate cells via interaction with TLR2, since treatment of TLR2-transfected 293 cells with several AGPs induced no NF-KB activity (data not shown). AGPs have not been evaluated for potential interaction with other TLRs at this time.

The precise nature of the interaction of lipid A with TLR4 and with other molecules such as LBP, CD14, and MD2 in the recognition pathway is currently an area of intense investigation.

Several studies have highlighted the important roles of accessory molecules, especially MD2, in LPS recognition (7, 40, 41, 44, 45). The emerging consensus is that LBP interacts with aggregates of LPS and promotes the formation of CD14/LPS monomeric complexes, which then facilitate the docking of LPS acyl chains into a hydrophobic pocket within MD-2; the negatively charged residues of the lipid A structure backbone interact with the positively charged residues along the edge of the pocket. This interaction presumably leads to a conformational change in MD-2 that locks the two entities together as a stable, soluble complex (42). The MD-2/LPS complex is then able to bind TLR4 on the cell surface and promote aggregation of the receptors into lipid rafts. Once a critical mass of aggregated TLR4 molecules is achieved, intracellular adaptor molecules are activated and subsequent induction of several signaling pathways results in the expression of a range of cellular activities relating to innate immune function. We showed previously that recognition of AGPs requires both TLR4 and MD2 (35). In this study, we found that CRX-527, an AGP with two negatively charged residues on its backbone (i.e. the phosphate residue on the sugar and the carboxyl group at R4), induces stronger protection than other AGPs (CRX-522, CRX-524, CRX-545) harboring a single negatively charged residue (**Figure 5**). CRX-573, which contains a carboxyethyl group at R4, was also found to be less protective than CRX-527. Because the carboxyl group in CRX-573 is more distant from the phosphate group on the sugar moiety due to the intervening ethyl group, the weaker activity induced by this AGP suggests that the distance between the ionizable group at R4 and the negatively charged phosphate residue on the sugar moiety is a critical determinant of binding to MD-2. This result is not unexpected, considering the importance of charged amino acid orientation within binding pockets for receptor/ligand interactions (26). We also found that increasing the length of the AGP backbone with carbon-based linkers led to diminished protective activity (**Figure 6**). Such changes might affect the strength of the interaction between the acyl chains of the AGP and the hydrophobic pocket of MD-2. Our findings from in vitro (35) and the in vivo studies described herein, thus, are consistent, and are supportive of the hypothesis that positively charged residues on the edge of the hydrophobic pocket of MD-2 (40) are important for binding to lipid A or its mimetics.

We found that secondary acyl chain length is the most critical determinant of protective activity of AGPs when combined with a constant primary acyl chain length of 14 carbons. Whereas AGPs with 8 to 14 carbon acyl chains at positions R1, R2 and R3 induced strong protection against *Listeria* or influenza challenge, compounds with 6 or 7 carbon acyl chains at these positions were inactive (**Figure 3**). The positional importance of the three acyl-oxy-acyl residues attached to the AGP backbone was demonstrated in the *Listeria* system. In this regard, an AGP with a 6 carbon acyl chain at R1 (CRX-566) was relatively inactive compared to compounds containing 6 carbon acyl chains at R2 or R3 (CRX-565 and CRX-569), both of which induced moderate levels of protection (**Figure 4, panel A**). We have observed similar differences in activity between these compounds in cytokine induction assays, both in vivo in mice (data not shown) and in vitro with human or murine cell lines and/or peripheral blood leukocytes (13). In the influenza system, however, differences in activity between AGPs with single 6 carbon secondary acyl chains at R1, R2 or R3 were not as apparent (**Figure 4, panel B**), which may mean that the influenza system is not as sensitive for quantifying differences in activity between compounds. Taken together, our results indicate that the length of the secondary acyl chains, particularly at R1, is a critical determinant for binding to MD-2. Although there is still much to learn about the binding of lipid A molecules to the MD-2/TLR4 complex, our findings suggest that this library of synthetic lipid A mimetics will ultimately be useful for dissecting the essential features of this interaction.

The finding that the AGPs are active in the airways further suggests that MD-2 and TLR4 are accessible in this compartment, and that TLR4 agonists may have a unique therapeutic role in modulation of innate immune responses when administered directly to the respiratory mucosa. TLR4 agonist activity can be potentially exploited to provide short-term resistance to infectious challenge such as might occur in the setting of exposure to bio-threat agents or epidemic infections. Indeed, the accessibility of TLR4 in the airways may allow relatively small doses of drug to be used compared to what would have to be administered systemically to obtain the same effect. Future studies of this unique family of TLR4 agonists will likely yield important insights into their potential clinical applications.

Figure And Table Legends

Figure 1: General Structure of AGPs.

Table 1: Specific Structure of AGPs.

Figure 2 (Panel A): Induction of non-specific resistance to challenge with *Listeria monocytogenes* by intravenous pretreatment of TLR4 mutant C3H/HeJ mice (hatched bars+/- sem) or wild-type C3H/HeOUJ mice (closed bars + sem) with CRX-524 (n= 5 mice per group). The average log10 number of splenic CFUs in vehicle-treated control mice was 7.46 +/- 0.08 (sem) for C3H/HeJ and 7.61 +/- 0.08 (sem) for C3H/HeOuJ (no significant difference between HeJ and HeOuH in this regard using Student's t-test).

Figure 2 (Panel B): Induction of non-specific resistance to intranasal influenza challenge by intranasal pretreatment of TLR4 mutant C3H/HeJ mice or wild-type C3H/HeOUJ mice with CRX-524 (n= 5 mice per group). Anesthetized mice received 5 ug of CRX-524 in 20 uL via the intranasal/intrapulmonary route. Closed bars = total weight and hatched bars = disease index. Percent survival for each group 21 days after infection is presented at the bottom of the graph.

Figure 3 (Panel A): Induction of non-specific resistance to challenge with *Listeria monocytogenes* by intravenous pretreatment with AGP compounds (1 ug dose = hatched bars + sem, 20 ug dose = closed bars + sem) that vary in acyl chain length at positions R1, R2 and R3 (n= 5 BALB/c mice per group). The average log10 number of splenic CFUs in vehicle-treated control mice was 7.51 +/- 0.13 (sem).

Figure 3 (Panel B): Induction of non-specific resistance to intranasal influenza challenge by intranasal pretreatment with AGP compounds that vary in acyl chain length at positions R1, R2 and R3 (n= 5 BALB/c mice per group). Closed bars = total weight and hatched bars = disease index. Percent survival for each group 21 days after infection is presented at the bottom of the graph.

Figure 4 (Panel A): Induction of non-specific resistance to challenge with *Listeria monocytogenes* by intravenous pretreatment with AGP compounds (1 ug dose = closed bars + sem) that have one or two "inactive" 6 carbon acyl chains at positions R1, R2 and/or R3 (n= 5 BALB/c mice per group). The average log10 number of splenic CFUs in vehicle-treated control mice was 7.38 +/- 0.17 (sem).

Figure 4 (Panel B): Induction of non-specific resistance to intranasal influenza challenge by intranasal pretreatment with AGP compounds that vary in acyl chain length at positions R1, R2 and

R3 (n= 5 BALB/c mice per group). Closed bars = total weight and hatched bars = disease index. Percent survival for each group 21 days after infection is presented at the bottom of the graph.

Figure 5: Induction of non-specific resistance to challenge with *Listeria monocytogenes* by intravenous pretreatment with AGP compounds (1 ug dose = closed bars + sem) that have various functional groups at position R4 on the aglycon unit (n= 5 BALB/c mice per group). The average log10 number of splenic CFUs in vehicle-treated control mice was 7.98 +/- 0.13 (sem).

Figure 6: Induction of non-specific resistance to challenge with *Listeria monocytogenes* by intravenous pretreatment with AGP compounds (1 ug dose = closed bars + sem) that have various spacer lengths between the sugar moiety and aglycon moieties (n= 5 BALB/c mice per group). The average log10 number of splenic CFUs in vehicle-treated control mice was 7.03 +/- 0.07 (sem).

References

1. Akira, S. 2003. Mammalian Toll-like receptors. Curr Opin Immunol 15:5-11.
2. Ayabe, T., D. P. Satchell, C. L. Wilson, W. C. Parks, M. E. Selsted, and A. J. Ouellette. 2000. Secretion of microbicidal alpha-defensins by intestinal Paneth cells in response to bacteria. Nat Immunol 1:113-8.
3. Baldridge, J. R., C. W. Cluff, J. T. Evans, M. J. Lacy, J. R. Stephens, V. G. Brookshire, R. Wang, J. R. Ward, Y. M. Yorgensen, D. H. Persing, and D. A. Johnson. 2002. Immunostimulatory activity of aminoalkyl glucosaminide 4-phosphates (AGPs): induction of protective innate immune responses by RC-524 and RC-529. J Endotoxin Res 8:453-8.
4. Berger, F. M. 1967. The effect of endotoxin on resistance to infection and disease. Adv Pharmacol 5:19-46.
5. Caamano, J., and C. A. Hunter. 2002. NF-kappaB family of transcription factors: central regulators of innate and adaptive immune functions. Clin Microbiol Rev 15:414-29.
6. Evans, J. T., C. W. Cluff, D. A. Johnson, M. J. Lacy, D. H. Persing, and J. R. Baldridge. 2003. Enhancement of antigen-specific immunity via the TLR4 ligands MPL adjuvant and Ribi.529. Expert Rev Vaccines 2:219-29.
7. Friedland, N., H. L. Liou, P. Lobel, and A. M. Stock. 2003. Proc Natl Acad Sci U S A 100:2512-2517.
8. Gioannini, T. L., A. Teghanemt, D. Zhang, N. P. Coussens, W. Dockstader, S. Ramaswamy, and J. P. Weiss. 2004. Isolation of an endotoxin-MD-2 complex that produces Toll-like receptor 4-dependent cell activation at picomolar concentrations. PNAS 101:4186-4191.
9. Gruber, A., M. Mancek, H. Wagner, and C. J. Kirschning. 2004. Sructural Model of MD-2 and Functional Role of Its Basic Amino Acid Clusters Involved in Cellular Lipopolysaccharide Recognition. The Journal of Biological Chemistry 279:28475-28482.
10. Hagberg, L., R. Hull, S. Hull, J. R. McGhee, S. M. Michalek, and C. Svanborg Eden. 1984. Difference in susceptibility to gram-negative urinary tract infection between C3H/HeJ and C3H/HeN mice. Infect Immun 46:839-44.
11. Hoebe, K., X. Du, P. Georgel, E. Janssen, K. Tabeta, S. O. Kim, J. Goode, P. Lin, N. Mann, S. Mudd, K. Crozat, S. Sovath, J. Han, and B. Beutler. 2003. Identification of Lps2 as a key transducer of MyD88-independent TIR signalling. Nature 424:743-8.
12. Johnson, A. G. 1994. Molecular adjuvants and immunomodulators: new approaches to immunization. Clin Microbiol Rev 7:277-89.
13. Johnson, D. A., D. S. Keegan, C. G. Sowell, M. T. Livesay, C. L. Johnson, L. M. Taubner, A. Harris, K. R. Myers, J. D. Thompson, G. L. Gustafson, M. J. Rhodes, J. T. Ulrich, J. R. Ward, Y. M. Yorgensen, J. L. Cantrell, and V. G. Brookshire. 1999. 3-O-Desacyl monophosphoryl lipid A derivatives: synthesis and immunostimulant activities. J Med Chem 42:4640-9.

14. Johnson, D. A., C. G. Sowell, C. L. Johnson, M. T. Livesay, D. S. Keegan, M. J. Rhodes, J. T. Ulrich, J. R. Ward, J. L. Cantrell, and V. G. Brookshire. 1999. Synthesis and biological evaluation of a new class of vaccine adjuvants: aminoalkyl glucosaminide 4-phosphates (AGPs). Bioorg Med Chem Lett 9:2273-8.
15. Kaisho, T., and S. Akira. 2002. Toll-like receptors as adjuvant receptors. Biochim Biophys Acta 1589:1-13.
16. Kawai, T., O. Adachi, T. Ogawa, K. Takeda, and S. Akira. 1999. Unresponsiveness of MyD88-deficient mice to endotoxin. Immunity 11:115-22.
17. Kennedy, M., G. Mullen, C. Leifer, C. Lee, A. Mazzoni, K. Dileepan, and D. Segal. 2004. A complex of soluble MD-2 and lipopolysaccharide serves as an activating ligand for toll-like receptor 4. J Biol Chem.
18. Macela, A., J. Stulik, L. Hernychova, M. Kroca, Z. Krocova, and H. Kovarova. 1996. The immune response against Francisella tularensis live vaccine strain in Lps(n) and Lps(d) mice. FEMS Immunol Med Microbiol 13:235-8.
19. Masihi, K. N., W. Lange, W. Brehmer, and E. Ribi. 1986. Immunobiological activities of nontoxic lipid A: enhancement of nonspecific resistance in combination with trehalose dimycolate against viral infection and adjuvant effects. Int J Immunopharmacol 8:339-45.
20. Medzhitov, R., and C. Janeway, Jr. 2000. Innate immune recognition: mechanisms and pathways. Immunol Rev 173:89-97.
21. Miyake, K. 2004. Innate recognition of lipopolysaccharide by Toll-like receptor 4-MD-2. TRENDS in Microbiology 12.
22. Mullen, G. E. D., M. N. Kennedy, A. Visintin, A. Mazzoni, C. A. Leifer, D. R. Davies, and D. M. Segal. 2003. The role of disulfide bonds in the assembly and function of MD-2. PNAS 100:3919-3924.
23. Muller, J. M., H. W. Ziegler-Heitbrock, and P. A. Baeuerle. 1993. Nuclear factor kappa B, a mediator of lipopolysaccharide effects. Immunobiology 187:233-56.
24. Myers, K. R., A. T. Truchot, J. Ward, Y. Hudson, and J. T. Ulrich. 1990. A critical determinant of lipid A endotoxic activity, p. 145-156. *In* A. Nowotny, J. J. Spitzer, and E. J. Ziegler (ed.), Cellular and Molecular Aspects of Endotoxin Reactions. Elsevier Sciences Publishers B V, Amsterdam.
25. Neter, E. 1969. Endotoxins and the immune response. Curr Top Microbiol Immunol 47:82-124.
26. Nikolic-Zugic, J., and F. R. Carbone. 1991. Peptide presentation by class-I major histocompatibility complex molecules. Immunol Res 10:54-65.
27. O'Brien, A. D., D. L. Rosenstreich, I. Scher, G. H. Campbell, R. P. MacDermott, and S. B. Formal. 1980. Genetic control of susceptibility to Salmonella typhimurium in mice: role of the LPS gene. J Immunol 124:20-4.
28. O'Neill, L. A., A. Dunne, M. Edjeback, P. Gray, C. Jefferies, and C. Wietek. 2003. Mal and MyD88: adapter proteins involved in signal transduction by Toll-like receptors. J Endotoxin Res 9:55-9.
29. Persing, D. H., R. N. Coler, M. J. Lacy, D. A. Johnson, J. R. Baldridge, R. M. Hershberg, and S. G. Reed. 2002. Taking toll: lipid A mimetics as adjuvants and immunomodulators. Trends Microbiol 10:S32-7.
30. Poltorak, A., X. He, I. Smirnova, M. Y. Liu, C. V. Huffel, X. Du, D. Birdwell, E. Alejos, M. Silva, C. Galanos, M. Freudenberg, P. Ricciardi-Castagnoli, B. Layton, and B. Beutler. 1998. Defective LPS signaling in C3H/HeJ and C57BL/10ScCr mice: mutations in Tlr4 gene. Science 282:2085-8.
31. Poltorak, A., I. Smirnova, X. He, M. Y. Liu, C. Van Huffel, O. McNally, D. Birdwell, E. Alejos, M. Silva, X. Du, P. Thompson, E. K. Chan, J. Ledesma, B. Roe, S. Clifton, S. N. Vogel, and B. Beutler. 1998. Genetic and physical mapping of the Lps locus: identification of the toll-4 receptor as a candidate gene in the critical region [published erratum appears in Blood Cells Mol Dis 1999 Feb;25(1):78]. Blood Cells Mol Dis 24:340-55.
32. Re, F., and J. L. Strominger. 2003. Seperate Functional Domains of Human MD-2 Mediate Toll-Like Receptor 4-Binding and Lipopolysaccharide Responsiveness. The Journal of Immunology 171:5272-5276.

33. Rosenstreich, D. L., A. C. Weinblatt, and A. D. O'Brien. 1982. Genetic control ofresistance to infection in mice. Crit Rev Immunol 3:263-330.
34. Singh, J., S. S. Sidhu, G. S. Dhaliwal, G. R. Pangaonkar, A. S. Nanda, and A. S. Grewal. 2000. Effectiveness of lipopolysaccharide as an intrauterine immunomodulator in curing bacterial endometritis in repeat breeding cross-bred cows. Anim Reprod Sci 59:159-66.
35. Stover, A. G., J. Da Silva Correia, J. T. Evans, C. W. Cluff, M. W. Elliott, E. W. Jeffery, D. A. Johnson, M. J. Lacy, J. R. Baldridge, P. Probst, R. J. Ulevitch, D. H. Persing, and R. M. Hershberg. 2003. Structure-activity relationship of synthetic toll-like receptor 4 agonists. J Biol Chem.
36. Sweet, M. J., and D. A. Hume. 1996. Endotoxin signal transduction in macrophages. J Leukoc Biol 60:8-26.
37. Toshchakov, V., B. W. Jones, P. Y. Perera, K. Thomas, M. J. Cody, S. Zhang, B. R. Williams, J. Major, T. A. Hamilton, M. J. Fenton, and S. N. Vogel. 2002. TLR4, but not TLR2, mediates IFN-beta-induced STAT1alpha/beta-dependent gene expression in macrophages. Nat Immunol 3:392-8.
38. Triantafilou, M., K. Miyake, D. T. Golenbock, and K. Triantafilou. 2002. Mediators of innate immune recognition of bacteria concentrate in lipid rafts and facilitate lipopolysaccharide-induced cell activation. Journal of Cell Science 115:2603-2611.
39. Ulrich, J. M., KN; Lange, W. 1988. Mechanisms of nonspecific resistance to microbial infections induced by trehalose dimycolate (TDM) and monophosphoryl lipid A (MPL). p. 167-178. *In* K. N. M. a. W. Lange (ed.), Advances in the Biosciences, vol. 68. Pergamon Journals Ltd., Oxford.
40. Visintin, A., E. Latz, B. G. Monks, T. Espevik, and D. T. Golenbock. 2003. Lysines 128 and 132 enable lipopolysaccharide binding to MD-2, leading to Toll-like receptor-4 aggregation and signal transduction. J Biol Chem 278:48313-20.
41. Visintin, A., A. Mazzoni, J. A. Spitzer, and D. M. Segal. 2001. Secreted MD-2 is a large polymeric protein that efficiently confers lipopolysaccharide sensitivity to Toll-like receptor 4. Proc Natl Acad Sci U S A 98:12156-61.
42. Weiss, J. P., T. L. Gioannini, A. Teghanemt, D. Zhang, N. P. Coussens, W. Dockstader, and S. Ramaswamy. 2004. Isolation of an endotoxin-MD-2 complex that produces Toll-like receptor 4-dependent cell activation at picomolar concentrations. PNAS 101:4186-4191.
43. Woods, J. P., J. A. Frelinger, G. Warrack, and J. G. Cannon. 1988. Mouse genetic locus Lps influences susceptibility to Neisseria meningitidis infection. Infect Immun 56:1950-5.
44. Wright, C. S., S. C. Li, and F. Rastinejad. 2000. J Mol Biol 304:411-422.
45. Wright, C. S., Q. Zhao, and F. Rastinejad. 2003. J Mol Biol 331:951-964.
46. Yamamoto, M., S. Sato, H. Hemmi, K. Hoshino, T. Kaisho, H. Sanjo, O. Takeuchi, M. Sugiyama, M. Okabe, K. Takeda, and S. Akira. 2003. Role of adaptor TRIF in the MyD88-independent toll-like receptor signaling pathway. Science 301:640-3.

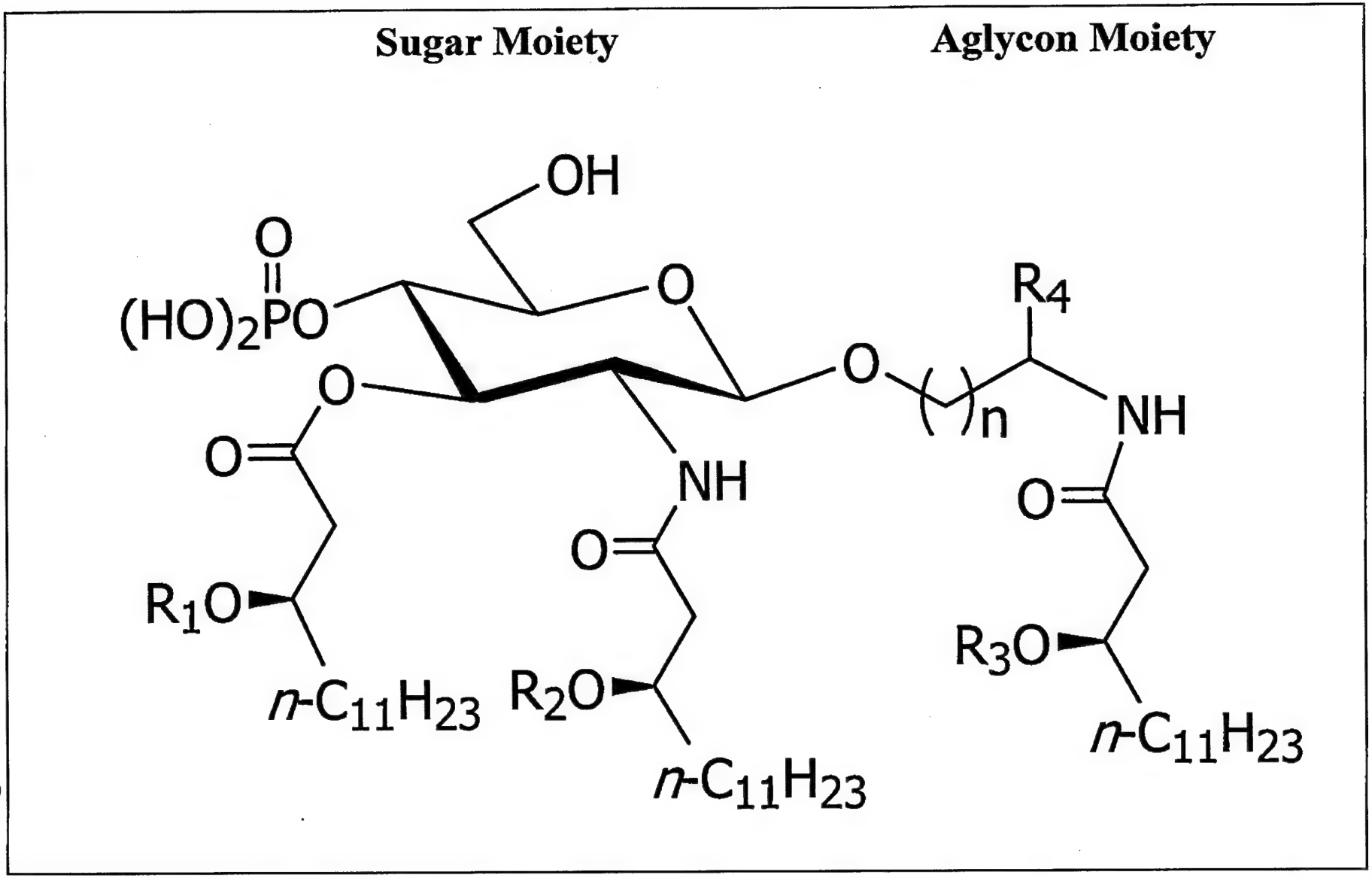
Sugar Moiety
Aglycon Moiety
OH
O
(HO)2PO
O
O
O
R4
O
n
NH
O
NH
O
R1O
R2O
R3O
n-C11H23
n-C11H23
n-C11H23

Figure 1

Table 1

AGP	R1 –Chain Length	R2 –Chain Length	R3 –Chain Length	R4 – Functional Group	Length of aglycon spacer (# carbon atoms = n+1)
CRX-526	6	6	6	CO_2H	2
CRX-554	7	7	7	CO_2H	2
CRX-555	8	8	8	CO_2H	2
CRX-537	9	9	9	CO_2H	2
CRX-527	10	10	10	CO_2H	2
CRX-538	11	11	11	CO_2H	2
CRX-560	12	12	12	CO_2H	2
CRX-512	14	14	14	CO_2H	2
CRX-566	6	10	10	CO_2H	2
CRX-565	10	6	10	CO_2H	2
CRX-569	10	10	6	CO_2H	2
CRX-568	6	6	10	CO_2H	2
CRX-567	6	10	6	CO_2H	2
CRX-570	10	6	6	CO_2H	2
CRX-529	14	14	14	H	2
CRX-525	14	14	14	H	3
CRX-557	14	14	14	H	4
CRX-571	14	14	14	H	6
CRX-524	10	10	10	H	2
CRX-522	10	10	10	$CONH_2$	2
CRX-545	10	10	10	CH_2OH	2
CRX-573	10	10	10	$CH_2CH_2CO_2H$	2

Figure 2A

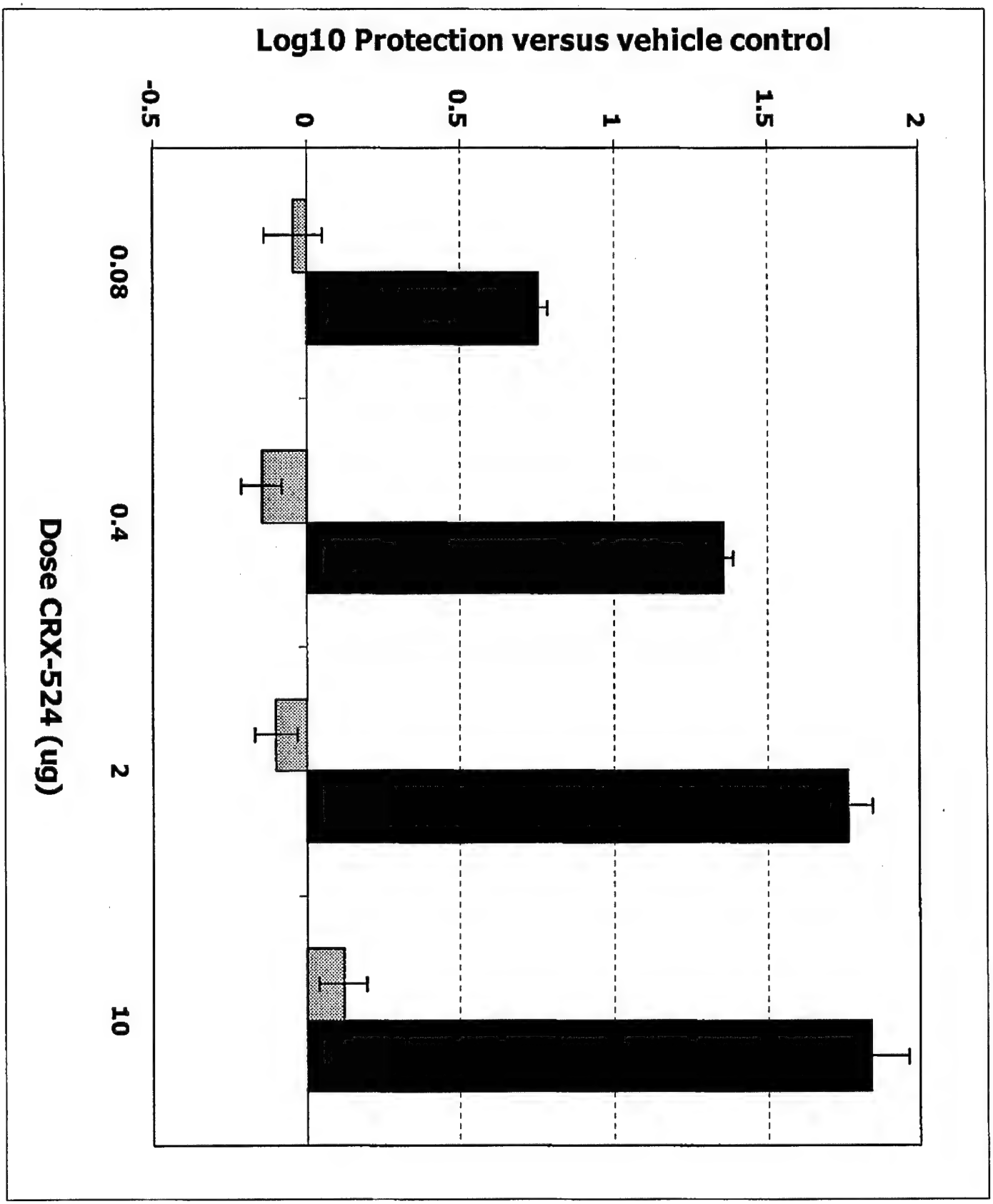
Log10 Protection versus vehicle control
-0.5
0
0.5
1
1.5
2
0.08
0.4
2
10
Dose CRX-524 (ug)

Figure 2B

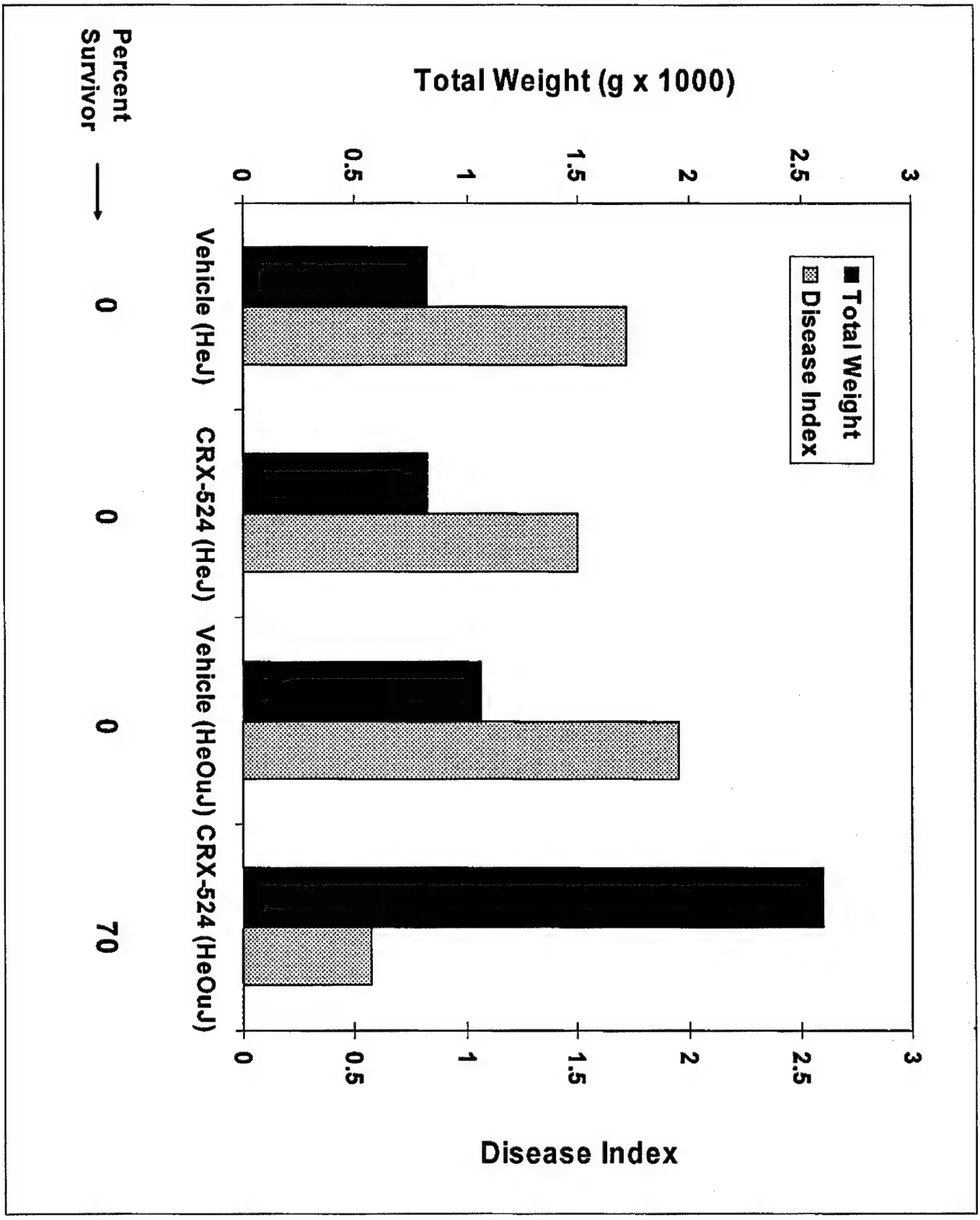
Total Weight (g x 1000)
0
0.5
1
1.5
2
2.5
3
Total Weight
Disease Index
Vehicle (HeJ)
CRX-524 (HeJ)
Vehicle (HeOuJ)
CRX-524 (HeOuJ)
Percent Survivor
0
0
0
70
Disease Index

Figure 3A

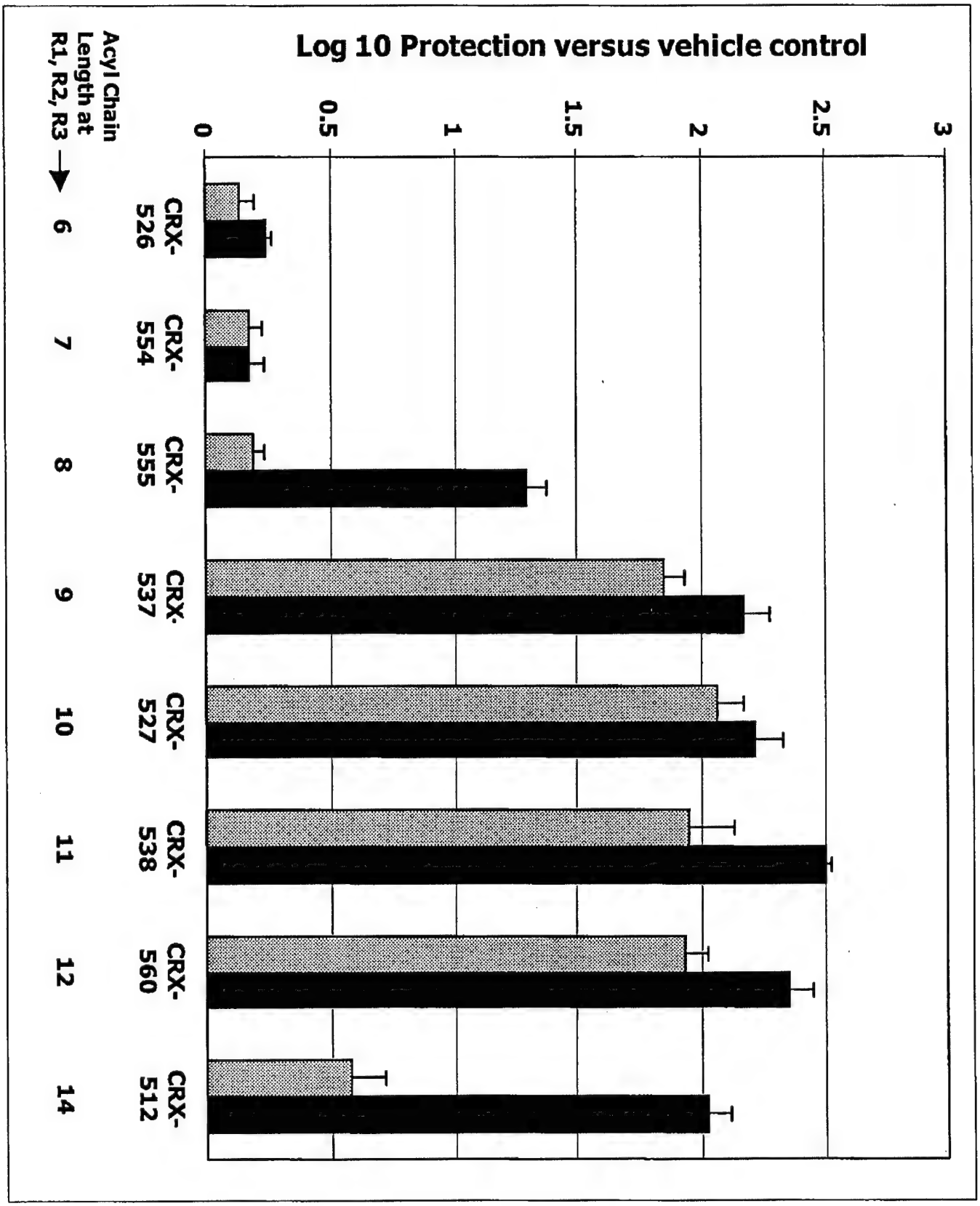
Log 10 Protection versus vehicle control
0
0.5
1
1.5
2
2.5
3
Acyl Chain Length at R1, R2, R3 →
CRX-526
6
CRX-554
7
CRX-555
8
CRX-537
9
CRX-527
10
CRX-538
11
CRX-560
12
CRX-512
14

Figure 3B

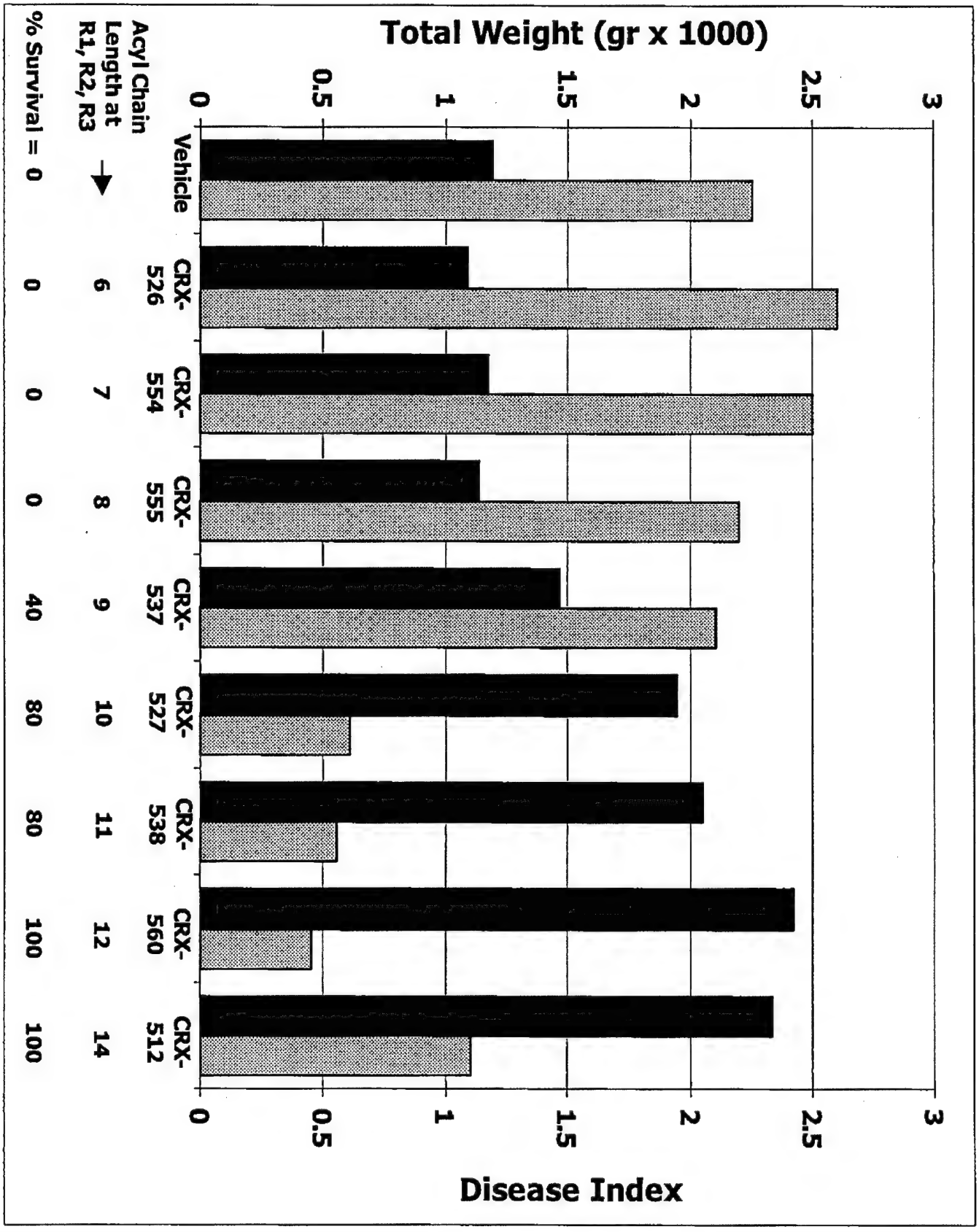
Total Weight (gr x 1000)
0
0.5
1
1.5
2
2.5
3
Vehicle
CRX-526
CRX-554
CRX-555
CRX-537
CRX-527
CRX-538
CRX-560
CRX-512
Acyl Chain Length at R1, R2, R3
6
7
8
9
10
11
12
14
% Survival = 0
0
0
0
40
80
80
100
100
Disease Index

Figure 4A

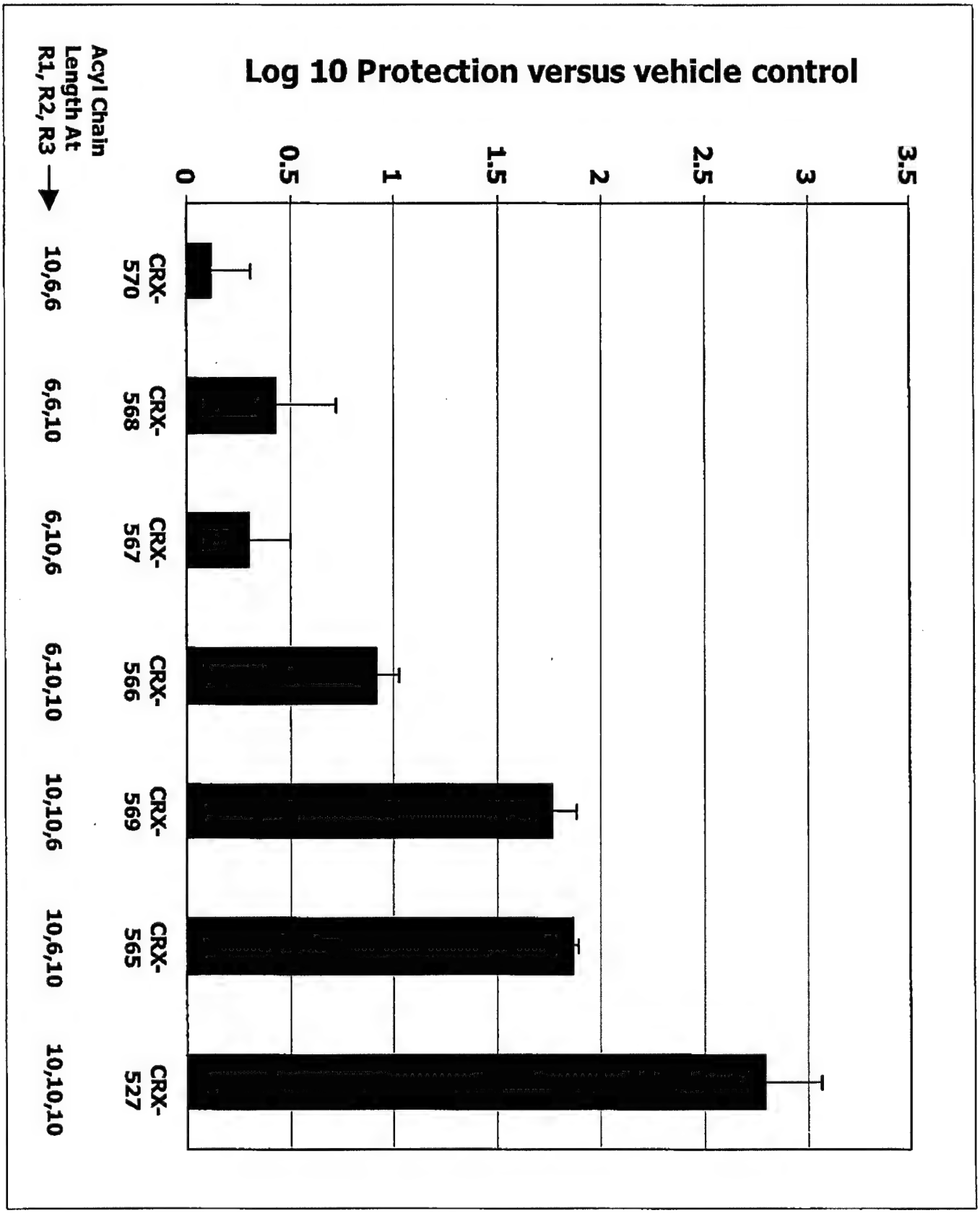
Log 10 Protection versus vehicle control
0
0.5
1
1.5
2
2.5
3
3.5
Acyl Chain Length At R1, R2, R3
CRX-570
10,6,6
CRX-568
6,6,10
CRX-567
6,10,6
CRX-566
6,10,10
CRX-569
10,10,6
CRX-565
10,6,10
CRX-527
10,10,10

Fig 4B

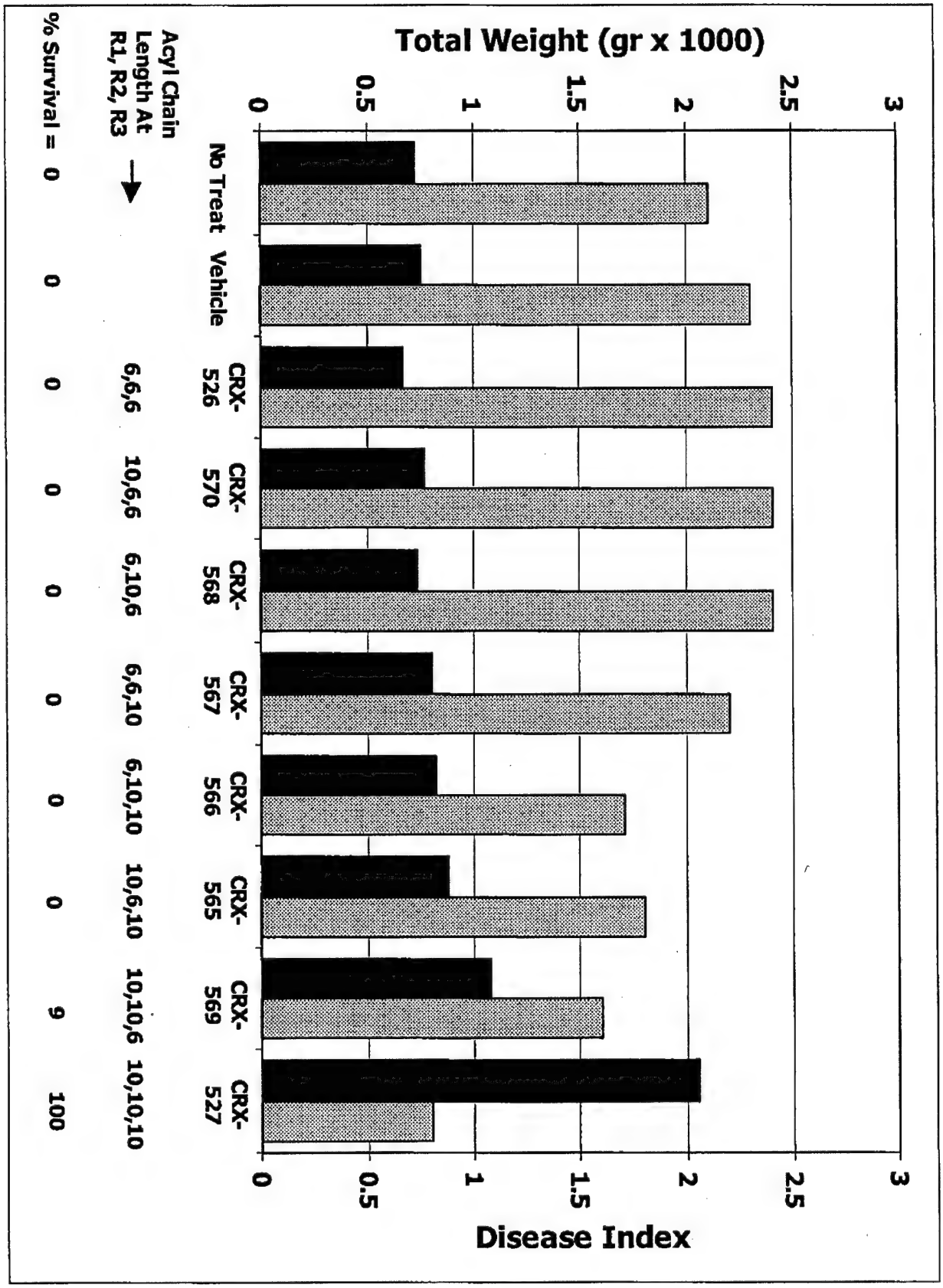
Total Weight (gr x 1000)
0
0.5
1
1.5
2
2.5
3
Disease Index
No Treat
Vehicle
CRX-526
CRX-570
CRX-568
CRX-567
CRX-566
CRX-565
CRX-569
CRX-527
Acyl Chain Length At R1, R2, R3
6,6,6
10,6,6
6,10,6
6,6,10
6,10,10
10,6,10
10,10,6
10,10,10
% Survival = 0 0 0 0 0 0 0 9 100

Figure 5

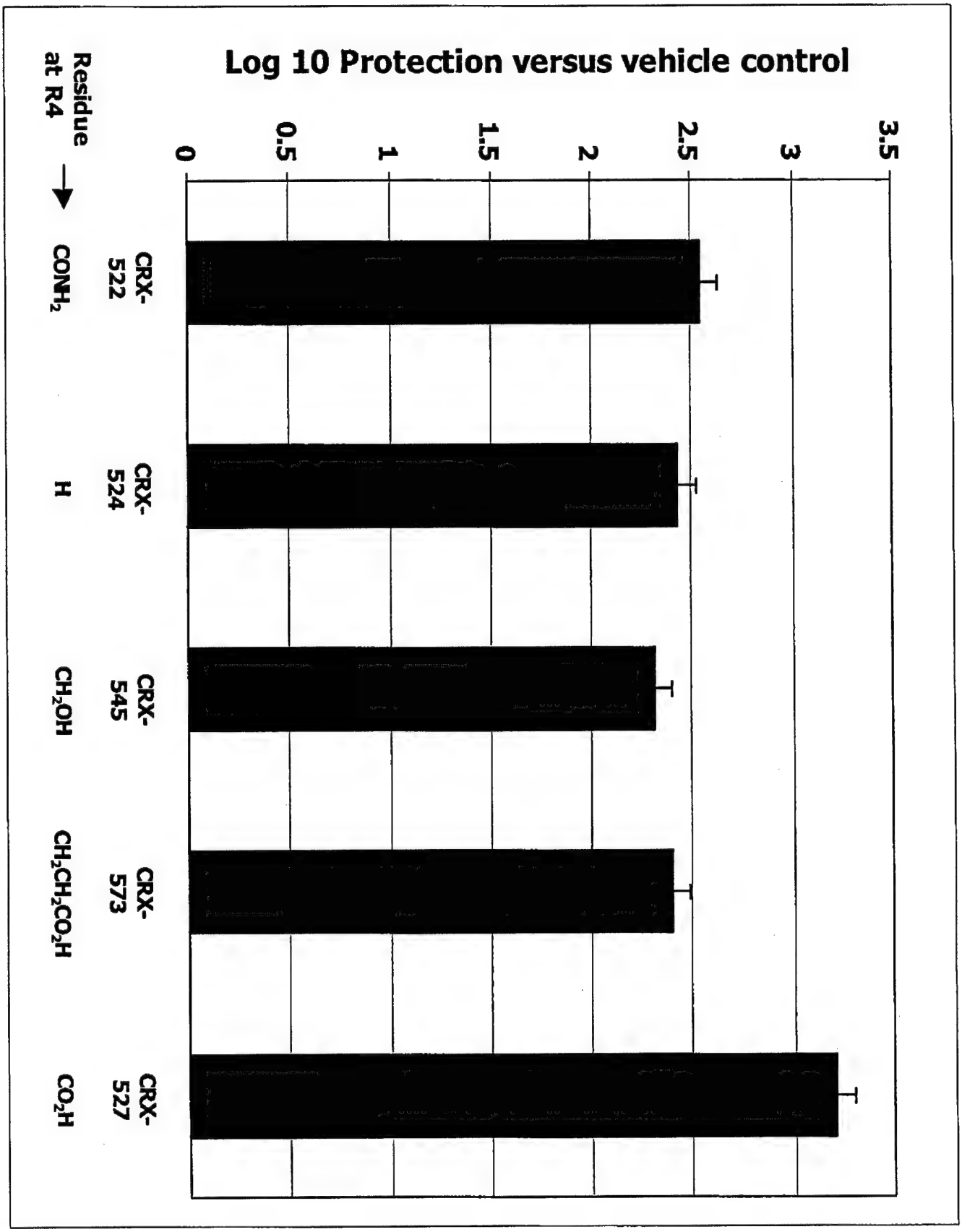
Log 10 Protection versus vehicle control
0
0.5
1
1.5
2
2.5
3
3.5
Residue at R4
CONH2
H
CH2OH
CH2CH2CO2H
CO2H
CRX-522
CRX-524
CRX-545
CRX-573
CRX-527

Figure 6

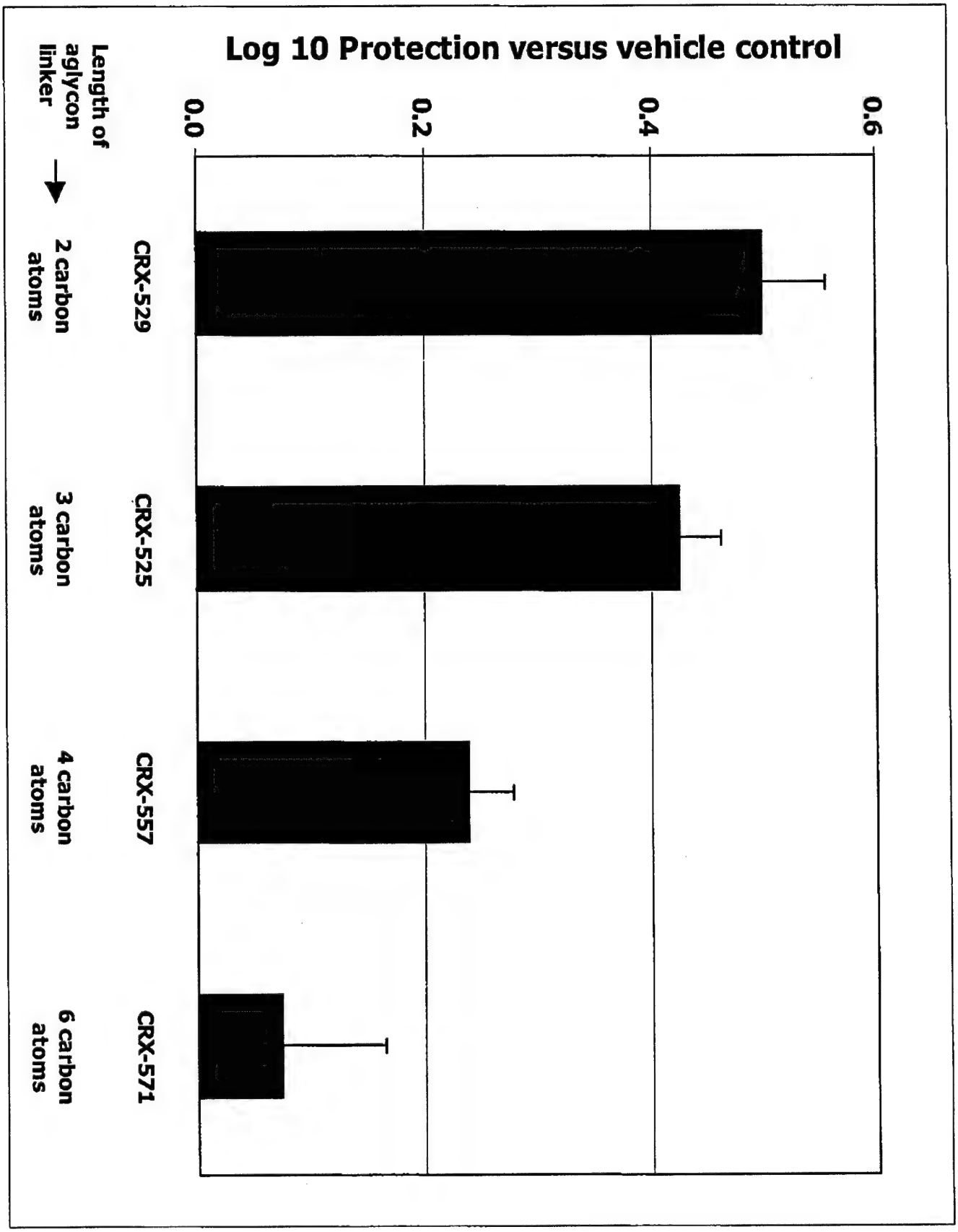
Log 10 Protection versus vehicle control
0.0
0.2
0.4
0.6
Length of aglycon linker
2 carbon atoms
3 carbon atoms
4 carbon atoms
6 carbon atoms
CRX-529
CRX-525
CRX-557
CRX-571

THE JOURNAL OF BIOLOGICAL CHEMISTRY
Vol. 279, No. 6, Issue of February 6, pp. 4440–4449, 2004
Printed in U.S.A.
© 2004 by The American Society for Biochemistry and Molecular Biology, Inc.

Structure-Activity Relationship of Synthetic Toll-like Receptor 4 Agonists*

Received for publication, September 30, 2003
Published, JBC Papers in Press, October 21, 2003, DOI 10.1074/jbc.M310760200

Axel G. Stöver‡, Jean Da Silva Correia§, Jay T. Evans¶, Christopher W. Cluff¶, Mark W. Elliott‡, Eric W. Jeffery‡, David A. Johnson¶, Michael J. Lacy¶, Jory R. Baldridge¶, Peter Probst‡, Richard J. Ulevitch§, David H. Persing‡‖‡‡, and Robert M. Hershberg‡‖**§§**

From the ‡Corixa Corporation, Seattle, Washington 98104, ¶Corixa Corporation, Hamilton, Montana 59840, §Department of Immunology, The Scripps Research Institute, La Jolla, California 92037, and ‖The Infectious Disease Research Institute, Seattle, Washington 98104

Important questions remain regarding the impact of variations in the structure of the lipid A portion of lipopolysaccharide on activation of cells via the Toll-like receptor 4 complex. We have studied a series of synthetic lipid A mimetic compounds known as aminoalkyl glucosaminide phosphates in which the length of the secondary acyl chain has been systematically varied. Using transcriptional profiling of human monocytes and responses of Toll-like receptor 4 complex cell transfectants, we demonstrate a clear dependence of length on secondary acyl chain on Toll-like receptor 4 activation. Compounds with secondary acyl chains less than eight carbons in length have dramatically reduced activity, and substitutions of the left-sided secondary acyl chain had the most important effect on the Toll-like receptor 4 agonist activity of these molecules. The structure-function relationships of these compounds assessed via the induction of chemokines and cytokines following *in vivo* administration closely mirrored those seen with cell-based studies. This novel set of synthetic lipid A mimetics will be useful for Toll-like receptor 4-based investigations and may have clinical utility as stand-alone immunomodulators.

The ability of an organism to protect itself from microbial challenge requires the rapid recognition of "pathogen-associated molecular patterns," conserved structural motifs found throughout the microbial world. Toll-like receptors are a family of structurally related surface receptors that play an important role in transducing an inflammatory signal in response to pathogen-associated molecular pattern recognition. Toll was originally identified as a *Drosophila* gene essential for embryonic development and antifungal immunity (1). Ten mammalian orthologues of Toll-like receptors (TLRs)[1] have been identified (2–4). While all TLRs have similar structural features (*e.g.* extracellular leucine-rich repeats and cytoplasmic domains with homology to the interleukin-1 (IL-1) receptor), each TLR alone as a homodimer (*e.g.* TLR4, TLR5, TLR7, and TLR9) or in combination with another TLR as a heterodimer (*e.g.* TLR1, TLR2, and TLR6) is capable of recognizing distinct pathogen-associated molecular patterns due to unique structural motifs (5). Interestingly several natural and synthetic TLR ligands have been demonstrated to have significant clinical utility both as vaccine adjuvants and as stand-alone immunomodulatory agents (6–8).

One of the best studied interactions between a microbial pathogen-associated molecular pattern and a TLR is the recognition of lipopolysaccharide (LPS), the major component of the outer membrane of Gram-negative bacteria, by TLR4 (for a review, see Ref. 9). Beutler and colleagues (10) first identified TLR4 as the "LPS receptor" by positional cloning studies in the LPS hyporesponder mouse strains C3H/HeJ and C57BL/10ScCr. The critical role of TLR4 in the transduction of an inflammatory signal by LPS has been confirmed in studies using mice with a deletion of TLR4. In addition, two additional proteins have been identified that interact with TLR4 and are implicated in LPS recognition, MD-2 and CD14. MD-2 is a secreted molecule that physically interacts with TLR4 (11), and genetic data (12) suggest that this molecule is required for LPS signaling via TLR4. CD14 is a glycosylphosphatidylinositol-linked membrane protein (devoid of a cytoplasmic signaling domain) with LPS binding activity. Collectively TLR4, MD-2, and CD14 form a trimolecular LPS receptor complex. The delineation of the precise molecular events associated with LPS binding and initiation of the signaling cascades via TLR4 remains an area of intense investigation.

Lipid A is the active component of the LPS molecule that stimulates the TLR4 receptor complex (13). Lipid A structures show considerable variability between bacterial species, and individual Gram-negative species can modulate the structure of the lipid A on their surface in the context of infection (14, 15). These structural differences, in particular the degree of acylation, can dramatically modify their proinflammatory capacity. In general, highly acylated (*e.g.* hexa-acylated lipid A from *Escherichia coli* or *Salmonella* species) tend to be potent inflammatory stimulators, while less acylated lipid A structures (*e.g.* $lipid_{IVA}$ and lipid A from certain periodontal bacteria such as *Porphyromonas gingivalis*) tend to be less inflammatory or even display LPS antagonist activity (16). Because these studies have generally used natural biological preparations of LPS,

* This work was supported by Defense Advanced Research Projects Agency Contract N66001-01-C-8007 (to D. H. P.). The costs of publication of this article were defrayed in part by the payment of page charges. This article must therefore be hereby marked "*advertisement*" in accordance with 18 U.S.C. Section 1734 solely to indicate this fact.

** Both authors contributed equally to this work.

‡‡ To whom correspondence and reprint requests may be addressed: Corixa Corp., 1124 Columbia St., Suite 200, Seattle, WA 98104. Tel.: 206-754-5879; Fax: 206-754-5917; E-mail: persing@corixa.com.

§§ To whom correspondence may be addressed: Dendreon Corp., 3005 First Ave., Seattle, WA 98121. Tel.: 206-829-1625; Fax: 206-219-7200; E-mail: rhershberg@dendreon.com.

[1] The abbreviations used are: TLR, Toll-like receptor; IL, interleukin; SAC, secondary acyl chain; AGP, aminoalkyl glucosaminide phosphate; LPS, lipopolysaccharide; ELISA, enzyme-linked immunosorbent assay; TNF, tumor-necrosis factor; RANTES, regulated on activation normal T cell expressed and secreted; MCP1, macrophage chemoattractant protein 1; MIP, monocyte inhibitory protein.

This paper is available on line at http://www.jbc.org

detailed structure-function studies of the interaction between lipid A and the TLR4 complex have not been possible. Important questions remain regarding the precise region of the lipid A molecule that is required to stimulate the TLR4 complex and the effect of specific changes in the lipid A molecule on CD14 and/or MD-2 dependence of TLR4 stimulation and the transcriptional responses that ensue. To address these questions, we have studied a series of synthetic lipid A mimetic compounds known as aminoalkyl glucosaminide phosphates (AGPs) (17). The AGP classes of lipids are monosaccharide lipid A mimetics of a biologically active hexa-acylated component present in the widely used adjuvant monophosphoryl lipid A (MPL® adjuvant). Because AGPs are prepared by chemical synthesis, we have been able to generate a library of closely related molecules with defined modifications in the acyl chain length. Using transcriptional profiling of human monocytes, responses of TLR4 receptor complex cell transfectants, and *in vivo* cytokine and chemokine responses, we were able to perform a detailed structure-function analysis of these hexa-acylated lipid A mimetics. Herein we demonstrate a clear dependence of TLR4 agonist activity on normal fatty acid ("secondary") chain length with changes in either of the sugar secondary acyl chains having a more dramatic effect on function of the molecules than changes in the aglycon secondary acyl chain. Furthermore we highlight the potential utility of certain members of this novel class of compounds as stand-alone immunomodulators based on their TLR4 agonist activity.

EXPERIMENTAL PROCEDURES

Chemical Synthesis of AGPs—The compounds used in this study are shown in Fig. 1 and were synthesized as described previously (17). Aminoalkyl glucosaminide 4-phosphates or AGPs are a class of lipid A mimetics in which the reducing sugar of lipid A has been replaced with an *N*-acylated aminoalkyl aglycon unit. The AGPs evaluated in this study (Fig. 1) contain an L-serine-based aglycon unit as well as three (*R*)-3-*n*-alkanoyloxytetradecanoyl residues comprised of even-numbered normal fatty acyl chains between 6 and 14 carbon atoms in length. The AGPs were prepared as described previously by a highly convergent method, which allowed chemical differentiation of the hydroxyl and amino groups and sequential introduction of the (*R*)-3-*n*-alkanoyloxytetradecanoyl residues. The seryl AGPs were purified by flash chromatography on silica gel (to >95% purity) and analyzed as their triethylammonium salts by standard analytical methods.

Reagents—LPS from *E. coli* 0127:B8 was used as a positive control stimulant in all experiments and was purchased from Sigma, reconstituted in water at a concentration of 1 mg/ml, and frozen at −20 °C until use. Recombinant human interferon γ was purchased from R&D Systems (Minneapolis, MN), reconstituted in phosphate-buffered saline, stored at −80 °C, and used at 1000 units/ml to activate macrophages.

Human Monocyte-derived Macrophages—Human peripheral blood mononuclear cells were derived by apheresis from healthy donors, purified over a Ficoll Hypaque 1.077 gradient, and stored in liquid nitrogen until use. Monocyte-derived macrophages were generated from adherent peripheral blood mononuclear cells as described previously (18). On the 5th day of culture, the medium was replaced with fresh medium supplemented with the indicated AGP concentrations. After 24 h of culture, the supernatant was removed and frozen at −20 °C until determination of cytokines by enzyme-linked immunosorbent assay (ELISA). To prepare RNA for microarray experiments, the cell concentration was adjusted to 8×10^6 cells/ml, and 1 ml of this cell suspension was placed into each well of a 12-well plate (Corning, Corning, NY). On the 5th day, the medium was replaced with fresh medium supplemented with an AGP at 1 μg/ml. After 6 h of stimulation, the medium was carefully removed from all wells of the same stimulation, pooled, frozen, and then analyzed by ELISA for the presence of tumor-necrosis factor-α (TNF-α). RNA was isolated from adherent cells by adding 0.5 ml of TRIzol (Invitrogen) to each well of the plates, the cells were resuspended by pipetting up and down repeatedly, and all liquid was immediately frozen at −80 °C. For RNA isolation, the samples were thawed, and the cells were lysed by adding 1-mm zirconia beads (BioSpec Products, Bartlesville, OK) and vortexing for 45 s. After a chloroform extraction, the RNA was precipitated, and the integrity was checked by gel electrophoresis.

RNA Amplification, cDNA Synthesis, and Probe Labeling—Total RNA was amplified by the modified Eberwine ("antisense") RNA amplification protocol (19–21). All reagents were purchased from Invitrogen. After amplification, the concentration of antisense RNA was measured by spectrophotometry, and the quality was determined by gel electrophoresis. Amplified RNA (1.2 μg) was diluted in 16 μl of water and used as template for cDNA synthesis. All reagents were purchased from Invitrogen. Probes were labeled as described elsewhere (22).

Transfection of HeLa Cells and Reporter Assay—A HeLa cell transient transfection system was used to determine the roles of human TLR4, CD14, and MD-2 in the cellular response to AGPs. HeLa cells were maintained in Dulbecco's modified Eagle's medium supplemented with 10% fetal bovine serum, 2 mM glutamine, 100 units/ml penicillin, and 10 μg/ml streptomycin (all from Invitrogen). HeLa cells were plated at 1×10^5 cells/well in a 12-well plate and transfected with 50 ng of IL-8 promoter-driven luciferase reporter and 10 ng of the indicated plasmids (23). The human CD14 cDNA used in this study was described previously (24). Human TLR4 cDNA was a kind gift of Dr. C. Janeway. Eighteen hours after transfection, cells were stimulated for 6 h, lysed, and then analyzed for luciferase and β-galactosidase activity. A β-galactosidase construct was used for the normalization of enzyme activity (23). 293 cells were stably transfected with TLR2, then transiently transfected with TLR1 and TLR6, and exposed to heat-killed *Staphylococcus aureus* at a concentration of 1 μg/ml.

Cytokine ELISA—Monocyte-derived macrophages were cultivated as described elsewhere (18). After 5 days of culture, the medium was removed and replaced with fresh medium to which AGPs were added at the concentrations indicated. After 24 h, the supernatants were collected and stored at −20 °C until the day of analysis. Supernatants were analyzed for TNF-α by ELISA assay using an anti-human TNF-α antibody and a biotinylated anti-human TNF-α antibody (BD Biosciences).

Clone Selection and PCR—Numerous human genes of interest were selected from the literature, and their cDNAs and expressed sequence tags were identified in GenBank™. This list of genes of interest included cytokines and cytokine receptors, chemokines and chemokine receptors, TLRs and TLR-associated proteins, adhesion molecules, kinases and phosphatases involved in signaling, transcription factors, a number of NFκB-controlled genes, apoptosis-related genes, and numerous miscellaneous genes of interest. Most of the cDNAs and expressed sequence tags used in this study were purchased from Research Genetics Invitrogen. A small number of clones were extracted form our in-house clone collections. *E. coli* clones were streaked on Luria-Bertani (LB) agar plates supplemented with an appropriate antibiotic, and single colonies served as the inoculum for the high throughput cultivation on 96-well plates (100 μl/well). After 24 h of cultivation, 1 μl of this cell suspension was collected and used as template to amplify plasmid inserts by PCR. PCR products were then screened on 1% agarose gels, purified using 96-well multiscreen PCR plates (Millipore, Bedford, MA), and eluted with 50% Me_2SO, resulting in a concentration of DNA averaging 150 ng/μl. Finally PCR products were submitted for nucleotide sequencing to our in-house sequencing facility. The nucleotide sequence was submitted for BLAST search against GenBank™ to identify the human gene. Suitable PCR products were transferred to 384-well plates and stored at −80 °C prior to printing.

Printing of Arrays—Approximately 1200 PCR products and controls were spotted onto 42 CMT-GAPS2 coated slides in triplicate (Corning) using an Affymetrix 417 arrayer (Affymetrix, Santa Clara, CA). Humidity control was maintained in the range of 45–52% using an ultrasonic humidifier (Model 696, Sunbeam, Boca Raton, FL). Following printing, the arrayed slides were UV cross-linked at 90 mJ overnight (Stratalinker, Stratagene, La Jolla, CA) and baked for 2 h at 80 °C. Prior to hybridization, the slides were prehybridized for a minimum of 45 min in a buffer consisting of 5× SSC, 1% bovine serum albumin, 25% formamide, and 0.1% SDS. Overall array quality was confirmed by hybridization to a Cy3 end-labeled, M13-reverse oligonucleotide (Qiagen Operon, Alameda, CA).

Probe Labeling and Hybridization—Fluorescently labeled probes were generated from 1.5 μg of antisense RNA amplified as described above. The Cy3- (treated) or Cy5 (untreated)-labeled probes were generated using the amino-allyl method described elsewhere (25) and included in the microarray resources section of The Institute of Genomic Research (TIGR) Web site. To determine the sensitivity of the microarray, validate the labeling reaction, and test RNA quality, *Arabidopsis* control RNA (Spot Report-3, Stratagene) was spiked into each probe sample prior to cDNA synthesis. The corresponding *Arabidopsis* cDNAs were arrayed on each slide with a variety of human housekeeping control genes (β-actin, α-tubulin, phospholipase A_2, transferrin, riboso-

mal protein s9, highly basic protein, and major histocompatibility complex class 1) in each of the four quadrants of the array. Probes were checked for successful labeling by spectrophotometry using a 2- or 5-μl cuvette and a Genespec 3 unit (MiraiBio Inc., Alameda, CA). Hybridizations and posthybridization washes were carried out as described by the slide manufacturer (Corning) for Me_2SO arrays using a formamide hybridization buffer. Hydrophobic coverslips (Hybrislip, Grace Biolabs, Bend, OR) were used in place of glass coverslips. Two individual hybridizations were performed for each sample with similar results, and results of one hybridization are shown.

Microarray Data Acquisition and Analysis—Following washing of arrays, slides were scanned using an Affymetrix 418 microarray scanner and saved as 16-bit TIFF files (Affymetrix). The Cy3 and Cy5 images for each array were overlaid, gridded, and quantified using Imagene software (Biodiscovery, Marina del Rey, CA). Hybridization data quality was evaluated using the mean signal to noise ratios for all cDNA spots, the mean signal to noise ratios for control spots, treated to untreated ratios for control, and spike-in spots and spot morphology. Normalization and further data analysis was performed using GeneSpring (Silicon Genetics, Redwood City, CA). The hybridization intensity of each spot was normalized to the median intensity of all non-control spots on the array. One-sample Student's *t* test *p* values (Table I) were calculated by GeneSpring to determine whether the mean normalized expression levels were statistically different from 1.0 (treated *versus* untreated).

In Vivo Characterization of AGPs—To test whether AGPs stimulate the innate immune system *in vivo*, each of the AGPs and LPS were dissolved in triethylammonium salts and injected at various concentrations into BALB/c mice (Jackson Laboratories, Bar Harbor, ME) via the intravenous route (tail vein, five mice/group). Blood was collected 2 h following administration of the compounds, and the concentrations of serum cytokines (TNF-α, IL-1β, IL-6, and IL-10) and chemokines (RANTES, MCP1, MIP1α, and KC) were determined using a custom Lincoplex cytokine array (Linco Research, St. Charles, MO) and a Luminex 100 IS system (Luminex, Austin, TX). The results presented are the average of five mice/group with the error bars based on S.E. values.

RESULTS

Chemical Structure of the Synthetic Lipid A Mimetics, AGPs—We previously described the synthesis of the AGP class of compounds, which are composed of a monosaccharide unit glycosidically linked to an *N*-acylated aminoalkyl aglycon unit (17). Chemical synthesis readily permits variations in the fatty acid residues and the chemical nature and charge of the aglycon unit. In this study, we focused on changes in acyl chain length within a family of AGP molecules possessing an L-serine-based aglycon unit, the so-called "L-seryl" family. As shown in Fig. 1, every member of this family has 14 carbon atoms in the "primary" fatty acid, which is the β-hydroxy fatty acid attached directly to the AGP backbone. β-Hydroxymyristic acid is the most common of the primary fatty acids present in lipid A. With respect to the normal or secondary fatty acid chain length, we have synthesized compounds with 6-, 8-, 10-, 12-, and 14-carbon acyl chains (Fig. 1*A*). In addition, we prepared a series of hybrid molecules based on the structure of CRX-527 (10-10-10) in which one or two of the 10-carbon acyl chains of CRX-527 (10-10-10) have been replaced with a six-carbon acyl chain (Fig. 1*B*). Collectively these compounds were used in a variety of cell-based and an *in vivo* model to determine structure-activity relationships related to AGP acyl chain length and stimulation via TLR4.

Cytokine Production by Human Monocytes Is Dependent on AGP Acyl Chain Length and Position—While TLR4 is expressed on a variety of hematopoietic and non-hematopoietic cells, monocytes and macrophages have been frequently studied as physiologically relevant LPS-sensitive cells (26, 27). The hallmark of monocyte and macrophage activation through Toll-like receptors is the activation of NFκB and the subsequent release of TNF-α and other cytokines and chemokines (28). To determine the activity of our synthetic lipid A mimetic, AGPs, we exposed human monocyte-derived macrophages (21) from three donors to various concentrations of these compounds and measured released TNF-α in the supernatant by ELISA. Fig. 2 shows the ELISA results for TNF-α presented as the average response from three donors.

As shown in Fig. 2*A*, the amount of TNF-α release in response to the AGPs varied as a function of the secondary acyl chain (SAC) length. Specifically treatment of cells with AGPs carrying SACs 10 carbons or greater in length (CRX-527 (10-10-10), CRX-560 (12-12-12), and CRX-512 (14-14-14)) resulted in the production of TNF-α (Fig. 2*A*). In marked contrast, the compounds with SACs less than 10 carbons (CRX-526 (6-6-6) and CRX-555 (8-8-8)) did not elicit the production of TNF-α by the same cells (Fig. 2*A*) alone or with co-incubation of the cells with interferon γ (data not shown). Co-administration of interferon γ to the cells in addition to the respective AGPs augmented the induced levels of TNF-α observed but did not alter the relationship between acyl chain length and activity (data not shown). We consistently found that the compound with the 10-carbon SAC (CRX-527 (10-10-10)) was the most potent tested, maximally active at a concentration of less than or equal to 1 ng/ml. Compounds with SAC lengths of 12 and 14 carbon atoms were considerably less potent than CRX-527 (10-10-10) and showed a more clear dose-response relationship in the ng/ml to μg/ml concentration range (Fig. 2*A*). The same potency relationship was seen when these compounds were tested for the production of TNF-α using the U937 and THP-1 monocyte/macrophage cell lines (data not shown).

These data highlighted a clear dependence on SAC length with regard to the stimulatory capacity of synthetic lipid A mimetics. Given the fact that CRX-526 (6-6-6) showed no activity in these assays and CRX-527 (10-10-10) was maximally active at less than or equal to 1 ng/ml, we evaluated compounds in which six-carbon acyl chains (hexanoic acid) were inserted into each position in CRX-527 (10-10-10). These compounds, shown in Fig. 1*B*, allowed us to further define the structural features of the lipid A molecule required for macrophage stimulation. As shown in Fig. 2*B*, substitution of one or two hexanoic acid chains into CRX-527 (10-10-10) dramatically reduced the activity of the molecule with regard to TNF-α production by human macrophages.

Analysis of Transcriptional Activation of Macrophages by AGPs—While our data clearly demonstrate the ability of AGPs to induce TNF-α production in human macrophages, we were interested in evaluating the structure-activity relationship associated with the more complex transcriptional response following stimulation with AGP compounds.

To this end, we developed a custom microarray containing ~300 inflammatory target genes with each target arrayed in triplicate to allow quality control and statistical analysis on each microarray slide. Total RNA derived from human macrophages stimulated with individual AGPs for 6 h was used as a template to generate Cy3- or Cy5-labeled cDNA used for hybridization to the microarray. In preliminary experiments, the 6-h time point was observed to result in the best signal to noise ratio of the majority of genes tested (data not shown). Identical cells stimulated with LPS from *E. coli* 0127:B8 served as a positive control. As shown in Fig. 3*A*, LPS stimulated the expression of 64 array elements more than 2-fold (*t* test *p* value for each element ≤0.05) compared with the complete lack of induced gene expression seen in the negative control (triethylammonium salts vehicle).

The analysis of the AGP-stimulated macrophage gene expression on this microarray confirmed the strict dependence on SAC length seen with the induction of TNF-α release by these cells. Specifically CRX-526 (6-6-6) did not induce any genes on

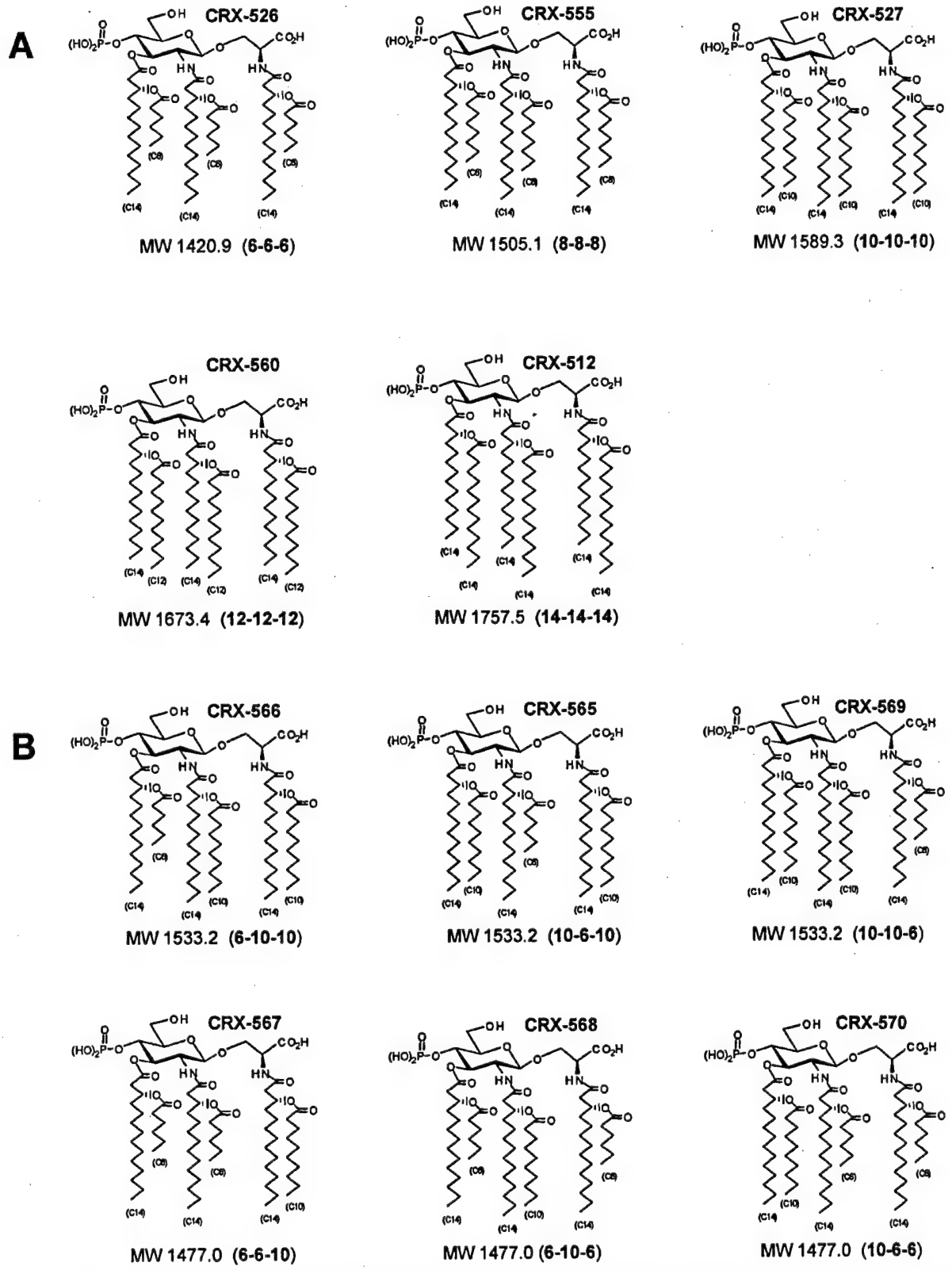

FIG. 1. **Chemical structure of the AGPs used in this study.** *A*, structures of AGP compounds in which the SACs within a given compound are the same length. *B*, structures of "substituted" AGP compounds in which SACs in a given compound are a combination of 10 and 6 carbons in length. *Numbers* in *parentheses* indicate the length of the SAC. All of the primary acyl chains are 14 carbons in length. *MW*, molecular weight in Daltons.

the array. While CRX-555 (8-8-8) did not induce TNF-α release in the macrophages when assayed by ELISA (Fig. 2*A*), we observed the induction of eight genes on the microarray following stimulation with this compound in the same cells. A dramatic increase in the transcriptional activation was seen with 68 genes induced by CRX-527 (10-10-10) and 59 and 50 genes

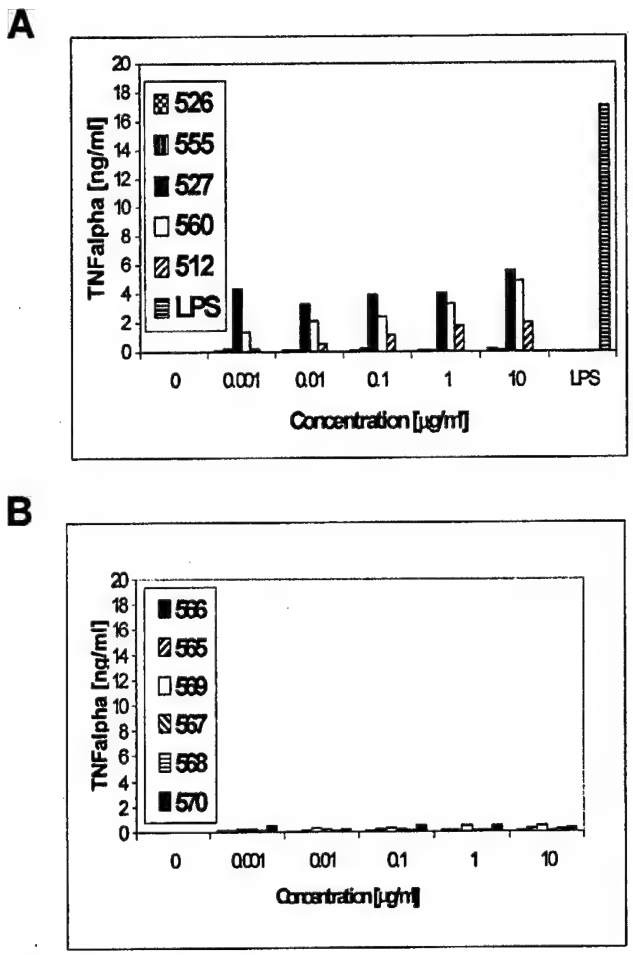

FIG. 2. **Cytokine release by human monocyte-derived macrophages.** *A*, AGPs with homogenous secondary acyl side chains of increasing length (CRX-526 (6-6-6), CRX-555 (8-8-8), CRX-527 (10-10-10), CRX-560 (12-12-12), and CRX-512 (14-14-14)). The positive control, LPS, was only tested at the concentration of 10 µg/ml. *B*, AGPs with heterogeneous secondary acyl chains (CRX-565 (10-6-10), CRX-566 (6-10-10), CRX-567 (6-6-10), CRX-568 (6-10-6), CRX-569 (10-10-6), and CRX-570 (10-6-6)). TNF-α was determined in the culture supernatants by ELISA after 24 h of stimulation with AGPs at the concentrations indicated.

induced by CRX-560 (12-12-12) and CRX-512 (14-14-14), respectively.

We also evaluated the transcriptional responses elicited by the substituted AGP compounds using the same microarray. As shown in Fig. 3*A*, the substitution of two decanoic acid chains with hexanoic acid chains dramatically resulted in a loss of stimulatory activity compared with CRX-527 (10-10-10). Interestingly, given the increased sensitivity of the microarray analysis compared with the TNF-α ELISA data, several of the compounds with substitutions of a single hexanoic acid onto the 10-10-10 backbone induced modest transcriptional responses (Fig. 3*A*). Specifically this partial response was seen with CRX-565 (10-6-10) and CRX-569 (10-10-6), compounds in which the left-sided decanoic acid was preserved. In marked contrast, CRX-566 (6-10-10) was essentially non-stimulatory, mirroring the lack of responsiveness seen with the doubly substituted compounds or CRX-526 (6-6-6).

The list of 68 genes affected by CRX-527 (10-10-10) is presented in Table I. Because stimulation with CRX-527 (10-10-10) resulted in the most significant transcriptional response of all of the AGPs tested, we focused our comparative analysis on the genes that were either up- or down-regulated by CRX-527

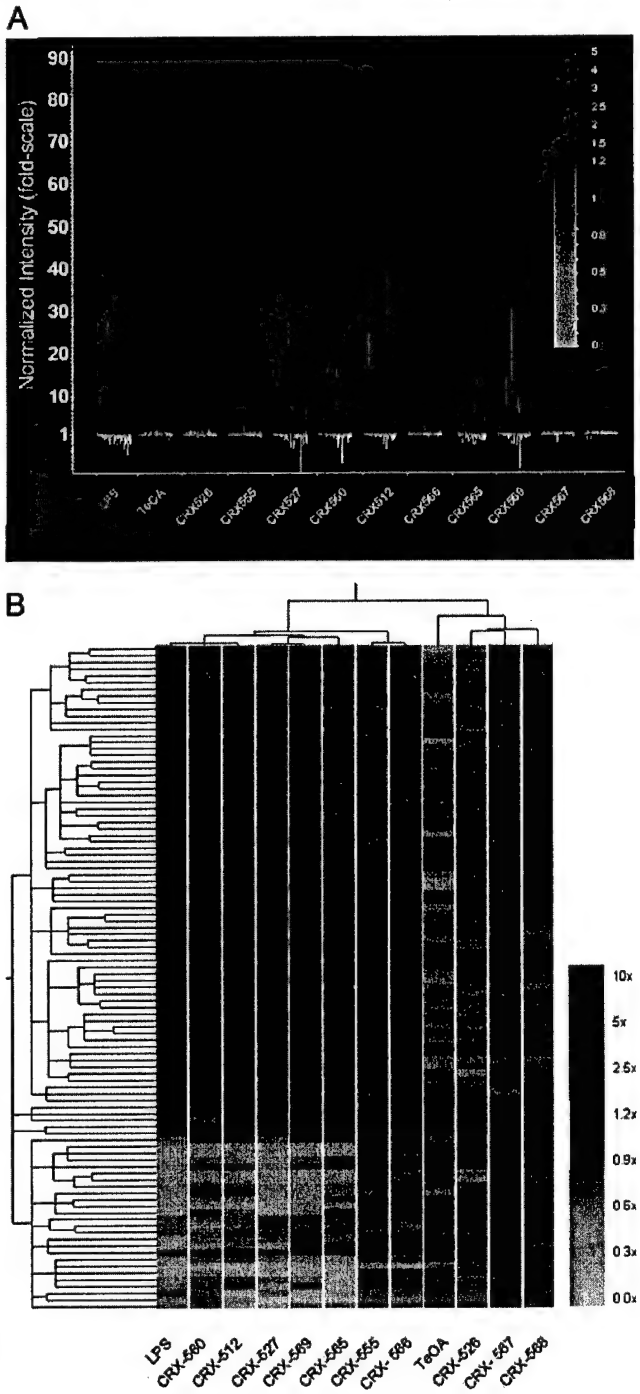

FIG. 3. *A*, bar graph of genes affected by AGPs in human monocyte-derived macrophages. Each *bar* represents a gene; its length indicates the normalized intensity (-fold scale), and its color indicates up-regulation (*red*) or down-regulation (*green*). *B*, dendrogram (hierarchical clustering) of genes affected by CRX-527 (10-10-10) and other stimuli in human monocyte-derived macrophages. Each *box* represents one microarray element. Its color indicates up-regulation (*red*) or down-regulation (*green*). *Gray boxes* indicate lack of data. *TeOA*, triethylammonium salts.

(10-10-10) with a *t* test *p* value of less than or equal to 0.05. Organization of the expression data by performing hierarchical clustering (29) into a gene tree was performed and is shown in Fig. 3*B*. The profiles of gene induction by LPS and CRX-527 (10-10-10) are very similar with LPS being a modestly stronger stimulant. Two exceptions to this rule are the small inducible cytokine SCYB10 and the monokine induced by interferon γ

TABLE I
Gene expression

Expression data (-fold scale) of genes affected in monocyte-derived macrophages are shown. Genes were selected based on stimulation with CRX-527 (10-10-10) (expression of ≥2- or ≤-0.5-fold with a *t* test *p* value ≤0.05) and are compared with CRX-560 (12-12-12), CRX-560 (14-14-14), and LPS. MIG, monokine induced by interferon γ; ICAM1, intercellular adhesion molecule 1; SOCS-1, suppressor of cytokine signaling-1; TRAF1, tumor necrosis factor receptor-associated protein 1; IRF1, interferon regulatory factor 1; TNFR, TNF receptor; TGF, transforming growth factor; STAT, signal transducers and activators of transcription; COX-2, cyclooxygenase-2; TAP1, transporter associated with antigen processing 1; HSP, heat shock protein; CSF-1, colony-stimulating factor-1.

Gene	Treatment			
	CRX-527 (10-10-10)	CRX-560 (12-12-12)	CRX-512 (14-14-14)	LPS
Chemokines				
SCYB10	46.4	6.6	3.1	23.4
SCYA8	33.4	25.3	19.6	41.6
SCYA4	23.6	16.6	14.5	23.2
Exodus-1	22.0	31.9	33.6	42.2
SCYB11	20.8	3.9	1.3	10.7
RANTES	16.3	14.7	6.0	24.5
MIP3α	15.3	11.6	19.0	34.9
SCYA1	13.0	17.0	9.6	20.4
MIG	11.1	2.2	1.3	5.2
MIP3β	7.9	7.4	2.4	11.0
SCYB13	7.7	7.0	1.3	10.4
IL-8	3.6	6.4	9.2	7.0
MIP2α	3.5	7.2	7.4	8.3
SCYA13	2.4	2.1	1.9	2.8
CCR5	2.2	1.6	1.4	1.5
Cytokines				
IL-6	27.0	17.4	25.5	61.1
IL-2 receptor-α	19.4	17.2	11.1	27.5
SOCS-1	19.3	5.3	4.9	6.9
TNF-α	10.8	5.6	7.6	9.5
TRAF1	8.1	4.5	4.6	6.8
TNFAIP3	8.1	3.8	3.0	5.5
TNFRSF5	5.5	4.0	3.0	4.8
IL-1RA	3.5	2.2	1.0	2.9
IRF1	3.3	2.8	1.9	3.0
IL-15	2.9	2.0	1.7	2.9
TNFRSF1B	2.8	2.7	1.9	2.8
Surface receptors				
CD38	20.0	12.3	3.8	20.3
CD80	4.2	2.6	2.7	5.7
CD44	4.1	3.5	2.6	3.6
ICAM1	3.5	2.9	2.9	3.1
Prostaglandin I_2 receptor	2.9	2.6	2.7	3.5
Prostaglandin E receptor 4	2.1	1.9	2.2	1.4
TLR5	0.3	0.3	0.5	0.3
TGF-β receptor 2	0.3	0.4	0.5	0.3
Interferon γ receptor 1	0.3	0.0	0.6	0.4
CD14	0.3	0.8	1.0	0.5
TGF-β receptor 1	0.3	0.4	0.5	0.3
Signaling				
STAT4	7.9	6.5	4.5	9.4
STAT2	6.3	3.1	1.6	4.4
MyD88	3.3	2.1	1.6	2.3
Lyn tyrosine kinase	2.9	2.6	2.3	2.6
MAP3K5	1.9	1.9	1.7	1.8
Transcription				
NFκBIA	5.0	3.7	3.2	4.9
NFκB1 (p105)	4.6	2.4	2.7	2.5
ETS2	2.6	3.5	2.6	3.6
Miscellaneous				
COX-2	14.9	25.6	20.5	42.1
Pentraxin-3	13.4	11.8	16.1	20.8
TAP1	5.5	4.6	1.9	4.3
Proteasome subunit, β-type, 9	4.0	3.3	1.3	4.3
IER3	3.7	4.6	4.1	3.7
Caspase 7	3.7	2.2	1.5	2.7
Proteasome subunit, α-type, 2	3.3	2.0	1.3	2.2
FOSL2	3.2	0.0	2.5	3.2
LAK-1	3.2	1.4	1.2	1.9
CARD15	3.0	2.2	1.2	2.7
Caspase 4	3.0	2.3	2.2	3.2
Caspase 1	2.3	2.0	1.7	1.9
β-Defensin-1	2.3	1.2	1.1	2.8
HSP 70-kDa 1A	2.2	1.5	1.1	1.6
TGFA	2.1	1.7	1.4	2.3
Proteasome subunit, α-type 3	2.0	1.4	1.3	1.4
WASPIP	0.5	0.7	0.5	0.4
Rho GDP dissociation inhibitor (GDI) β	0.4	0.5	0.6	0.4
Sprouty 2	0.4	0.5	0.7	0.3
CSF-1	0.3	0.7	1.1	0.4
Leukotriene-A4 hydrolase	0.3	0.3	0.4	0.2
Arachidonate 5-lipoxygenase	0.3	0.4	0.4	0.3
Plasminogen activator, urokinase-type	0.1	0.4	0.4	0.2

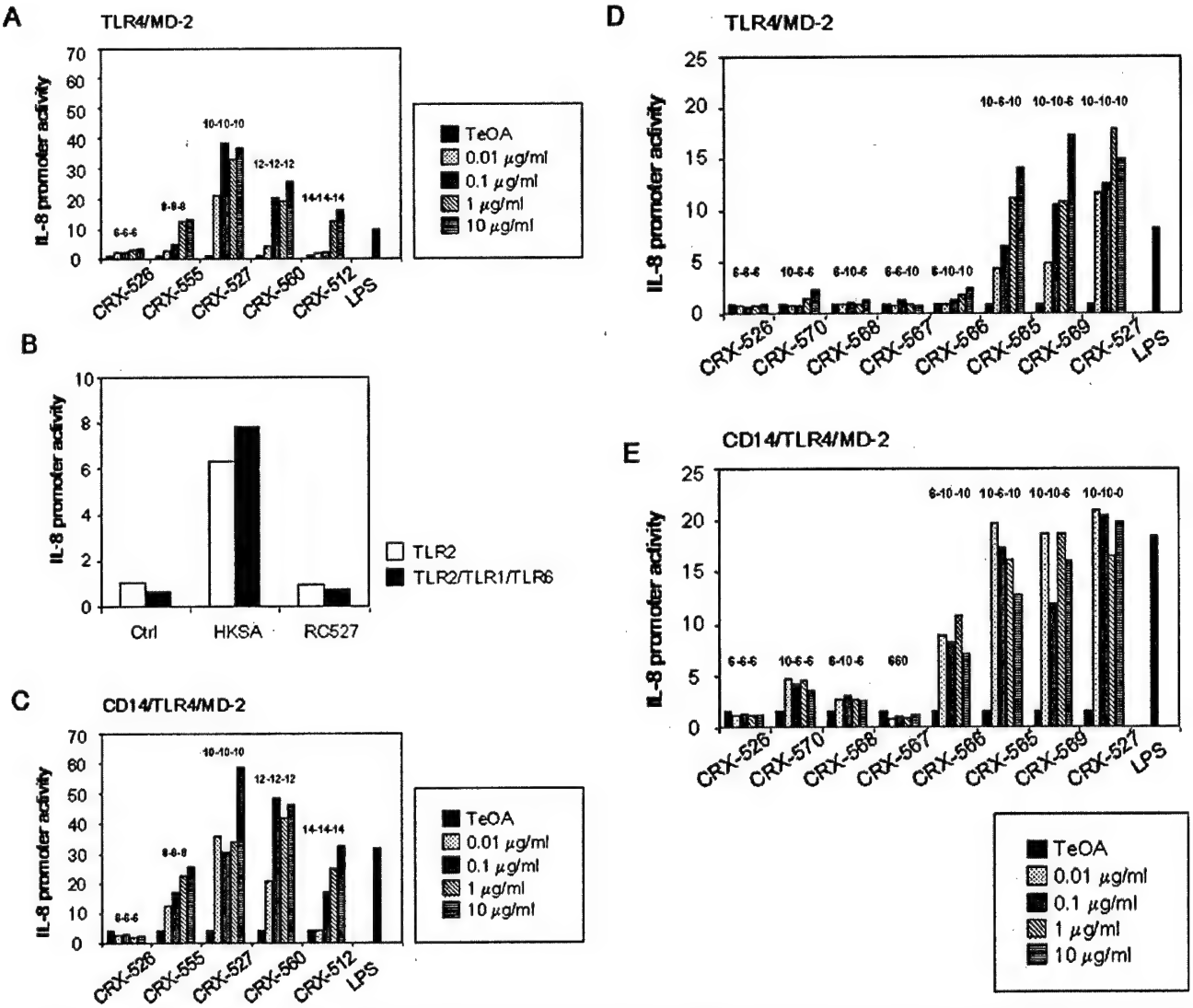

FIG. 4. **IL8 promoter activity.** *A–D*, HeLa cells were transfected with TLR4, MD-2, and CD14 as indicated and stimulated with AGPs as indicated, and IL-8 promoter activity was measured. *E*, 293 cells were stably transfected with TLR2, transiently transfected with TLR1 and TLR6 as indicated, and stimulated with CRX-527 (1 μg/ml), heat-killed *S. aureus* (*HKSA*, 1 μg/ml), or medium alone (Ctrl), and IL-8 promoter activity was determined. *TeOA*, triethylammonium salts.

(MIG; CXCL9); the transcripts of these genes are more than twice as abundant when stimulated by CRX-527 (10-10-10) when compared with LPS (46.4-fold *versus* 23.4-fold and 11.1-fold *versus* 5.2-fold, respectively). While some genes may not be present in the LPS-induced sample due to filtering of the data set using a strict cutoff (*t* test *p* value of ≤0.05), in general, we were not able to detect any genes specifically induced by any of the stimulatory AGPs tested alone (CRX-527 (10-10-10), CRX-560 (12-12-12), CRX-512 (14-14-14), CRX-565 (10-6-10), and CRX-569 (10-10-6)) that were not induced by LPS. The transcriptional profiles of CRX-527 (10-10-10) and CRX-569 (10-10-6) are highly similar. Likewise CRX-560 (12-12-12) and CRX-512 (14-14-14) clustered together with LPS, indicating that these two AGPs and LPS similarly affect the expression of the 149 array elements analyzed. CRX-555 (8-8-8) and CRX-566 (6-10-10) also cluster together, suggesting strong similarities between the effects of these two AGPs. Most strikingly, the non-stimulatory AGPs CRX-526 (6-6-6), CRX-567 (6-6-10), and CRX-568 (6-10-6) cluster together with the vehicle control triethylammonium salts.

Analysis of AGPs Using Transfectants Expressing the TLR4 Receptor Complex—TLR4 is expressed on the surface as part of a trimolecular complex with both MD-2 and CD14 (23). MD-2 has been shown to physically associate with nascent TLR4 in the endoplasmic reticulum but is also secreted and interacts with the extracellular domain of TLR4 expressed on the cell surface (30). Based on biochemical and genetic data, MD-2 is required for LPS-induced stimulation via TLR4. CD14 is a glycosylphosphatidylinositol-linked protein to which LPS has been shown to be transferred via lipopolysaccharide-binding protein circulating in the serum (31). We have previously demonstrated that HeLa cells directed to express TLR4, MD-2, and CD14 following transient transfection respond to LPS (23). We have used a luciferase reporter plasmid containing a portion of the IL-8 promoter, known to be readily induced by LPS via the activation of NFκB, as readout in this assay.

HeLa cells were transiently transfected with TLR4 alone, or in combination with MD-2 and/or CD14, and stimulated with varying concentrations of AGPs. As shown in Fig. 4*A*, HeLa cells transfected with TLR4 and MD-2 gained responsiveness to LPS and CRX-527 (10-10-10); co-expression of CD14 potentiated the response (Fig. 4, *B* and *E*). Cell supernatants of HeLa cells were also examined for the production of IL-8 by ELISA, and a similar pattern of response was observed (data not

shown). In addition, HeLa cells transfected with *Drosophila* Toll (with or without MD-2) or with TLR2 alone were not stimulated by LPS or the AGPs (data not shown). The ability of the AGPs to stimulate the transfectants was strictly dependent on the length of the SAC with results closely mirroring those seen with the human macrophages. Co-expression of CD14 in the transfectants was not required for stimulation but did augment responses to the stimulatory AGPs, particularly at lower concentrations and with the compounds with suboptimal SAC lengths (*e.g.* 8- and 14-carbon, Fig. 4*B*). Similar to the human macrophage cytokine and microarray results, we did not see any TLR4-mediated activation by CRX-526 (6-6-6), which contains hexanoic acid residues in all three of the secondary positions. These data demonstrate the TLR4 dependence and specificity of stimulation with the AGP compounds.

We similarly evaluated a set of partially substituted AGP compounds in this TLR4 transfectant system. As seen in the microarray analysis of stimulated human monocytes (Fig. 3), we found that compounds with a single six-carbon acyl chain in the middle or right position (CRX-565 (10-6-10) and CRX-569 (10-10-6)) in the context of the 10-carbon SAC structure had significant activity in the TLR4/MD-2 transfectants (Fig. 4*C*). The compound with a substitution of a six-carbon acyl chain, the left-sided SAC (CRX-566 (6-10-10), which showed minimal activation via microarray)) was similarly unable to stimulate the TLR4/MD-2 transfectants. Interestingly co-expression of CD14 with TLR4 and MD-2 conferred slight responsiveness to CRX-566 (6-10-10) and augmented the responses to CRX-565 (10-6-10) and CRX-569 (10-10-6) (Fig. 4*D*). Consistent with the data from the microarray experiment, the compounds in which two hexanoic acids were substituted for decanoic acids had minimal to no stimulatory capacity in the transfectants (Fig. 4*D*). These data further highlight the relative importance of the left-sided acyl chain length in lipid A structures in stimulation via the TLR4 complex.

To determine whether TLR1, TLR2, or TLR6 could respond to the AGP, experiments were carried out with 293 cells expressing TLR2 in the presence or absence of TLR1 and TLR6. CRX-527 (10-10-10) did not activate cells through TLR2, TLR1, or TLR6 alone or in combination (Fig. 4*E*). In these latter experiments, heat-killed *S. aureus*, a potent stimulus of TLR2, was used as positive control. In addition, HeLa cells transfected with *Drosophila* Toll (with or without MD-2) were not stimulated by LPS or the AGPs (data not shown).

Analysis of AGP Structure-Function Relationships following in Vivo Administration—The analysis of the response of human macrophages and TLR4 complex transfectants to the AGP compounds has demonstrated the potent activity of these compounds and a substantial dependence on the activity with SAC length. To extend these observations to an *in vivo* model, we determined the effect of intravenous administration of these AGP compounds on cytokine and chemokine production in BALB/c mice. Mice were injected with five different doses of AGPs, and serum was analyzed after 2 h for levels of RANTES, MCP-1, MIP1α, KC (a mouse IL-8 homologue), IL-1β, TNF-α, IL-10, and IL-6. Levels of RANTES, MCP-1, MIP1α, and KC following AGP administration are presented in Fig. 5 and were representative of the patterns observed with all of the cytokines and chemokines tested. In all cases, there was a strict dependence on SAC length that closely mirrored that seen in human macrophages and the TLR4 transfectant analyses. No cytokine or chemokine induction was observed with CRX-526 (6-6-6), and maximal activity was seen with CRX-527 (10-10-10). The dose-response relationship between AGP and *in vivo* chemokine induction revealed the relative potencies of CRX-527 (10-10-10) > CRX-555 (8-8-8) ≥ CRX-560 (12-12-12) > CRX-512 (14-14-14).

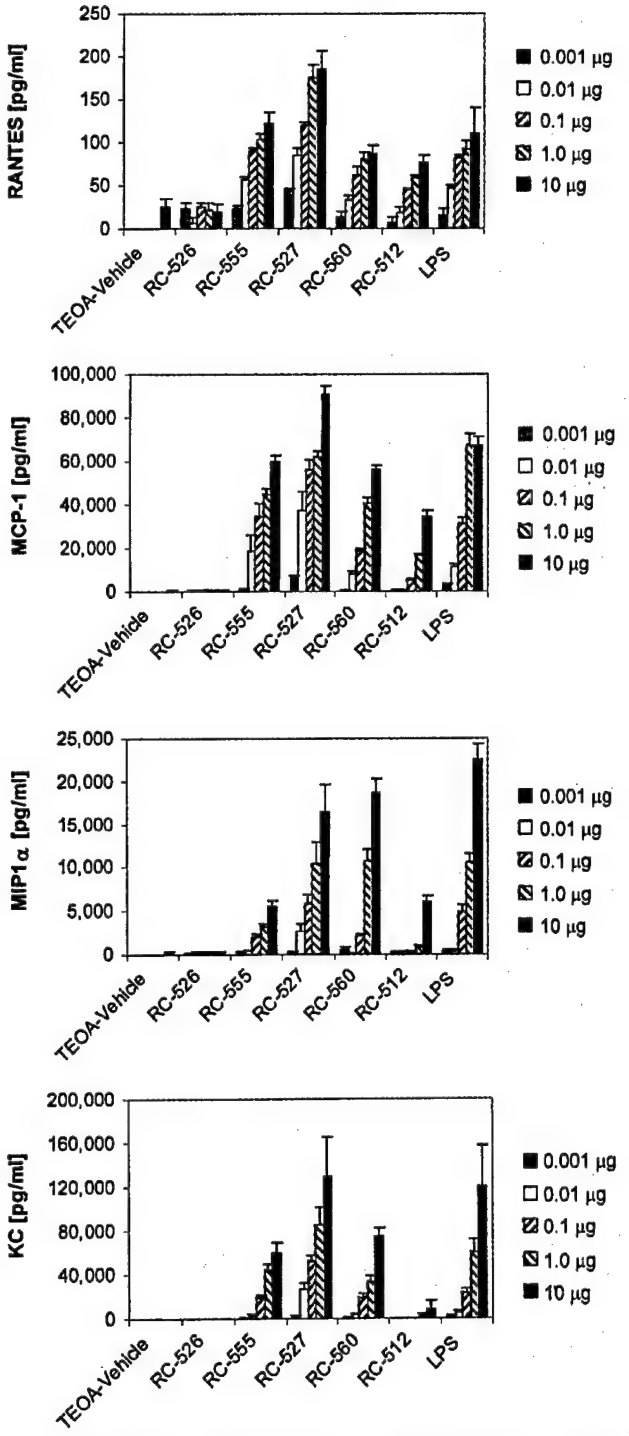

FIG. 5. Chemokine concentration in mouse serum 2 h after intravenous injection of indicated AGP. The chemokine concentrations were determined using a custom Lincoplex cytokine array and Luminex 100 IS system. *TeOA*, triethylammonium salts.

DISCUSSION

In this report, we studied a panel of synthetic lipid A mimetics to investigate the critical relationship between the acyl chain length in the lipid A structure and cellular activation via TLR4. Using both TLR4-positive human macrophages and a TLR4 transfection system, we demonstrate that within a defined family of hexa-acylated molecules, a secondary acyl chain

length of eight carbon atoms is necessary for TLR4 stimulation, and a length of 10 carbon atoms is optimal. Maintenance of this acyl chain length was especially critical for the secondary fatty acid on the left side of the lipid A structure. The responses of these compounds *in vitro* using cell-based assays and TLR4 transfectants strongly correlated with their *in vivo* activity.

The development of the AGP family of lipid A mimetics was based on our previous observations with monophosphoryl lipid A (MPL® adjuvant), a detoxified version of LPS from *Salmonella minnesota* widely used as an immunological adjuvant in human vaccines (6). MPL® adjuvant, a product resulting from sequential acid and base hydrolysis of native *S. minnesota* LPS, is a mixture of multiple congeners including hexa-, penta-, tetra-, and triacylated species. The most active pharmacophore was determined to be a hexa-acylated species in both human and rodent studies. These data are in agreement with the results from Hajjar *et al.* (32) in which natural hexa-acylated species of *Pseudomonas* lipid A stimulated the strongest inflammatory response from human TLR4-positive cells compared with less acylated lipid A moieties. Interestingly that group identified a hypervariable region specific to human TLR4 itself that confers the ability to discriminate between penta-acylated and hexa-acylated lipid A species. Consistent with these data, the synthetic hexa-acylated species used in our studies were more potent than the naturally derived MPL® adjuvant and a limited number of synthetic penta-acylated AGP compounds generated (data not shown). Recently Tamai *et al.* (33) reported TLR4-specific antagonist activity *in vitro* using a synthetic hexa-acylated disaccharide molecule based on the structure of *E. coli* lipid A but not the reduced tetra-acylated species. Curiously that group also reported the induction of several inflammatory cytokines in human peripheral blood mononuclear cells by triacylated monosaccharide lipid A-like compounds. It is tempting to speculate that the macromolecular structure of these compounds in solution mimics the conical hexa-acylated structure thought to be associated with TLR4 agonist activity (34).

Within a defined family of synthetic hexa-acylated compounds with an identical backbone structure, we were able to identify a strict dependence on secondary acyl chain length and TLR4 agonist activity. Specifically a secondary acyl chain length of eight carbons or more was necessary to elicit any inflammatory response, and a length of 10 carbons was optimal relative to longer acyl chains of 12 or 14 carbons. Within the optimal 10-carbon framework, substitutions of six-carbon acyl chains into the left, middle, or right secondary acyl chain position resulted in greatly diminished TLR4 agonist activity, particularly when there were multiple substitutions or changes in the left-sided acyl chain position. It should be noted that the response to even the most potent compound (*i.e.* CRX-527 (10–10-10)) was strictly dependent on TLR4 and MD-2 but not CD14 in the cell transfectants. While we cannot exclude the possibility that soluble CD14 was present in the serum and contributed to the responses seen in the cell transfectants, it was clear that CD14 was capable of enhancing the response to the compounds with shorter acyl chains (*e.g.* CRX-566 (6-10-10) and CRX-555 (8-8-8), Fig. 4). These data suggest that CD14 may preferentially enhance responsiveness to variant lipid A molecules that are not optimally recognized by the TLR4·MD-2 complex, thus potentially expanding the range of molecules that can elicit an inflammatory response from a cell expressing TLR4 and MD-2.

We observed that the results of the microarray analysis from the AGP-stimulated monocytes most closely mirrored the data from the TLR4/MD-2 transfectants. Specifically both systems were able to detect weak or partial agonist activity (*e.g.* with CRX-565 (10-6-10)) that was not as readily apparent when TNF-α was analyzed from stimulated macrophages. The clustering analysis from the microarray data highlighted the fact that the synthetic TLR4 agonists induce a transcriptional response nearly identical to that of native LPS. Comparing the transcriptional responses across the family of compounds suggested that the weaker agonists induced a qualitatively similar response to the stronger agonists or LPS, *i.e.* reduced levels and/or a limited subset of genes induced. While the data presented herein reflect a highly selected group of target genes, further analysis using microarrays in which more than 1000 "unselected" genes induced by LPS were arrayed as targets have revealed the same pattern.[2] Interestingly the results from the various *in vitro* analyses correlated with the biological potency of the respective molecules *in vivo* in the context of chemokine induction.

The intended application for MPL® adjuvant is as an immunological vaccine adjuvant, which would potentiate both B and T cell responses to co-administered antigen. Indeed MPL® adjuvant has been administered to more than 12,000 humans in the context of numerous infectious disease and cancer vaccine trials. Similarly the "prototype" AGP, RC529 (6), has been used successfully in a Phase III clinical trial combined with a conventional alum-based hepatitis B vaccine. More recently, we have been able to demonstrate the ability of members of the AGP family to confer protection against *Listeria* or influenza virus challenge in the absence of co-administration of the microbe itself or microbial antigen.[3] Taken together, the potent chemokine/cytokine induction and ability to confer protection against infectious challenge in the absence of antigen highlight the possibility that TLR4 agonists may be used as stand-alone agents in infectious and/or atopic/allergic disease. The success of synthetic TLR7 agonists (imiquimod/R-848) (35) and TLR9 agonists (CpG oligonucleotides) (36) as stand-alone immunomodulators in clinical development provides a clear precedent for this approach and paves the way for TLR4-based immunomodulatory approaches. Regardless these synthetic compounds have proved helpful in elucidating structure-function relationships relevant to the interaction between lipid A and TLR4 and will prove to be useful compounds in a variety of cell-based and animal studies investigating TLR4.

REFERENCES

1. Lemaitre, B., Nicolas, E., Michaut, L., Reichhart, J. M., and Hoffmann, J. A. (1996) *Cell* **86,** 973–983
2. Rock, F. L., Hardiman, G., Timans, J. C., Kastelein, R. A., and Bazan, J. F. (1998) *Proc. Natl. Acad. Sc. i U. S. A.* **95,** 588–593
3. Takeuchi, O., Kawai, T., Sanjo, H., Copeland, N. G., Gilbert, D. J., Jenkins, N. A., Takeda, K., and Akira, S. (1999) *Gene (Amst.)* **231,** 59–65
4. Chuang, T., and Ulevitch, R. J. (2001) *Biochim. Biophys. Acta* **1518,** 157–161
5. Takeda, K., Kaisho, T., and Akira, S. (2003) *Annu. Rev. Immunol.* **21,** 335–376
6. Persing, D. H., Coler, R. N., Lacy, M. J., Johnson, D. A., Baldridge, J. R., Hershberg, R. M., and Reed, S. G. (2002) *Trends Immunol.* **10,** S32–S37
7. Martin, M., Michalek, S. M., and Katz, J. (2003) *Infect. Immun.* **71,** 2498–2507
8. Krieg, A. M. (2000) *Vaccine* **19,** 618–622
9. Kimbrell, D. A., and Beutler, B. (2001) *Nat. Rev. Genet.* **2,** 256–267
10. Poltorak, A., He, X., Smirnova, I., Liu, M. Y., Van Huffel, C., Du, X., Birdwell, D., Alejos, E., Silva, M., Galanos, C., Freudenberg, M., Ricciardi-Castagnoli, P., Layton, B., and Beutler, B. (1998) *Science* **282,** 2085–2088
11. da Silva Correia, J., Soldau, K., Christen, U., Tobias, P. S., and Ulevitch, R. J. (2001) *J. Biol. Chem.***276,** 21129–21135
12. Poltorak, A., Ricciardi-Castagnoli, P., Citterio, S., and Beutler, B. (2000) *Proc. Natl. Acad. Sci. U. S. A.* **97,** 2163–2167
13. Baker, P. J., Hraba, T., Taylor, C. E., Myers, K. R., Takayama, K., Qureshi, N., Stuetz, P., Kusumoto, S., and Hasegawa, A. (1992) *Infect. Immun.* **60,** 2694–2701
14. Bishop, R. E., Gibbons, H. S., Guina, T., Trent, M. S., Miller, S. I., and Raetz, C. R. (2000) *EMBO J.* **19,** 5071–5080
15. Guo, L., Lim, K. B., Poduje, C. M., Daniel, M., Gunn, J. S., Hackett, M., and Miller, S. I. (1998) *Cell* **95,** 189–198

[2] A. G. Stöver, M. W. Elliot, E. W. Jeffery, D. H. Persing, and R. M. Hershberg, unpublished observations.

[3] C. W. Cluff, J. R. Baldridge, A. G. Stöver, D. H. Persing, and R. M. Hershberg, manuscript in preparation.

16. Mullarkey, M., Rose, J. R., Bristol, J., Kawata, T., Kimura, A., Kobayashi, S., Przetak, M., Chow, J., Gusovsky, F., Christ, W. J., and Rossignol, D. P. (2003) *J. Pharmacol. Exp. Ther.* **304,** 1093–1102
17. Johnson, D. A., Sowell, C. G., Johnson, C. L., Livesay, M. T., Keegan, D. S., Rhodes, M. J., Ulrich, J. T., Ward, J. R., Cantrell, J. L., and Brookshire, V. G. (1999) *Bioorg. Med. Chem. Lett.* **9,** 2273–2278
18. Probst, P., Skeiky, Y. A., Steeves, M., Gervassi, A., Grabstein, K. H., and Reed, S. G. (1997) *Eur. J. Immunol.* **27,** 2634–2642
19. Luo, L., Salunga, R. C., Guo, H., Bittner, A., Joy, K. C., Galindo, J. E., Xiao, H., Rogers, K. E., Wan, J. S., Jackson, M. R., and Erlander, M. G. (1999) *Nat. Med.* **5,** 117–122
20. Eberwine, J., Yeh, H., Miyashiro, K., Cao, Y., Nair, S., Finnell, R., Zettel, M., and Coleman, P. (1992) *Proc. Natl. Acad. Sci. U. S. A.* **89,** 3010–3014
21. Van Gelder, R. N., von Zastrow, M. E., Yool, A., Dement, W. C., Barchas, J. D., and Eberwine, J. H. (1990) *Proc. Natl. Acad. Sci. U. S. A.* **87,** 1663–1667
22. Mujumdar, S. R., Mujumdar, R. B., Grant, C. M., and Waggoner, A. S. (1996) *Bioconjug. Chem.* **7,** 356–362
23. da Silva Correia, J., and Ulevitch, R. J. (2002) *J. Biol. Chem.* **277,** 1845–1854
24. Lee, J. D., Kravchenko, V., Kirkland, T. N., Han, J., Mackman, N., Moriarty, A., Leturcq, D., Tobias, P. S., and Ulevitch, R. J. (1993) *Proc. Natl. Acad. Sci. U. S. A.* **90,** 9930–9934
25. Hegde, P., Qi, R., Abernathy, K., Gay, C., Dharap, S., Gaspard, R., Hughes, J. E., Snesrud, E., Lee, N., and Quackenbush, J. (2000) *BioTechniques* **29,** 548–550
26. Yang, S., Sugawara, S., Monodane, T., Nishijima, M., Adachi, Y., Akashi, S., Miyake, K., Hase, S., and Takada, H. (2001) *Infect. Immun.* **69,** 2025–2030
27. Flo, T. H., Ryan, L., Latz, E., Takeuchi, O., Monks, B. G., Lien, E., Halaas, O., Akira, S., Skjak-Braek, G., Golenbock, D. T., and Espevik, T. (2002) *J. Biol. Chem.* **277,** 35489–35495
28. Xing, Z., Jordana, M., Kirpalani, H., Driscoll. K. E., Schall, T. J., and Gauldie, J. (1994) *Am. J. Respir. Cell Mol. Biol.* **10,** 148–153
29. Eisen, M. B., Spellman, P. T., Brown, P. O., and Botstein, D. (1998) *Proc. Natl. Acad. Sci. U. S. A.* **95,** 14863–14868
30. Visintin, A., Mazzoni, A., Spitzer, J. A., and Segal, D. M. (2001) *Proc. Natl. Acad. Sci. U. S. A.* **98,** 12156–12161
31. Tobias, P. S., and Ulevitch, R. J. (1993) *Immunobiology* **187,** 227–232
32. Hajjar, A. M., Ernst, R. K., Tsai, J. H., Wilson, C. B., and Miller S. I. (2002) *Nat. Immunol.* **3,** 354–359
33. Tamai, R., Asai, Y., Hashimoto, M., Fukase, K., Kusumoto, S., Ishida, H., Kiso, M., and Ogawa, T. (2003) *Immunology* **110,** 66–72
34. Brandenburg, K., Matsuura, M., Heine, H., Müller, M., Kiso, M., Ishida, H., Koch, M. H. J., and Seidel, U. (2002) *Biophys. J.* **83,** 322–333
35. Hemmi, H., Kaisho, T., Takeuchi, O., Sato, S., Sanjo, H., Hoshino, K., Horiuchi, T., Tomizawa, H., Takeda, K., and Akira, S. (2002) *Nat. Immunol.* **3,** 196–200
36. Bauer, S., Kirschning, C. J., Hacker, H., Redecke, V., Hausmann, S., Akira, S., Wagner, H., and Lipford, G. B. (2001) *Proc. Natl. Acad. Sci. U. S. A.* **98,** 9237–9242

Abstracts of presentations resulting from Army and DARPA Contract (due to space limitations; funding acknowledgements are not noted in abstracts, but were included in presentation slides)

Toll meeting, Italy, 2004

Differential induction of cytokines and type I interferons in human monocytes and dendritic cells by synthetic TLR-4 and TLR-3 agonists

Probst P., Engardt S., Stolk J., Evans J., Johnson D.A. and Persing D.
Corixa Corporation, Seattle, U.S.A.

Toll like receptors (TLRs) play an essential role in the innate resistance to microbial pathogens. Recently, it has been shown by our group that aminoalkyl glucosamine phosphates (AGPs) a family of synthetic lipid A mimetic TLR-4 ligands induce high level of protection against bacterial and viral challenge in mice. Recognition of microbial products by TLRs activates monocytes, macrophages and dendritic cells (DC) to produce anti-microbial effector molecules like TNF-α and type I interferons. The goal of the present study was to characterize the activation of human monocytes, macrophages and monocyte-derived DC by AGPs. The response of human monocytic cells to the AGP RC-527, a strong inducer of anti-microbial activity in the murine system, was compared to *E. coli* LPS and to the synthetic TLR-3 agonist poly I:C by determining the secretion of IFN-α, IFN-β, IL-1β, IL-6, IL-10, IL-12p70 and TNF-α. As expected poly I:C induced IFN-α and to a lesser extend IFN-β in all three types of antigen presenting cells. In contrast, only IFN-γ-activated monocytes but not DC and macrophages produced IFN-α and IFN-β in response to RC527 and LPS. Interestingly, activated monocytes secreted the type I interferons faster in response to RC527 than in response to poly I:C suggesting that the secretion of type I interferons in response to TLR-3 and TLR-4 agonists is regulated differentially. Monocytes secreted lower levels of the inflammatory cytokines IL-1β, IL-6 and TNF-α in response to RC527 than in response to LPS. Notably, RC527 and LPS induced similar levels of IL-12, but RC527 induces 5 to 10 times lower levels of IL-10 in activated monocytes suggesting that RC527 preferentially induces the secretion of IL-12. Poly I:C induced very limited amounts of the inflammatory cytokines in monocytes. In contrast to the TLR4 agonists the activation of monocytes with GMCSF but not IFN-γ increased the cytokine production in response to poly I:C. In summary, these data indicate that although the TLR-3 and TLR-4 signaling cascades share the same adapter molecules (Trif and MyD88) the secretion of type I interferons as well as the induction of inflammatory cytokines are regulated differentially in response to TLR-3 and TLR-4 agonists. Furthermore, RC-527 induces anti-microbial effector molecules like IFN-α, IFN-β, TNF-α and IL-12 in human monocytes suggesting that RC-527 may be used as a monotherapeutic agent to enhance resistance against microbial infections.

Macrae Respiratory Viral Infections Meeting, Fort Myers, FL, 2004

Rapid Acting Vaccines: Synthetic Toll-Like Receptor 4 (TLR-4) Agonists Induce Sequential Innate and Adaptive Mucosal Immune Responses

J.T. Evans, C.W. Cluff, D.A. Johnson, J.R. Baldridge, and D.H. Persing
Corixa Corporation, Seattle, WA and Hamilton, MTCorixa scientists have designed a
new class of synthetic lipid A mimetics, termed Aminoalkyl Glucosaminide 4-Phosphates (AGPs), which act as potent agonists of TLR4. Pre-clinical and clinical studies have demonstrated that some AGPs have potent vaccine adjuvant activity. In addition to enhancing adaptive immune responses, certain AGPs are potent inducers of the innate immune system providing immediate non-specific resistance (NSR) to a variety of pathogens. Taking advantage of the combined properties of these AGPs to mediate NSR and provide adjuvant activity, we have developed a rapid-acting vaccine approach that provides both immediate (innate) and long-term (adaptive) immunity. Our results demonstrate that intranasal administration of AGPs provides immediate non-specific protection against viral (influenza) and bacterial (*Listeria monocytogenes*) pathogens that lasts 3-5 days and can be extended by repeated administration. Inclusion of these AGPs in mucosal vaccines provides the added advantage of short-term non-specific resistance during the time required for development of adaptive mucosal immunity, thereby enabling the development of vaccines that are protective immediately following administration. This rapid-acting vaccine approach was demonstrated by inclusion of an AGP (RC-527) with the FluShield™ Influenza vaccine. Intranasal administration of this vaccine protected mice against influenza infection during the lag time required for the generation of adaptive immunity. This concept was also supported in the *Listeria* system, where AGP pre-treated mice remained healthy and generated significant *Listeria*-specific $CD8^+$ effector T-cell responses upon challenge with *Listeria*. Mucosal administration of a potent synthetic TLR4 agonist (AGP) with vaccine antigens induces immediate non-specific resistance while promoting long-term protective immunity.

Gordon Conference on Chemical & Biological Terrorism Defense; Buellton, CA, 2004

Rapid Acting Vaccines: Aminoalkyl Glucosaminide 4-Phosphates (AGPs) Are Potent Inducers of Sequential Innate and Adaptive Mucosal Immune Responses

C.W. Cluff, J.T. Evans, D.A. Johnson, J.R. Baldridge, and D.H. Persing

Corixa Corporation, Seattle, WA and Hamilton, MTCorixa scientists have designed a new class of synthetic lipid A mimetics, termed Aminoalkyl Glucosaminide 4-Phosphates (AGPs), which act as potent agonists of Toll-like receptor 4 (TLR4). Pre-clinical and clinical studies have demonstrated that some AGPs have potent vaccine adjuvant activity. In addition to enhancing adaptive immune responses, certain AGPs are potent inducers of the innate immune system providing immediate non-specific resistance (NSR) to a variety of pathogens. Taking advantage of the combined properties of these AGPs to mediate NSR and provide adjuvant activity we have developed a rapid-acting vaccine approach that provides both immediate (innate) and long-term (adaptive) immunity to viral or bacterial pathogens. Our results demonstrate that intranasal administration of AGPs provides immediate non-specific protection against viral (influenza) and bacterial (*Listeria monocytogenes*) pathogens that lasts 3-5 days and can be extended by repeated administration with no apparent ill effects. Inclusion of AGPs in mucosal vaccines provides the added advantage of short-term non-specific resistance during the time required for development of adaptive mucosal immunity, thereby enabling the development of vaccines that are protective within hours of first administration. This rapid-acting vaccine approach was demonstrated by inclusion of an AGP (RC-527) with the FluShield^{TM}Influenza vaccine. Intranasal administration of this vaccine protected mice against influenza infection during the lag time required for the generation of adaptive immunity. This concept was also supported in the *Listeria* system, where AGP pre-treated mice remained healthy and generated significant *Listeria*-specific $CD8^+$ effector T cell responses upon challenge with *Listeria*. **Conclusions:** Our results demonstrate that a heightened state of innate immunity can be induced and maintained by treatment with AGPs, and that mucosal administration of these compounds with vaccine antigens provides both immediate and long-term protective immunity.

ASM Biodefense Meeting, Baltimore, MD, 2004

Rapid Acting Vaccines: Synthetic Toll-Like Receptor 4 (TLR-4) Agonists Induce Sequential Innate and Adaptive Mucosal Immune Responses

J.T. Evans, C.W. Cluff, D.A. Johnson, J.R. Baldridge, and D.H. Persing
Corixa Corporation, Seattle, WA and Hamilton, MT**Background:** Corixa scientists have designed a new class of synthetic lipid A mimetics, termed Aminoalkyl Glucosaminide 4-Phosphates (AGPs), which act as potent agonists of TLR4. Pre-clinical and clinical studies have demonstrated that some AGPs have potent vaccine adjuvant activity. In addition to enhancing adaptive immune responses, certain AGPs are potent inducers of the innate immune system providing immediate non-specific resistance (NSR) to a variety of pathogens. **Methods and Results:** Taking advantage of the combined properties of these AGPs to mediate NSR and provide adjuvant activity, we have developed a rapid-acting vaccine approach that provides both immediate (innate) and long-term (adaptive) immunity. Our results demonstrate that intranasal administration of AGPs provides immediate non-specific protection against viral (influenza) and bacterial (*Listeria monocytogenes*) pathogens that lasts 3-5 days and can be extended by repeated administration. Inclusion of these AGPs in mucosal vaccines provides the added advantage of short-term non-specific resistance during the time required for development of adaptive mucosal immunity, thereby enabling the development of vaccines that are protective immediately following administration. This rapid-acting vaccine approach was demonstrated by inclusion of an AGP (RC-527) with the FluShield™ Influenza vaccine. Intranasal administration of this vaccine protected mice against influenza infection during the lag time required for the generation of adaptive immunity. This concept was also supported in the *Listeria* system, where AGP pre-treated mice remained healthy and generated significant *Listeria*-specific $CD8^+$ effector T-cell responses upon challenge with *Listeria*. **Conclusions:** Mucosal administration of a potent synthetic TLR4 agonist (AGP) with vaccine antigens induces immediate non-specific resistance while promoting long-term protective immunity.